

# Appendix for Approximately Right?: Global v. Local Methods for Open-Economy Models with Incomplete Markets\*

Oliver de Groot  
University of Liverpool & CEPR

C. Bora Durdu  
Federal Reserve Board

Enrique G. Mendoza  
University of Pennsylvania & NBER

## Abstract

This appendix provides a review of the closure methods used in the academic literature and policy circles, details on the global and local solution methods used to solve the endowment, RBC and Sudden Stops models in the main paper. The appendix also includes some mathematical derivations of expressions and results referred to in the paper, and additional quantitative results for each model.

**JEL Classification:** *C63, F41, E44*

---

\*Correspondence: [oliverdegroot@gmail.com](mailto:oliverdegroot@gmail.com), [bora.durdu@frb.gov](mailto:bora.durdu@frb.gov), [egme@sas.upenn.edu](mailto:egme@sas.upenn.edu). The views expressed in this paper are those of the authors and should not be attributed to the Board of Governors of the Federal Reserve System or its staff.

# Contents

<b>A</b>	<b>Review of the solution methods used in the literature</b>	<b>3</b>
<b>B</b>	<b>Endowment economy</b>	<b>7</b>
B.1	Global methods . . . . .	7
B.1.1	FiPIt method . . . . .	8
B.1.2	VFI method . . . . .	8
B.2	Local methods . . . . .	10
B.2.1	Perturbation methods . . . . .	10
B.2.2	Risk-adjusted steady state method . . . . .	14
B.2.3	Linear-with-occasionally-binding-constraint methods . . . . .	17
B.3	Calibration & comparison of quantitative results . . . . .	19
B.3.1	Calibration . . . . .	19
B.3.2	NFA decision rule and Net Exports . . . . .	20
B.3.3	Long-run moments & impulse response functions . . . . .	24
B.3.4	Spectral densities . . . . .	26
B.3.5	Interest rate shocks . . . . .	29
B.3.6	Alternative calibration of local solutions: Targeting mean vs. autocorrelation of NFA	29
B.3.7	Alternative local solutions: 2OA vs. 3OA . . . . .	30
B.3.8	Comparison of DEIR vs. Endogenous Discounting . . . . .	31
B.3.9	Comparison of global solutions . . . . .	38
B.3.10	Linear with occasionally binding constraint method: DynareOBC . . . . .	38
B.3.11	Analytical solution under savings-under-uncertainty framework . . . . .	43
<b>C</b>	<b>The RBC and Sudden Stops models</b>	<b>47</b>
C.1	FiPIt Global Solution Method . . . . .	50
C.2	Calibration of the RBC and Sudden Stops models . . . . .	57
C.3	Quantitative results of the RBC Model . . . . .	57
C.3.1	Coefficients of RBC decision rules . . . . .	59
C.3.2	Long-run moments and performance metrics . . . . .	60
C.3.3	Impulse response functions . . . . .	63
C.3.4	Spectral analysis . . . . .	72

C.3.5	Sensitivity Analysis . . . . .	74
C.4	Quantitative results of the Sudden Stops model . . . . .	80
C.4.1	Spectral analysis . . . . .	80
C.4.2	<i>FiPIt</i> v. DynareOBC speed comparisons . . . . .	80
C.4.3	Financial premia & quintile analysis for Sudden Stops model . . . . .	82

## A Review of the solution methods used in the literature

Global and local methods have been widely used in research and policy applications. Tables 1 and 2 document the usage of these methods for solving open-economy models with incomplete markets in research articles and policy institutions. Table 1 includes 61 papers. This list is meant to be illustrative, since constructing a complete list of the literature that uses these methods is beyond the scope of this paper. It includes the 50 most cited papers in *Google Scholar* that cite [Schmitt-Grohé and Uribe \(2003\)](#), excluding textbooks and review articles. It also includes all quantitative papers in the references of this paper that are not in that top-50 list, and several well-known papers going back to the early 1990s when the first numerical solutions of open-economy models with incomplete markets were produced. Table 2 lists the models used in eight policy institutions, using information obtained from publicly available documents.

Table 1: Methods Used to Solve Open-Economy Incomplete Markets Models

Authors	Year	Publication	Type of model	Solution method	Stationarity assumption	$\psi$
Adolfson et al.	2007	JIE	SOE	1OA	DEIR	.145(e)
Aguiar and Gopinath	2007	JPE	SOE	1OA	DEIR	.001(s)
Angeloni and Ehrmann	2007	BEJ Macro	$N = 12$	1OA	DEIR	.1(c)
Arellano	2008	AER	SOE	GLB		
Arellano and Mendoza	2002	NBER	SOE	GLB		
Baxter and Crucini	1995	IER	$N = 2$	1OA	AHC	
Bengui et al.	2012	JME	$N = 2$	GLB		
Benigno and Thoenissen	2008	JIMF	$N = 2$	1OA	AHC	
Benigno et al.	2016	JME	SOE	GLB		
Bergin	2006	JIMF	$N = 2$	1OA	DEIR	.00384(e)
Bianchi	2011	AER	SOE	GLB		
Bianchi and Mendoza	2018	JPE	SOE	GLB		
Bianchi et al.	2012	IMFER	SOE	GLB		
Bianchi et al.	2016	JIE	SOE	GLB		
Bodenstein	2011	JIE	$N = 2$	1OA	ED	
Bodenstein et al.	2011	JIE	$N = 2$	1OA	DEIR	0.0001(s)
Boz et al.	2011	JME	SOE	1OA	DEIR	.001(s)
Boz and Mendoza	2014	JME	SOE	GLB		

Continued on next page

Table 1 – continued from previous page

Authors	Year	Journal	Type of model	Solution method	Stationarity assumption	$\psi$
Buch et al.	2005	JIMF	$N = 2$	1OA	AHC	
Cavallo and Ghironi	2002	JME	$N = 2$	1OA	OLG	
Coeurdacier et al.	2011	AER P&P	SOE	RSS		
Correia et al.	1995	EER	SOE	1OA	AHC	
Corsetti et al.	2008	RESTUD	$N = 2$	1OA	ED	
Cuadra and Sapriza	2008	JIE	SOE	GLB		
Devereux et al.	2006	EJ	SOE	1OA	AHC	
Devereux and Sutherland	2010	JMCB	$N = 2$	1OA	ED	
Devereux and Sutherland	2011	JEEA	$N = 2$	1OA	ED	
Durdu et al.	2009	JDE	SOE	GLB		
Durdu and Mendoza	2006	JIE	SOE	GLB		
Enders et al.	2011	JIE	$N = 2$	1OA	ED	
Engel and Wang	2011	JIE	$N = 2$	1OA	AHC	
Fernandez and Chang	2013	IER	SOE	1OA	DEIR	.001 (s)
Fernandez-Villaverde et al.	2011	AER	SOE	3OA	AHC	
Fogli and Perri	2006	NBER	$N = 2$	GLB		
Garcia-Cicco et al.	2010	AER	SOE	1OA	DEIR	.001 (s),2.8(e)
Gertler et al.	2007	JMCB	SOE	1OA	DEIR	0.0001(s)
Ghironi	2006	JIE	$N = 2$	1OA	OLG	
Ghironi and Melitz	2005	QJE	$N = 2$	1OA	AHC	
Hatchondo and Martinez	2009	JIE	SOE	GLB		
Heathcote and Perri	2002	JME	$N = 2$	1OA	AHC	
Heathcote and Perri	2013	JPE	$N = 2$	2OA, 3OA		
Jaimovich and Rebelo	2008	JMCB	SOE	1OA	DEIR	.00001(s)
Justiniano and Preston	2010	JIE	SOE	1OA	DEIR	.01(c)
Lubik and Schorfheide	2005	NBER Macro	$N = 2$	1OA	CM	
Mendoza	1991	AER	SOE	GLB		
Mendoza	1992	IMFSP	SOE	GLB		
Mendoza	1995	IER	SOE	GLB		
Mendoza	2010	AER	SOE	GLB		
Mendoza and Smith	2006	JIE	SOE	GLB		
Mendoza et al.	2009	JPE	$N = 2, 3$	GLB		

Continued on next page

Table 1 – continued from previous page

Authors	Year	Journal	Type of model	Solution method	Stationarity assumption	$\psi$
Mendoza and Yue	2012	QJE	SOE	GLB		
Monacelli	2005	JMCB	SOE	1OA	CM	
Nason and Rogers	2006	JIE	SOE	1OA	DEIR	.00014, .007(e)
Neumeyer and Perri	2005	JME	SOE	1OA	AHC	
Rabanal and Tuesta	2010	JEDC	$N = 2$	1OA	AHC	
Raffo	2008	JIE	$N = 2$	1OA	AHC	
Rebelo and Vegh	1995	RESTUD	SOE	1OA	AHC	
Smets and Wouters	2002	JME	SOE	1OA	OLG	
Uribe and Yue	2006	JIE	SOE	1OA	AHC	

Note: SOE denotes a small open economy model.  $N =$  denotes a multicountry model with  $N$  countries. 1OA, 2OA and 3OA are the first-, second- and third-order approximation methods respectively, RSS is the risky steady state method, and GLB indicates models solved with global methods (including models with standard preferences and  $\beta R < 1$ , endogenous discounting, or overlapping generations). The approaches used to induce stationarity when using local methods are the debt-elastic interest rate (DEIR), asset holding costs (AHC), endogenous discounting (ED), overlapping generations (OLG) and complete markets (CM). For cases using DEIR, (s), (c) and (e) denote whether the debt-elasticity parameter  $\psi$  was chosen to be small, estimated, or calibrated respectively.

Table 2: Solution Methods Used in Policy Models

Institution	Model name	Type of model	Solution method	Stationarity assumption	$\psi$
Bank of Canada	GEM	$N = 5$	1OA	DEIR	n.d.
Bank of England	COMPASS	SOE	1OA	ED	
ECB	NAWM	$N = 2$ and SOE	1OA	DEIR	.01(s)
European Commission	QUEST	SOE	1OA	DEIR	.02(e)
Federal Reserve Board	SIGMA	$N = 2$	1OA	PAC	
IMF	GIMF	$N \geq 2$	1OA	OLG	
Norges Bank	NEMO	SOE	1OA	DEIR	n.d.
Riksbank	RAMSES	SOE	1OA	DEIR	.01(c)

Note: See note to Table 1 for details on abbreviations. n.d. denotes that there is no public document disclosing what value was used.

When local methods are used, 1OA is the most common in research and is used in all eight policy models, and from the assumptions to induce stationarity, DEIR is the most common followed by NFA adjustment costs and ED preferences. From all DEIR solutions, the  $\psi$  values range from 0.00001 to 0.01, and the most common is 0.001, which is the value proposed by [Schmitt-Grohé and Uribe \(2003\)](#).<sup>1</sup> In other cases, the value of  $\psi$  is set by calibration or obtained via estimation. In calibrated cases (three research papers and three policy models),  $\psi$  ranges from 0.01 to 0.1, and in estimated cases (four research papers and one policy model), the point estimates or the medians of posterior distributions in Bayesian estimation range from 0.00014 to 2.8. See the main draft for more discussion on these tables.

Global (GLB) methods are also widely used. Their use dates back to the [Mendoza \(1991\)](#) RBC model of a small open economy, and there are many applications in quantitative studies of sovereign default (e.g., [Aguar and Gopinath, 2007](#); [Arellano, 2008](#)), emerging markets business cycles (e.g., [Mendoza, 1995](#); [Neumeyer and Perri, 2005](#); [Uribe and Yue, 2006](#)), global imbalances (e.g., [Mendoza et al., 2009](#)), Sudden Stops (e.g., [Durdu et al., 2009](#); [Mendoza, 2010](#); [Mendoza and Smith, 2006](#)), and financial regulation (e.g., [Benigno et al., 2016](#); [Bianchi, 2011](#); [Bianchi and Mendoza, 2018](#); [Schmitt-Grohé and Uribe, 2017](#))

We now turn into presenting details for each of the endowment, RBC and the Sudden Stops model.

<sup>1</sup>Note, however, that the DEIR functional forms are not always the same, so  $\psi$  values are not directly comparable. When relevant for our quantitative analysis, we control for this by making comparisons in terms of the elasticity of the interest rate with respect to percent deviations of NFA from steady state.

## B Endowment economy

As described in the main draft, we use a small-open-economy model with stochastic endowment income to derive analytical results and characterize NFA dynamics under incomplete markets. The economy is inhabited by a representative agent with preferences given by:

$$E_0 \left\{ \sum_{t=0}^{\infty} \beta^t u(c_t) \right\}, \quad u(c_t) = \frac{c_t^{1-\sigma}}{1-\sigma}, \quad (1)$$

where  $\beta \in (0, 1)$  is the subjective discount factor,  $c_t$  is consumption and  $\sigma$  is the CRRA coefficient.

The economy's resource constraint is given by

$$c_t = e^{z_t} \bar{y} - A + b_t - qb_{t+1}, \quad (2)$$

term  $e^{z_t}$ ,  $b_t$  denotes the NFA position in one-period, non-state-contingent discount bonds traded where  $e^{z_t} \bar{y}$  is stochastic income that fluctuates around a mean  $\bar{y}$  with shocks  $z_t$  of exponential in a frictionless global credit market at exogenous price  $q = \frac{1}{1+r}$ , where  $r$  is the world real interest rate, and  $A$  is a constant that represents investment and government expenditures (which is introduced so the model can be calibrated to observed average consumption-GDP ratios). Income shocks follow an AR(1) process:  $z_t = \rho_z z_{t-1} + \sigma_z \varepsilon_t^z$  where  $\varepsilon_t^z$  is i.i.d.

For further details of the model and the definition of competitive equilibrium, see the main draft. Now we turn to the description of the quantitative methods we used to solve this model.

### B.1 Global methods

GLB methods solve the model in recursive form over a discrete state space of  $(b, z)$  pairs. Since the competitive equilibrium is efficient, it can be represented as a dynamic programming problem:

$$V(b, z) = \max_{c, b'} \left\{ \frac{c^{1-\sigma}}{1-\sigma} + \beta \sum_{z'} \pi(z', z) V(b', z') \right\}, \quad (3)$$

*s.t.*  $c = e^z \bar{y} - A + b - qb', \quad b' \geq \varphi.$

The AR(1) process of income is approximated as a discrete Markov chain with transition probability matrix  $\pi(z', z)$ . The solution to the Bellman equation is characterized by a decision rule  $b'(b, z)$  and the associated value function  $V(b, z)$ . This decision rule and the Markov process of the shocks induce a joint ergodic (unconditional) distribution of NFA and income  $\lambda(b, z)$ .

We use two alternative global solution methods: *FiPit* method and Value Function Iteration

(VFI) method.

### B.1.1 FiPIt method

While using the *FiPIt* method, we solve for  $b'(b, z)$ , by solving for the recursive equilibrium conditions using a fixed-point iteration algorithm (see [Mendoza and Villalvazo, 2020](#), for details).<sup>2</sup> In this case, the *FiPIt* method iterates on the following representation of the Euler equation:

$$c_{j+1}(b, z) = \left\{ \beta (1 + r) \sum_{z'} \pi(z', z) \left[ c_j(\hat{b}'_j(b, z), z') \right]^{-\sigma} \right\}^{-\frac{1}{\sigma}}. \quad (4)$$

Given a conjecture of the decision rule  $\hat{b}'_j(b, z)$  in iteration  $j$ , the associated consumption function is  $c_j(b, z) = e^z \bar{y} - A + b - q \hat{b}'_j(b, z)$ . This consumption function is interpolated over its first argument in order to determine  $c_j(\hat{b}'_j(b, z), z')$ , so that the above equation solves directly for a new consumption function  $c_{j+1}(b, z)$ . Using the resource constraint, the new consumption function yields a new decision rule for bonds  $b'_{j+1}(b, z)$ , which is re-set to  $b'_{j+1}(b, z) = \varphi$  if  $b'_{j+1}(b, z) \leq \varphi$ . Then the decision rule conjecture is updated to  $\hat{b}'_{j+1}(b, z)$  as a convex combination of  $\hat{b}'_j(b, z)$  and  $b'_{j+1}(b, z)$ , and the process is repeated until  $b'_{j+1}(b, z) = \hat{b}'_j(b, z)$  up to a convergence criterion.

### B.1.2 VFI method

The VFI algorithm is implemented as follows: Given the endogenous state variable  $b$  and exogenous state  $z = \varepsilon^z$ , the equilibrium of the endowment model is represented as the solution to this dynamic programming problem:

$$V(b, z) = \max_{b', c} \left\{ \frac{c^{1-\sigma}}{1-\sigma} + \beta E [V(b', z')] \right\} \quad (5)$$

s.t.

$$c = e^z \bar{y} - A - q^b b' + b \quad (6)$$

where  $V(b, z)$  is the value function and  $q^b = \frac{1}{1+r}$ . The VFI algorithm solves this problem in the following steps:

---

<sup>2</sup>This method solves Euler equations directly instead of using a non-linear solver. It is fast and easy to implement in Matlab. [Mendoza and Villalvazo \(2020\)](#) show that it performs better than standard time iteration and endogenous grids methods, particularly for models with two endogenous state variables and occasionally binding constraints, because the time iteration method requires solving nonlinear equations and the endogenous grids method requires complex interpolation techniques because the endogenous grids are irregular.

1. Define grids for  $b$  and  $z$  with  $nb$  nodes for the bonds grid and  $ne$  nodes for the income shocks, and set also a convergence criterion for the value function  $\epsilon$ .
2. Define grids of bonds  $\{b_1, b_2, b_3, \dots, b_{nb}\}$  and shocks  $\{z_1, z_2, z_3, \dots, z_{ne}\}$ . The bonds grid is defined by a set of nodes with a lower bound equal to the natural or ad-hoc debt limits, and an upper bound high enough to have zero mass in the ergodic distribution of bonds. The grid of shocks is defined by a Markov process with  $ne$  nodes, usually constructed to approximate an AR(1) process of an actual income process in the data using Tauchen's quadrature method.
3. For each state  $(b_i, z_h)$ , set a value for the initial value function (at iteration  $j = 0$ , where  $j$  is the iteration counter) so as to construct  $V^0(b, z)$ . A trivial initial condition is  $V^0(b, z) = 0$ .
4. Maximization step: Update the value function to obtain  $V^{j+1}(b, z)$  as follows:

- a For each state  $(b_i, z_h)$ , evaluate the value of consumption if the decision rule for bonds  $b_{ii}$  were to be assigned to each of the  $nb$  possible values it can take on the bonds grid (i.e., for  $ii = 1, \dots, nb$ ):

$$c(b_i, z_h; b_{ii}) = e^{z_h \bar{y}} - A - q^b b_{ii} + b_i$$

- b Compute the value of choosing  $b_{ii}$  if the state of nature is  $(b_i, z_h)$ , denoted  $W(b_i, z_h; b_{ii})$ , by evaluating the Bellman equation as follows:

$$W^j(b_i, z_h; b_{ii}) = \frac{c(b_i, z_h; b_{ii})^{1-\sigma}}{1-\sigma} + \beta E_{hh} [V^j(b_{ii}, z_{hh})]$$

- c For each  $(b_i, z_h)$ , maximize  $W^j(b_i, z_h; b_{ii})$  over  $b_{ii}$ . The decision rule for bonds at iteration  $j$  is given by  $b^j(b_i, z_h) = \operatorname{argmax}_{b_{ii}} \{W^j(b_i, z_h; b_{ii})\}$  and the "new" value function is defined by  $V^{j+1}(b_i, z_h) = W^j(b_i, z_h; b^j(b_i, z_h))$

5. Compare  $V^j$  and  $V^{j+1}$  and compute the convergence criterion  $d$  as

$$d^j = \max_{i \in \{1, \dots, nb\}, h \in \{1, \dots, ne\}} |V^j(b_i, z_h) - V^{j+1}(b_i, z_h)|$$

6. If  $d > \epsilon$ , convergence has not been attained Set  $V^j(b, z) = V^{j+1}(b, z)$  and go back to step 4.
7. If  $d \leq \epsilon$ , the value function has converged to  $V(b, z) = V^{j+1}(b, z)$  with associated decision rules given by  $b'(b, z) = b^j(b_i, z_h)$ .

## B.2 Local methods

This section provides a textbook treatment of the local solution methods used for the endowment economy model: first- and second-order perturbation (1OA and 2OA, respectively); risk-adjusted steady state (RSS); and linear-with-occasionally-binding-constraint (DynareOBC). We keep the notation generic so that our description also applies to the RBC model for the first three solution method, and the solution of the Sudden Stops model with DynareOBC. Note that all four solutions are local in that they construct an approximation in the neighborhood of a steady state. However, the aim of all four methods is to construct good numerical approximations of *non-local* features.

**Notation** Let the set of equilibrium conditions for the dynamic general equilibrium model we wish to study be written as

$$0 = \mathbb{E}_t f(y_{t+1}, y_t, y_{t-1}, \varepsilon_t), \quad (7)$$

where  $\mathbb{E}_t$  denotes the expectations operator. The vector  $y_t$  of variables is of size  $n_y$  and the vector  $\varepsilon_t$  of shocks is of size  $n_\varepsilon$ . The function  $f$  maps  $\mathbb{R}^{n_y} \times \mathbb{R}^{n_y} \times \mathbb{R}^{n_y} \times \mathbb{R}^{n_\varepsilon}$  into  $\mathbb{R}^{n_y}$ . The vector  $\varepsilon_t$  is assumed to have bounded support and be independently and identically distributed with mean zero and with variance-covariance matrix  $I$ , the identity matrix.<sup>3</sup> The unknown solution (or decision rule) to the model given in (7) that we wish to approximate is of the form

$$y_t = g(y_{t-1}, \varepsilon_t), \quad (8)$$

where  $g$  maps  $\mathbb{R}^{n_y} \times \mathbb{R}^{n_\varepsilon}$  into  $\mathbb{R}^{n_y}$ .

This method is slow in models with more than one endogenous state variable and cannot be used when equilibria are inefficient, but does not require differentiability or convexity of optimization problems. Compared to VFI, *FiPIt* is a fast, simple method that applies fixed-point iteration to solve Euler equations. It can be used when equilibria are inefficient but requires differentiability (see [Mendoza and Villalvazo, 2020](#), for details).

### B.2.1 Perturbation methods

Although linearizing around a steady state is a special version of perturbation methods and has been used to solve dynamic equilibrium models since the early 1980s, perturbation methods were only formerly introduced into Economics by [Judd and Judd \(1998\)](#). In Judd, the methods were

---

<sup>3</sup>This is without loss of generality since the var-cov structure of the fundamental shocks can be specified in  $f$ .

based upon a value function formulation of the problem. In this paper, we follow [Schmitt-Grohé and Uribe \(2004\)](#) in constructing a second-order perturbation method using the equilibrium conditions directly rather than a value function formulation. Toolkits for applying perturbation methods abound. Dynare, in particular, is an efficient, user friendly, and freely available toolkit.

The basic idea of perturbation methods is to find a particular case of the model that has a known solution and use that particular case and its solution as a starting point for computing approximate solutions to nearby problems. This approach relies on the implicit function theorem and Taylor series expansion. A special version of perturbation methods is linearizing around a steady state.

In particular, with perturbation methods we approximate the decision rule of the model near the steady state of the model's deterministic counterpart. The method then uses local information to calculate linear and higher-order approximations of the solution near the steady state.

The result of perturbation methods is a polynomial which approximates the true solution in the neighborhood of the deterministic steady state. To construct this approximation, we add an auxiliary *perturbation* parameter,  $\sigma$ , to the unknown decision rule in (8) as follows

$$\mathbf{y}_t = g(\mathbf{y}_{t-1}, \varepsilon_t, \sigma) \quad \text{and} \quad \mathbf{y}_{t+\tau} = g(\mathbf{y}_{t+\tau-1}, \sigma \varepsilon_{t+\tau}, \sigma) \quad \text{for } \tau > 0, \quad (9)$$

The perturbation parameter takes a value between 0 and 1. When  $\sigma = 1$ , we have the full stochastic model in (7) and when  $\sigma = 0$  we instead have the perfect-foresight analog of that model—i.e., the model without future uncertainty.

The perturbation methods begins by finding a known solution to a nearby problem. In a dynamic stochastic model, this known solution is the deterministic steady state, when  $\sigma = 0$ ,  $\varepsilon_t = 0$ , and  $\mathbf{y}$  solves

$$0 = f(\mathbf{y}, \mathbf{y}, \mathbf{y}, 0). \quad (10)$$

Notice that when  $\sigma = 0$  the expectations operator disappears because there is no future uncertainty. Armed with the deterministic steady state, the perturbation method proceeds as follows. Substituting (8) into (7) gives

$$0 = \mathbb{E}_t f(g(g(\mathbf{y}_{t-1}, \varepsilon_t, \sigma), \sigma \varepsilon_{t+1}, \sigma), g(\mathbf{y}_{t-1}, \varepsilon_t, \sigma), \mathbf{y}_{t-1}, \varepsilon_t). \quad (11)$$

Equation (11) can be written more concisely as

$$0 = \mathbb{E}_t F(\mathbb{y}_{t-1}, \varepsilon_t, \sigma). \quad (12)$$

Since (12) is equal to zero, all derivatives of (12) must also be equal to zero. These derivatives provide identifying restrictions for determining the partial derivatives of  $g$ .

*First-order Differentiating (12) with respect to  $\mathbb{y}_{t-1}$  and  $\varepsilon_t$  gives*

$$[F_{\mathbb{y}}]_j^i = [f_1]_k^i [g_{\mathbb{y}}]_l^k [g_{\mathbb{y}}]_j^l + [f_2]_k^i [g_{\mathbb{y}}]_j^k + [f_3]_j^i = 0; \quad i, j, k, l = 1, \dots, n_{\mathbb{y}}, \quad (13)$$

$$[F_{\varepsilon}]_m^i = [f_1]_k^i [g_{\mathbb{y}}]_l^k [g_{\varepsilon}]_m^l + [f_2]_k^i [g_{\varepsilon}]_m^k + [f_4]_m^i = 0; \quad m = 1, \dots, n_{\varepsilon}, \quad (14)$$

respectively, where all the derivatives of  $f$  have been evaluated at the deterministic steady state:  $(\mathbb{y}_{t-1}, \varepsilon_t, \sigma) = (\mathbb{y}, 0, 0)$ , and are therefore known.

A word on the notation is necessary here. The term  $[f_3]_j^i$ , for example, is the  $(i, j)$  element of the Hessian of  $f$  with respect its third argument,  $\mathbb{y}_{t-1}$ . Also,  $[f_2]_k^i [g_{\mathbb{y}}]_j^k$ , for example, is short-hand for

$$\sum_{k=1}^n \frac{\partial f^i}{\partial \mathbb{y}_t^k} \frac{\partial g^k}{\partial \mathbb{y}_{t-1}^j}. \quad (15)$$

The derivatives of  $f$  evaluated at  $(\mathbb{y}, \mathbb{y}, \mathbb{y}, 0)$  are known. The first expression above represents a system of  $n_{\mathbb{y}} \times n_{\mathbb{y}}$  quadratic equations in  $n_{\mathbb{y}} \times n_{\mathbb{y}}$  unknowns given by the elements of  $g_{\mathbb{y}}$ . Similarly, with  $g_{\mathbb{y}}$  known, the second expression above represents a system of  $n_{\mathbb{y}} \times n_{\varepsilon}$  (linear) equations in  $n_{\mathbb{y}} \times n_{\varepsilon}$  unknowns given by the elements of  $g_{\varepsilon}$ .

Thus, using standard results on the solution of quadratic matrix equations,  $g_{\mathbb{y}}$  and  $g_{\varepsilon}$  can be found as solutions. In general, in the neighborhood of the deterministic steady state, up to first-order, we have that  $g_{\sigma} = 0$ . This result holds because the system of equations  $[F_{\sigma}]^i = 0$  are linear and homogenous in  $g_{\sigma}$ . We do not prove the result here but direct the interested reader to [Schmitt-Grohé and Uribe \(2004\)](#). This result is important though, because it says that a first-order approximation in the neighborhood of the deterministic steady state is always certainty equivalent.

The first-order approximation of the solution in the neighborhood of the deterministic steady state is therefore given by

$$g(\mathbb{x}_t, \sigma) = g(\mathbb{x}, 0) + g_{\mathbb{x}}(\mathbb{x}, 0)(\mathbb{x}_t - \mathbb{x}), \quad (16)$$

where, for simplicity, we write  $\mathbb{x}_t \equiv [y'_{t-1}, \varepsilon'_t]'$ . It follows that the deterministic steady state,  $\mathbb{x}$ , is simply  $\mathbb{x} = (y, 0)$ .

*Second-order* Given the deterministic steady state, the first-derivatives of (12) provided identifying restrictions to solve for the  $g_{\mathbb{x}}$  terms of the unknown decision rule. Similarly, we will use second-derivatives of (12) combined with the deterministic steady state and the known values for  $g_{\mathbb{x}}$  to derive identifying restrictions for  $g_{\mathbb{x}\mathbb{x}}$  and  $g_{\sigma\sigma}$ . Specifically

$$\begin{aligned} [F_{yy}]_{jn}^i &= \left( [f_{11}]_{ko}^i [g_y]_p^o [g_y]_n^p + 2 [f_{12}]_{ko}^i [g_y]_n^o + 2 [f_{13}]_n^i \right) [g_y]_l^k [g_y]_j^l \\ &+ \left( [f_{22}]_{ko}^i [g_y]_n^o + 2 [f_{23}]_n^i \right) [g_y]_j^k + [f_{33}]_n^i \\ &+ [f_1]_k^i \left( [g_{yy}]_{lo}^k [g_y]_n^o [g_y]_j^l + [g_y]_l^k [g_{yy}]_{jn}^l \right) + [f_2]_k^i [g_{yy}]_{jn}^k = 0, \end{aligned} \quad (17)$$

$$\begin{aligned} [F_{y\varepsilon}]_{jm}^i &= \left( [f_{11}]_{ko}^i [g_y]_p^o [g_\varepsilon]_m^p + 2 [f_{12}]_{ko}^i [g_\varepsilon]_m^o + 2 [f_{14}]_m^i \right) [g_y]_l^k [g_y]_j^l \\ &+ \left( [f_{22}]_{ko}^i [g_\varepsilon]_m^o + [f_{24}]_m^i \right) [g_y]_j^k + \left( [f_{31}]_{ko}^i [g_y]_p^o [g_\varepsilon]_m^p + [f_{32}]_{ko}^i [g_\varepsilon]_m^o + [f_{34}]_m^i \right) \\ &+ [f_1]_k^i \left( [g_{yy}]_{lo}^k [g_\varepsilon]_m^o [g_y]_j^l + [g_y]_l^k [g_{y\varepsilon}]_{jm}^l \right) + [f_2]_k^i [g_{y\varepsilon}]_{jm}^k = 0, \end{aligned} \quad (18)$$

$$\begin{aligned} [F_{\varepsilon\varepsilon}]_{mq}^i &= \left( [f_{11}]_{ko}^i [g_y]_p^o [g_\varepsilon]_q^p + [f_{12}]_{ko}^i [g_\varepsilon]_q^o + [f_{14}]_q^i \right) [g_y]_l^k [g_\varepsilon]_m^l \\ &+ \left( [f_{21}]_{ko}^i [g_y]_p^o [g_\varepsilon]_q^p + [f_{22}]_{ko}^i [g_\varepsilon]_q^o + [f_{24}]_q^i \right) [g_\varepsilon]_m^k + [f_{44}]_q^i \\ &+ [f_1]_k^i \left( [g_{yy}]_{lo}^k [g_\varepsilon]_1^o [g_\varepsilon]_m^l + [g_y]_l^k [g_{y\varepsilon}]_{jq}^l \right) + [f_2]_k^i [g_{\varepsilon\varepsilon}]_{mq}^k = 0; \end{aligned} \quad (19)$$

$$n, o, p = 1, \dots, n_y; \quad q = 1, \dots, n_\varepsilon$$

The first expression above represents a system of  $n_y \times n_y \times n_y$  linear equations in  $n_y \times n_y \times n_y$  unknowns given by the elements of  $g_{yy}$ . With  $g_{yy}$  known, the second expression above represents a system of  $n_y \times n_y \times n_\varepsilon$  linear equations in  $n_y \times n_y \times n_\varepsilon$  unknowns given by the elements of  $g_{y\varepsilon}$ . And, with  $g_{y\varepsilon}$  known, the third expression above represents a system of  $n_y \times n_\varepsilon \times n_\varepsilon$  linear equations in  $n_y \times n_\varepsilon \times n_\varepsilon$  unknowns given by the elements of  $g_{\varepsilon\varepsilon}$ .

In general, in the neighborhood of the deterministic steady state,  $g_{y\sigma} = g_{\varepsilon\sigma} = 0$ . This results because the system of equations  $[F_{y\sigma}]_j^i = 0$  and  $[F_{\varepsilon\sigma}]_j^i = 0$  are homogenous in  $g_{y\sigma}$  and  $g_{\varepsilon\sigma}$ , respectively. Finally, the  $n_y$  unknowns given by the elements of  $g_{\sigma\sigma}$  can be obtained by solving the  $n_y \times 1$  linear equations

$$[F_{\sigma\sigma}]^i = [f_{11}]_{jk}^i [g_\varepsilon]_m^j [g_\varepsilon]_q^k [I]_m^q + [f_2]_j^i [g_{\sigma\sigma}]^j + [f_1]_j^i \left( [g_y]_k^j [g_{\sigma\sigma}]^k + [g_{\varepsilon\varepsilon}]_{mq}^j [I]_q^m + [g_{\sigma\sigma}]^j \right) = 0. \quad (20)$$

The second-order approximation of the decision rule in the neighborhood of the deterministic steady state of a stochastic model differs from that of its non-stochastic counterpart only in a constant term,  $g_{\sigma\sigma}$ . The second-order approximation of the solution in the neighborhood of the deterministic steady state is therefore given by

$$[g(\mathbf{x}_t, \sigma)]^i = [g(x, 0)]^i + [g_{\mathbf{x}}(x, 0)]_r^i [\mathbf{x}_t - \mathbf{x}]^r + \frac{1}{2} [g_{\mathbf{x}\mathbf{x}}(x, 0)]_{rs}^i [\mathbf{x}_t - \mathbf{x}]^r [\mathbf{x}_t - \mathbf{x}]^s + \frac{1}{2} [g_{\sigma\sigma}(x, 0)]^i, \quad r, s = 1, \dots, n_y + n_\varepsilon. \quad (21)$$

An increase in uncertainty—increasing the standard deviation of the shock innovations—will change  $g_{\sigma\sigma}$  and shift the mean of the endogenous variables away from the deterministic steady state.

*m<sup>th</sup>-order* In principle, one can solve a polynomial approximation of  $g$  up to any order,  $m$ , using perturbation methods. In each step, the  $(m - 1)^{th}$  approximation of  $g$  is known and the  $m^{th}$  derivatives of (12) will provide identifying restrictions for the  $m^{th}$  coefficients of  $g$ . In each case, the system of equations are linear. However, the number of unknowns increase rapidly in  $m$ . Thus, even for a medium-size DSGE model, orders of approximation above 3 are computationally demanding.

## B.2.2 Risk-adjusted steady state method

The risk-adjusted steady state method differs from standard perturbation methods in constructing an approximate solution, not in the neighborhood of the deterministic steady state, but rather in the neighborhood of an approximation of the full stochastic model's steady state. In principle, just like standard perturbation methods, an approximate decision rule can be constructed up to any order. However, we focus attention on a first-order approximation in the neighborhood of a risk-adjusted steady state. Several approaches to constructing such approximations have been proposed in the literature, beginning with [Collard and Juillard \(2001\)](#), and with more recent contributions by [Coourdacier et al. \(2011\)](#), [Juillard \(2011\)](#), [de Groot \(2013\)](#), and [Meyer-Gohde \(2015\)](#). The method proposed by [Coourdacier et al. \(2011\)](#) is a focus of this section since they apply their *risky* steady state method to solving a small open economy model as we do.

Unlike (9), the solution is not parameterized explicitly by the perturbation parameter. Rather

$$\mathbf{y}_t = g(\mathbf{y}_{t-1}, \varepsilon_t) \quad \text{and} \quad \mathbf{y}_{t+\tau} = g(\mathbf{y}_{t+\tau-1}, \sigma \varepsilon_{t+\tau}) \quad \text{for} \quad \tau > 0. \quad (22)$$

Substituting (9) into (7) gives

$$0 = \mathbb{E}_t f(g(g(y_{t-1}, \varepsilon_t), \sigma \varepsilon_{t+1}), g(y_{t-1}, \varepsilon_t), y_{t-1}, \varepsilon_t). \quad (23)$$

We can define the *exact* risk-adjusted steady state: When  $\sigma = 1$  and  $\varepsilon = 0$ ,  $y^{er}$  is the exact risk-adjusted steady state if it solves the problem

$$0 = \mathbb{E}_t f(g(y^{er}, \varepsilon_{t+1}), y^{er}, y^{er}, 0). \quad (24)$$

However, this object is not very useful since the definition relies on  $g$  in order to solve for  $y^{er}$ . Instead, it is possible to solve jointly for an approximation of the risk-adjusted steady state and linear dynamics.<sup>4</sup> Equation (23) can be written more concisely as

$$0 = F(x_t, \sigma). \quad (25)$$

Consider the Taylor expansion of this function up to second-order in the neighborhood of an approximate risk-adjusted steady state ( $y^r$ ), given by

$$[F(y_{t-1}, \varepsilon_t, \sigma)]^i = [F(y^r, 0, 0)]^i + \frac{1}{2} [F_{\sigma\sigma}]^i + [F_y]_j^i [x_t - x]_j + \frac{1}{2} [F_{yy}]_{jk}^i [x_t - x]_j [x_t - x]_k. \quad (26)$$

All the derivatives of  $F$  are evaluated at  $(y^r, 0, 0)$ , although for notational simplicity this information has been removed. So far we haven't made much progress since even the derivatives of  $F$  are unknown. However, for this equation to hold for any  $x_t$  then it must be the case that

$$[F]^i + \frac{1}{2} [F_{\sigma\sigma}]^i = 0, \quad [F_y]_j^i = 0, \quad \text{and} \quad [F_{yy}]_{jk}^i = 0. \quad (27)$$

All of these terms above have exactly the same structure as those given for the perturbation methods except  $[F_{\sigma\sigma}]^i$ , which is given by

$$[F_{\sigma\sigma}]^i = [f_{11}]_{jk}^i [g_\varepsilon]_m^j [g_\varepsilon]_q^k [I]_m^q + [f_1]_j^i [g_{\varepsilon\varepsilon}]_{mq}^j [I]_q^m = 0. \quad (28)$$

This shows that for a second-order approximation in  $\sigma$ , we get second-order terms,  $g_{\varepsilon\varepsilon}$ . Thus, to construct a linear (first-order approximation), we follow Couerdacier et al. (2011) and assume that

---

<sup>4</sup>The exact risk-adjusted steady state is not the mean of the ergodic distribution of  $y$ . The ergodic mean requires an unconditional expectations operator, while in (24) the expectations operator is conditional on time  $t$  information.

the second-order terms,  $g_{\sigma\sigma}$ , are equal to zero, and ignore the second-derivative conditions,  $F_{yy}$ .

Bringing everything together, we have the following set of equations: The steady state equations

$$\mathbb{F}(\mathbf{y}^r, g_{\mathbf{x}}) \equiv [f(\mathbf{y}^r, \mathbf{y}^r, \mathbf{y}^r, 0)]^i + [f_{11}]_{jk}^i [g_{\varepsilon}]_m^j [g_{\varepsilon}]_q^k [I]_m^q = 0, \quad (29)$$

and the first-derivative conditions

$$[F_{\mathbf{y}}]_j^i = [f_1]_k^i [g_{\mathbf{y}}]_l^k [g_{\mathbf{y}}]_j^l + [f_2]_k^i [g_{\mathbf{y}}]_j^k + [f_3]_j^i = 0; \quad i, j, k, l = 1, \dots, n_{\mathbf{y}}, \quad (30)$$

$$[F_{\varepsilon}]_m^i = [f_1]_k^i [g_{\mathbf{y}}]_l^k [g_{\varepsilon}]_m^l + [f_2]_k^i [g_{\varepsilon}]_m^k + [f_4]_m^i = 0; \quad m = 1, \dots, n_{\varepsilon}. \quad (31)$$

Since both sets of equations depend on both the steady state  $\mathbf{y}^r$  and on the linearized dynamics,  $g_{\mathbf{y}}$  and  $g_{\varepsilon}$ , these equations need to be solved simultaneously. We use the following algorithm:

1. Use the deterministic steady state as an initial guess,  $\mathbf{y}^0$ , of the risk-adjusted steady state and calculate the linearized dynamics,  $g_{\mathbf{x}}^0$ .
2. Evaluate (29) using  $(\mathbf{y}^0, g_{\mathbf{x}}^0)$ .  
if  $|\mathbb{F}(\mathbf{y}^0, g_{\mathbf{x}}^0)| > \epsilon$  (where  $\epsilon$  is a tolerance parameter) then update the steady state guess to  $\mathbf{y}^1$  and proceed to step 3.  
else STOP. A solution to the fixed-point problem has been found.
3. Use  $\mathbf{y}^1$  to calculate the updated linearized dynamics  $g_{\mathbf{x}}^1$ . Return to step 2 using  $(\mathbf{y}^1, g_{\mathbf{x}}^1)$  in the place of  $(\mathbf{y}^0, g_{\mathbf{x}}^0)$ .

The linear approximation of the solution in the neighborhood of the risk-adjusted steady state is therefore given by

$$g(\mathbf{y}_{t-1}, \varepsilon_t, \sigma) = \mathbf{y}^r + g_{\mathbf{y}}(\mathbf{y}^r, 0)(\mathbf{y}_{t-1} - \mathbf{y}^r) + g_{\varepsilon}(\mathbf{y}^r, 0)\varepsilon_t. \quad (32)$$

Notice that, unlike its standard perturbation counterpart, this linear approximation of the decision rule is not certainty equivalent. Changes in the variance-covariance of shocks will alter both the steady state and the linearized dynamics around that steady state.

Alternative risk-adjusted approximations are possible. [Juillard \(2011\)](#) solves the system of equations in (27) and thus constructs a second-order approximation in the neighborhood of the deter-

ministic steady state. In contrast, [de Groot \(2013\)](#) derives the second-order approximation in the neighborhood of the deterministic steady state and takes a first-order Taylor expansion of this function to construct a linear approximation in the neighborhood of the risk-adjusted steady state. This method benefits from not requiring a fixed-point problem to be solved.

### B.2.3 Linear-with-occasionally-binding-constraint methods

In this section, we describe how perturbation solutions can handle the model with an occasionally binding collateral constraint. Since the zero lower bound became a binding constraint for monetary policy during the 2007-08 financial crisis, the literature has developed extensions to local approximation methods to solve models with occasionally binding constraints. There are two main computational toolkits publicly available. For the model in this paper, both approaches delivered the same candidate solution paths for endogenous variables.<sup>5</sup> The first, `OccBin` ([Guerrieri and Iacoviello \(2015\)](#)), exploits a piecewise linear solution technique. The second, `DynareOBC` ([Holden \(2016\)](#)), exploits the use of “news” shocks to construct a solution.<sup>6</sup>

**Holden (2016):** We first present the set up without the constraint. The linearized version of (7) can be written as

$$0 = (C + B + A)\mathbb{x} + C\mathbb{x}_{t+1} + B\mathbb{x}_t + A\mathbb{x}_{t-1}, \quad (33)$$

where  $\mathbb{x}_t \equiv [y'_t, \varepsilon'_{t+1}]'$  and  $\mathbb{x}$  is the deterministic steady state. Assume the first element of the steady state vector,  $\mathbb{x}_1$ , is positive. We will return to this assumption below. The matrices are given by

$$C \equiv \begin{bmatrix} f_1 & 0 \\ 0 & 0 \end{bmatrix}, \quad B \equiv \begin{bmatrix} f_2 & 0 \\ 0 & I \end{bmatrix}, \quad \text{and} \quad A \equiv \begin{bmatrix} f_3 & f_4 \\ 0 & 0 \end{bmatrix}. \quad (34)$$

where, for example,  $f_1$  is the Hessian of  $f$  with respect to the first argument, evaluated at the deterministic steady state. The solution to this problem is the linearized decision rule

$$\mathbb{x}_t = (I - g_{\mathbb{x}})\mathbb{x} + g_{\mathbb{x}}\mathbb{x}_{t-1} \quad \text{where} \quad g_{\mathbb{x}} = -(B + Cg_{\mathbb{x}})^{-1}A. \quad (35)$$

<sup>5</sup>Other local approximation methods may also be amenable to solving models with occasionally binding constraints. For extended path algorithms, see [Adjemian and Juillard \(2013\)](#). For penalty based methods see [McGrattan \(1996\)](#).

<sup>6</sup>Antecedents of this approach include [Laséen and Svensson \(2011\)](#) and [Holden and Paetz \(2012\)](#).

The occasionally binding constraint is introduced by augmenting (33) as follows

$$\mathbb{x}_{1,t} = \max(0, (C_1 + B_1 + A_1)\mathbb{x} + C_1\mathbb{x}_{t+1} + (B_1 + I_1)\mathbb{x}_t + A_1\mathbb{x}_{t-1}), \quad (36)$$

$$0 = (C_{-1} + B_{-1} + A_{-1})\mathbb{x} + C_{-1}\mathbb{x}_{t+1} + B_{-1}\mathbb{x}_t + A_{-1}\mathbb{x}_{t-1}, \quad (37)$$

where  $C_1$ , for example, denotes the first row of  $C$  and  $C_{-1}$  denotes  $C$  excluding the first row. The occasionally binding constraint has been introduced using a max operator in the first equation. The fact that the constraint has been introduced as a positivity constraint is without loss of generality since it is always possible to rewrite a constraint in this form.

The problem that needs to be solved can be formulated as follows: Given a vector of initial conditions,  $\mathbb{x}_0$ , find a sequence  $\{\mathbb{x}_t\}_{t=0}^{\infty}$  in  $\mathbb{R}^n$  such that (36) and (37) hold and that  $\mathbb{x}_t \rightarrow \mathbb{x}$  as  $t \rightarrow \infty$ . Above we assume that  $\mathbb{x}_1 > 0$ . This means i) that the constraint does not bind in the steady state and ii) we consider only solutions in which there is some  $T \in \mathbb{N}$  such that for  $t > T$  the constraint no longer binds.

The problem described above is solved by solving a complementary problem using “news” shocks. Consider the following system

$$0 = (C + B + A)\mathbb{x} + C\mathbb{x}_{t+1} + B\mathbb{x}_t + A\mathbb{x}_{t-1} + I_{c1}y_{1,t-1} \quad (38)$$

In time 0 there is a  $T \times 1$  vector,  $y_0$ , of news shocks, where  $y_{t,0}$  is the shock  $t$  periods ahead. Thus,  $y_{i+1,t-1} = y_{i,t}$  and, for  $t > T$ ,  $y_{1,t-1} = 0$ .  $I_{c1}$  denotes the first column of the identity matrix. The algorithm then searches for  $y_{1,t-1}$  such that the max operator in (36) is adhered to in all periods.

**Guerrieri and Iacoviello (2015):** In contrast to using news shocks to enforce the constraint, this method concatenate decision rules to construct a piecewise-linear solution. They begin by defining two regimes, the “unconstrained” and “constrained” regimes

$$0 = (C + B + A)\mathbb{x} + C\mathbb{x}_{t+1} + B\mathbb{x}_t + A\mathbb{x}_{t-1}, \quad (39)$$

$$0 = (C^* + B^* + A^*)\mathbb{x} + C^*\mathbb{x}_{t+1} + B^*\mathbb{x}_t + A^*\mathbb{x}_{t-1}, \quad (40)$$

where the latter is the constrained regime (i.e., the first term in the max operator above). The coefficients of this second (constrained) set of linearized equilibrium conditions are evaluated at the

same deterministic steady state as the first (unconstrained) set of linearized equilibrium conditions. A solution for the model is then a function that maps  $\mathbb{x}_{t-1}$  into  $\mathbb{x}_t$  such that the conditions under the unconstrained or constrained set of equilibrium conditions hold, depending on the evaluation of the constraint in (36). The algorithm used to solve for this time-varying decision rule employs a guess-and-verify approach. In effect, for any initial state configuration,  $\mathbb{x}_0$ , the algorithm guesses the periods  $t \geq 0$  for which the economy is in the constrained and unconstrained regimes. This guess is characterized by a vector of 0s and 1s. Again, let  $T$  denote the last period in which the constraint binds. For  $t \geq T$ , the decision rule will be (35). For period  $T - 1$ , the solution for  $\mathbb{x}_{T-1}$  given  $\mathbb{x}_{T-2}$  can then be derived by solving the following equation

$$0 = (C^* + B^* + A^*)\mathbb{x} + C^* ((I - g_{\mathbb{x}})\mathbb{x} + g_{\mathbb{x}}\mathbb{x}_{t-1}) + B^*\mathbb{x}_{t-1} + A^*\mathbb{x}_{t-2}. \quad (41)$$

It is possible to iterate back in this fashion, using either (35) or (41), depending on the regime, until  $\mathbb{x}_0$  is reached, giving a candidate equilibrium path. Next, the max function is used to check the vector that summarizes the initial guess of regimes against the actual outturn in the candidate path. If the sequence of regime guesses is verified, then the solution is complete. Otherwise, the guess for when regimes apply is updated and the process is repeated.

Next, we describe the calibration used for the endowment model and present quantitative results that highlight differences and similarities implied by the local and global solutions.

### B.3 Calibration & comparison of quantitative results

#### B.3.1 Calibration

We use the same baseline calibration as in [Durdu et al. \(2009\)](#), which was based on annual data for Mexico. The common baseline calibration parameters are set as follows:  $\sigma = 2$ , a standard value,  $\bar{y} = 1$  as a normalization,  $r = 0.059$ , which is the average of the [Uribe and Yue \(2006\)](#) real interest rate including the EMBI spread for Mexico. The target average NFA-GDP ratio is set to  $-44$  percent, which is the average for Mexico over the period 1985–2004 in the database constructed by [Lane and Milesi-Ferretti \(2007\)](#), and the target consumption-GDP ratio is 0.692, which is the average ratio in Mexican data for the 1965–2005 period. These parameter values and the resource constraint imply  $A = \bar{y} + rb - c = 0.282$ . The standard deviation and first-order autocorrelation of the AR(1) income process were estimated at  $\sigma_z = 0.0327$  and  $\rho_z = 0.597$  using the HP-detrended cyclical component of GDP computed with Mexican data. For further details of the calibration see

the main draft Section 2.4.

### B.3.2 NFA decision rule and Net Exports

In this section, we provide details on the derivations of the decision rules reported in Section 2.4 of the main draft.

#### *Analytical solution*

Assume the dynamics of NFA can be represented as a first-order autoregressive process for which  $\rho$ ,  $\mu_b$ , and  $\sigma_B^2$  denote the autocorrelation, mean, and variance of NFA, respectively. Recall that net exports ( $nx_t$ ) are equal to  $qb_{t+1} - b_t$ , where  $q \equiv 1/R$  denotes the price of discount bonds. The autocorrelation of  $nx$  implied by the NFA autoregressive process is derived as follows:

$$\begin{aligned}
E[(nx_t - \bar{nx})(nx_{t-1} - \bar{nx})] &= E[nx_t nx_{t-1}] - \bar{nx}^2 \\
&= E[(qb_{t+1} - b_t)(qb_t - b_{t-1})] - \mu_b^2(q-1)^2 \\
&= q^2 E[b_{t+1}b_t] + E[b_t b_{t-1}] - qE[b_t^2] - qE[b_{t+1}b_{t-1}] - \mu_b^2(q-1)^2 \\
&= (\rho\sigma_B^2 + \mu_b^2)(1+q^2) - q(\sigma_B^2 + \mu_b^2) - q((1-\rho)\mu_b^2 + \rho(\rho\sigma_B^2 + \mu_b^2)) - \mu_b^2(q-1)^2 \\
&= \sigma_b^2(q^2\rho + \rho - q - q\rho^2)
\end{aligned}$$

$$\rho(nx) = \frac{q^2\rho + \rho - q - q\rho^2}{1 + q^2 - 2q\rho}. \quad \square \quad (42)$$

This relationship implies that there is a highly nonlinear relationship between autocorrelation of net foreign assets and net exports. This nonlinear relationship is a key aspect we will refer through out the appendix and main draft while interpreting local and global solutions.

#### *Local solution*

To derive decision rules using the local solutions, we use the following equilibrium conditions (with  $\bar{y} = 1$  and  $A = 0$ , for simplicity)

$$\begin{aligned}
c_t &= e^{z_t} + b_t - \frac{b_{t+1}}{1+r_t}, \\
1 &= \beta \mathbb{E}_t (c_t/c_{t+1})^\sigma (1+r_t), \\
r_t &= r + \psi \left( e^{b^* - b_{t+1}} - 1 \right), \\
z_t &= \rho_z z_{t-1} + \sigma_z \varepsilon_t^z.
\end{aligned}$$

Written in the form of (7), we have

$$\mathbb{E}_t f(y_{t+1}, y_t, y_{t-1}, \varepsilon_t) = \mathbb{E}_t \begin{bmatrix} -y_t^1 + \exp(y_t^3) + y_{t-1}^2 - \frac{y_t^2}{1+r+\psi(\exp(b-y_t^2)-1)} \\ -1 + \beta (y_t^1/y_{t+1}^1)^\sigma (1+r+\psi(\exp(b^*-y_t^2)-1)) \\ -y_t^3 + \rho_z y_{t-1}^3 + \sigma_z \varepsilon_t^z \end{bmatrix}, \quad (43)$$

where  $y_t \equiv [c_t, b_{t+1}, z_t]'$ . The deterministic steady states of NFA,  $b^{dss}$ , is pinned down by the parameter  $b^*$ . The endowment process,  $z_t$ , has a steady state of 0. The deterministic steady state of consumption is given by  $c^{dss} = 1 - b^{dss}r/(1+r)$ . We can derive numerical values for the policy functions. Using the baseline calibration,  $\{r = 0.08571, b^* = -0.51, \sigma = 2, \psi = 0.001, \rho_z = 0.597, \sigma_z = 0.0327\}$ , the 1OA decision rule is given by

$$\begin{bmatrix} c^{dss} \\ b^{dss} \end{bmatrix} = \begin{bmatrix} .960 \\ -.510 \end{bmatrix} \quad \text{and} \quad g_x = \begin{bmatrix} .084 & .186 \\ .995 & .884 \end{bmatrix}, \quad (44)$$

where the rows are the endogenous variables,  $[c_t, b_{t+1}]$ , and the columns are the state variables,  $[b_t, z_t]'$ . The additional 2OA decision rule terms are given by

$$g_{xx}^c = \begin{bmatrix} -.005 & -.005 \\ -.005 & .104 \end{bmatrix}, \quad g_{xx}^b = \begin{bmatrix} .004 & .005 \\ .005 & .972 \end{bmatrix}, \quad \text{and} \quad g_{\sigma\sigma} = \begin{bmatrix} -4.8 \times 10^{-5} \\ 5.2 \times 10^{-5} \end{bmatrix}. \quad (45)$$

For the RSS decision rules, the steady state conditions are given by

$$0 = -c^{rss} + 1 + b^{rss} - \frac{b^{rss}}{1+r+\psi(e^{b^*-b^{rss}}-1)}, \quad (46)$$

$$0 = -1 + \beta \left(1 + r + \psi \left(e^{b^*-b^{rss}} - 1\right)\right) \left(1 + \frac{\gamma(\gamma-1)}{2} \mathbb{E}_t (c_{t+1} - c^{rss})^2\right), \quad (47)$$

where  $\mathbb{E}_t (c_{t+1} - c^{rss})^2 = g_z^c \sigma_z^2$ . Solving jointly for the risk-adjusted steady state,  $[c^{rss}, b^{rss}]'$ , and the first-order coefficients,  $g_x^{rss}$ , gives

$$\begin{bmatrix} c_t \\ b_{t+1} \end{bmatrix} = \begin{bmatrix} c^{rss} \\ b^{rss} \end{bmatrix} + g_x^{rss} \begin{bmatrix} b_t - b^{rss} \\ z_t \end{bmatrix} \quad (48)$$

where

$$\begin{bmatrix} c^{rss} \\ b^{rss} \end{bmatrix}' = \begin{bmatrix} .970 \\ -.376 \end{bmatrix}, \quad g_x^{rss} = \begin{bmatrix} .083 & .184 \\ .995 & .886 \end{bmatrix}. \quad (49)$$

Since the DynareOBC method generates time-and-state dependent decision rules, it is not possible to write down decision rules as we have for the perturbation and RSS methods.

*Analytical results using local solutions for a simplified endowment model with log-utility and i.i.d. shocks*

It is possible derive analytical expressions for the 2OA and RSS decision rules in a simplified endowment economy. In particular, we set  $b^* = 0$  so the deterministic steady state is  $[c, b] = [1, 0]$ ;  $\rho_z = 0$  so endowment fluctuations are i.i.d.; and  $\sigma = 1$  so we have log-preferences. Finally, we set  $r = 0$  and  $\beta = 1$ . The 2OA decision rules are given by

$$\begin{aligned}\tilde{c}_t &= g(b_t, z_t, \sigma) = g_b b_t + g_z z_t + \frac{1}{2} (g_{bb} b_t^2 + g_{zz} z_t^2 + g_{\sigma\sigma}) + g_{bz} b_t z_t, \\ b_{t+1} &= h(b_t, z_t, \sigma) = h_b b_t + h_y z_t + \frac{1}{2} (h_{bb} b_t^2 + h_{zz} z_t^2 + h_{\sigma\sigma}) + h_{bz} b_t z_t,\end{aligned}$$

where  $\tilde{c}_t \equiv \log(c_t)$ . Substituting into the Euler equation and budget constraint gives

$$\begin{aligned}1 &= \mathbb{E}_t \exp(g(b_t, z_t, \sigma_z) - g(h(b_t, z_t, \sigma_z), \sigma_z \sigma \varepsilon_{t+1}, \sigma)) (1 + \psi(\exp(-h(b_t, z_t, \sigma_z)) - 1)), \\ \exp(g(b_t, z_t, \sigma_z)) &= \exp(z_t) + b_t - h(b_t, z_t, \sigma_z) (1 + \psi(\exp(-h(b_t, z_t, \sigma_z)) - 1))^{-1}.\end{aligned}$$

*2OA solution*

Solving for  $h_b$  gives

$$\begin{aligned}h_b(\psi) &= 1 - \frac{1}{2} \left( \sqrt{\psi^2 + 4\psi} - \psi \right), \\ &= 1 - 2 \frac{\psi}{\psi + \sqrt{\psi^2 + 4\psi}} < 1,\end{aligned}$$

for  $\psi > 0$ . It also tells us that  $h_b(0) = 1$ ,  $h'_b(\psi) < 0$ ,  $h''_b(\psi) > 0$ ,  $\lim_{\psi \rightarrow \infty} h_b(\psi) = 0$ , and  $\lim_{\psi \rightarrow 0} h'_b(\psi) = -\infty$ . We also have that

$$\begin{aligned}0 &= g_z - h_z(g_b + \psi), \\ 0 &= 1 - g_z - h_z.\end{aligned}$$

As a result, it is straightforward to show that  $h_z = h_b$  and  $g_b = g_z = 1 - h_b$ . The 2OA coefficients

for NFA are given by

$$\begin{aligned}
h_{bb} = h_{bz} &= -\psi^3 + \sqrt{\psi + 4}\psi^{5/2} - 4\psi^2 + 2\sqrt{\psi + 4}\psi^{3/2} - \frac{5\psi}{2} + \frac{(\psi + 1)\sqrt{\psi + 4}\sqrt{\psi}}{2(\psi + 3)}, \\
h_{zz} &= -\psi^3 + \sqrt{\psi + 4}\psi^{5/2} - 4\psi^2 + 2\sqrt{\psi + 4}\psi^{3/2} - 2\psi - \frac{\sqrt{\psi + 4}\sqrt{\psi}}{\psi + 3} + 1, \\
h_{\sigma\sigma} &= \frac{(-2\psi^2 + 2\sqrt{\psi + 4}\psi^{3/2} - 7\psi + 5\sqrt{\psi + 4}\sqrt{\psi} - 4)}{(\psi + 3)(\psi + \sqrt{\psi + 4}\sqrt{\psi} + 2)}.
\end{aligned}$$

Clearly, the coefficients quickly become complicated functions of  $\psi$ . However,  $h_{bb}(0) = h_{bz}(0) = 0$ ,  $h_{zz}(0) = 1$ , and  $h_{\sigma\sigma}(0) = -2/3$ .

### RSS solution

In the simplified endowment economy with i.i.d. endowment risk and a simplified DEIR function of the form  $1 + r_t = (1 + r)e^{\psi(b^* - b_{t+1})}$ , the “full RSS” solution is identical to the “partial RSS” solution described in the main paper. We begin by substituting into the Euler equation, giving

$$1 = \beta(1 + r)\mathbb{E}_t \exp \left( \begin{array}{c} -\gamma(\tilde{c}^{rss} + g_b b_{t+1} + g_z(\rho_y z_t + \sigma_z \varepsilon_{t+1})) \\ +\gamma(\tilde{c}^{rss} + g_b(b_t - b^{rss}) + g_z z_t) + \psi(b^* - b_{t+1}) \end{array} \right).$$

The steady state equation is given by

$$\begin{aligned}
1 &= \beta(1 + r)\mathbb{E}_t \exp(-\gamma g_z \sigma_z \varepsilon_{t+1} - \psi(b^{rss} - b^*)) \\
&= \beta(1 + r) \exp\left(\frac{1}{2}\gamma^2 g_z^2 \sigma_z^2 - \psi(b^{rss} - b^*)\right).
\end{aligned}$$

The second line is either derived from the properties of the log-normal distribution, or by taking a second-order expansion around  $\sigma_z = 0$  and then applying  $\log(1 + x) \approx x$  for small  $x$ . Rearranging gives

$$b^{rss} = b^* + \frac{\gamma^2 g_z^2 \sigma_z^2}{2\psi}.$$

When  $b^* = 0$  and  $\gamma = 1$  (log-preferences), this simplifies to  $b^{rss} = \frac{g_z^2 \sigma_z^2}{2\psi}$ . After setting  $\beta = 1$  and  $r = 0$ , the IOA term,  $h_b$ , is given by

$$h_b = \frac{1}{2} \left( e^{-b\psi} + (1 - b\psi) - \sqrt{(e^{-b\psi} - (1 - b\psi))^2 + 4e^{-b\psi}\psi} \right). \quad (50)$$

where, for clarity,  $b$  denotes  $b^{r_{ss}}$ . The only difference between  $h_b$  under RSS and 2OA is that the expression is evaluated at  $b^{r_{ss}}$  rather than  $b^{d_{ss}} = 0$ . The remaining 1OA terms are given by

$$h_z = \frac{1}{1 - e^{b\psi}(h_b + b\psi - 1)}, \quad g_b = \frac{e^{b\psi}(h_b + b\psi) - 1}{(e^{b\psi} - 1)b - 1}, \quad g_z = \frac{1 - e^{b\psi}(h_b + b\psi)}{(1 - (e^{b\psi} - 1)b)(1 - e^{b\psi}(h_b + b\psi - 1))}.$$

These coefficients clarify that the first-order dynamics of the RSS solution differ from the dynamics of the 1OA solution.

### B.3.3 Long-run moments & impulse response functions

In this subsection, we provide pertinent details for the results related to the long-run moments and impulse response functions in the main draft.

The result showing that precautionary savings nearly vanish from 2OA and partial RSS solutions as  $\psi$  rises implies that the terms driving the deviation of the unconditional average of  $b$  from  $b^{d_{ss}}$  in their decision rules are vanishing too. To shed light on why this happens, we use again the decision rules for log utility and i.i.d. shocks (together with the quantitative result that the quadratic and interaction terms of the 2OA solutions are negligible) to obtain these expressions:<sup>7</sup>

$$E[b]^{2OA} = b^{d_{ss}} + \sigma_z^2 \frac{h_{\sigma\sigma}}{2(1 - h_b)}, \quad E[b]^{RSS} = b^{d_{ss}} + \sigma_z^2 \frac{g_y^2}{2\psi}, \quad (51)$$

where  $g_y$  is the coefficient of the consumption decision rule on income. Since  $h_b$  is decreasing in  $\psi$  for  $\psi < 0.5$  (recall Figure 1 in the main draft), the denominators in the right-hand-side of the above expressions rise with  $\psi$ , which brings the unconditional means closer to  $b^{d_{ss}}$ . The coefficients  $h_{\sigma_z\sigma_z}$  and  $g_y$  also depend on  $\psi$ ,

#### *Second-order terms & moments*

The main text of the paper argues that the quadratic and interaction terms of the 2OA solutions are negligible. This section addresses this point in more detail. Figure 1 plots three rows of unconditional moments (mean, standard deviation, and persistence of NFA) from the endowment model using [Andreasen et al. \(2018\)](#) pruning. Each of the three columns varies one structural parameter at a time ( $\psi$ ,  $\sigma$ , and  $\rho_z$ , respectively) while holding the rest at the baseline calibration. We compare the true SOA solution with a ‘‘poor man’s’’ analog in which we set  $h_{bb} = h_{bz} = h_{zz} = 0$  (i.e., leaving only the  $h_{\sigma\sigma}$  term from the true SOA decision rule).

<sup>7</sup>When  $\psi$  is small and  $h_b$  is close to 1 (e.g., when  $\psi = 0.001$ ), the other quadratic and interaction terms do matter for the value of  $E[b]$ . However, they become negligible again if  $\psi > 0.01$ . See Online Appendix C.3.3 for details.

The top-left panel shows that the mean-NFA under the true SOA and under the poor-man's SOA only diverge for small value of  $\psi$  when NFA is highly persistent. The difference is significant for the baseline calibration ( $\psi = 0.001$ ) but not for the targetted calibration ( $\psi = 0.047$ ). Rows 2 and 3 show that first-order moments such as the standard deviation and persistence of NFA are unaffected by the existence of second-order terms, except in the case when the calibration is extreme and far from the baseline (e.g., when risk averse or the persistence of the endowment shocks is very high).

To see why the unconditional mean-NFA is affected by second-order terms, it is helpful to write out its analytical expression. The pruned SOA decision rule is given by

$$b_{t+1} = b_{1t+1} + b_{2t+1}, \quad (52)$$

$$b_{1t+1} = h_b b_{1t} + h_z z_t, \quad (53)$$

$$b_{2t+1} = h_b b_{2t} + \frac{1}{2} (h_{bb} b_{1t}^2 + h_{zz} z_t^2 + h_{\sigma\sigma}) + h_{bz} b_{1t} z_t. \quad (54)$$

Taking unconditional expectations gives

$$\mathbb{E}(b_{t+1}) = \frac{1}{1-h_b} \frac{1}{2} (h_{bb} \mathbb{E}(b_{1t}^2) + 2h_{bz} \mathbb{E}(b_{1t} z_t) + h_{zz} \mathbb{E}(z_t^2) + h_{\sigma\sigma}), \quad (55)$$

and since

$$\mathbb{E}(b_{1t+1}^2) = \frac{1}{1-h_b^2} h_z \frac{\sigma_z^2}{1-\rho_z^2}, \quad \mathbb{E}(b_{1t} z_t) = \frac{\sigma_z^2}{1-\rho_z^2}, \quad \mathbb{E}(z_t^2) = \rho_z \frac{\sigma_z^2}{1-\rho_z^2}, \quad (56)$$

we can combine these terms to give

$$\mathbb{E}(b_{t+1}) = \frac{1}{1-h_b} \frac{1}{2} \left( \left( h_{bb} \frac{1}{1-h_b^2} h_z + 2h_{bz} \rho + h_{zz} \right) \frac{\sigma_z^2}{1-\rho_z^2} + h_{\sigma\sigma} \right) \quad (57)$$

The poor man's [pm] SOA ignores all second-order terms except for  $h_{\sigma\sigma}$ . In this case:

$$b_{t+1}^{pm} = h_b b_t^{pm} + h_z z_t + \frac{1}{2} h_{\sigma\sigma}, \quad (58)$$

and

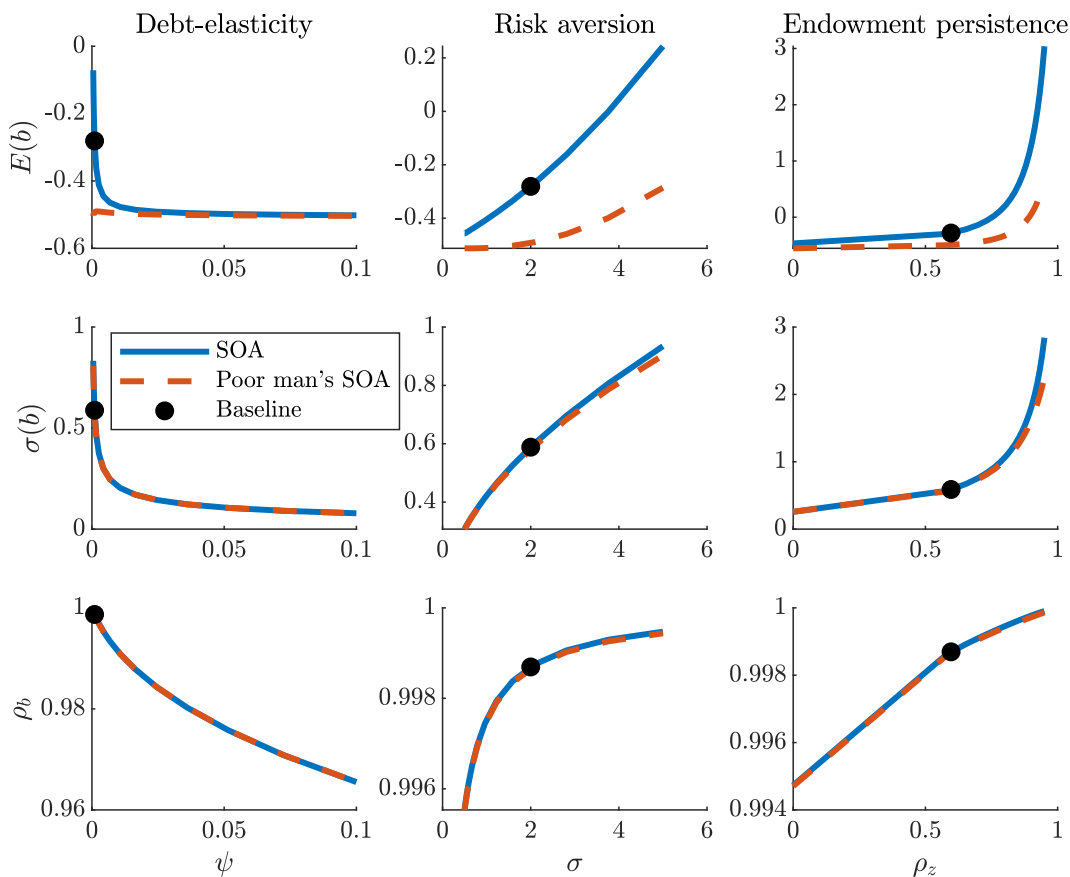
$$\mathbb{E}(b_{t+1}^{pm}) = \frac{1}{1-h_b} \frac{1}{2} h_{\sigma\sigma}. \quad (59)$$

Thus, the discrepancy, err, is given by

$$\text{err} = \frac{1}{1-h_b} \frac{1}{2} \left( \left( h_{bb} \frac{1}{1-h_b^2} h_z + 2h_{bz} \rho_z + h_{zz} \right) \frac{\sigma_z^2}{1-\rho_z^2} \right). \quad (60)$$

This final expression clarifies that when  $h_b$  is close to 1, that all interaction terms, but especially  $h_{bb}$ , gets magnified, and becomes important for accurately calculating mean-NFA.

Figure 1: Second-order terms & moments



Note: Moments calculated analytically using the [Andreasen et al. \(2018\)](#) pruning algorithm. The Poor man's SOA sets  $h_{bb} = h_{zz} = h_{bz} = 0$ .

### B.3.4 Spectral densities

In this section, we examine nonparametric sample periodograms of simulated data produced by the various solution methods. A summary of our discussion here is also presented in the main draft. The goal is to determine whether they yield different predictions about the relevance of

fluctuations at different frequencies for overall variability. Figure 2 shows periodograms of  $b$ ,  $c$  and  $nx$  for a multivariate spectrum from long time-series simulations with 4500 periods and a Bartlett window with the smoothing parameter set to 100.<sup>8</sup> The y-axis shows the population spectrum, the x-axis shows the frequency in years, and the vertical lines isolate the business cycle frequency. The panels on the left (right) are for the baseline (targeted) calibrations. As in the previous charts, the plots for the GLB solution are identical in both sets of plots, because the global solution has a single calibration. In addition, as with the time-series results, the spectral density functions are nearly identical for 2OA and RSS methods, because the local decision rules have similar  $h_b$  terms and the quadratic and interaction terms of the 2OA solutions are irrelevant.

All the periodograms are generally downward sloping because the equilibrium stochastic processes are similar to AR(1) processes. Hence, the contribution of lower frequencies to the variances of the variables exceeds that of business cycle and lower frequencies. The results show, however, that the local methods under the baseline calibration overestimate the contribution of low frequency movements to the total variance of all three series, which is consistent with their slower mean-reversion and higher values of  $\rho_b$  relative to the GLB solution. Moreover, while the contribution of fluctuations at the business cycle frequency or higher for the variability of  $b$  is slightly higher with the local solutions than in the GLB solution, for  $nx$  the local methods overestimate it and for  $c$  they underestimate it. In particular, the local methods underestimate significantly the fraction of consumption fluctuations explained by business cycle and higher frequencies and under-predict significantly the contribution of low frequencies.

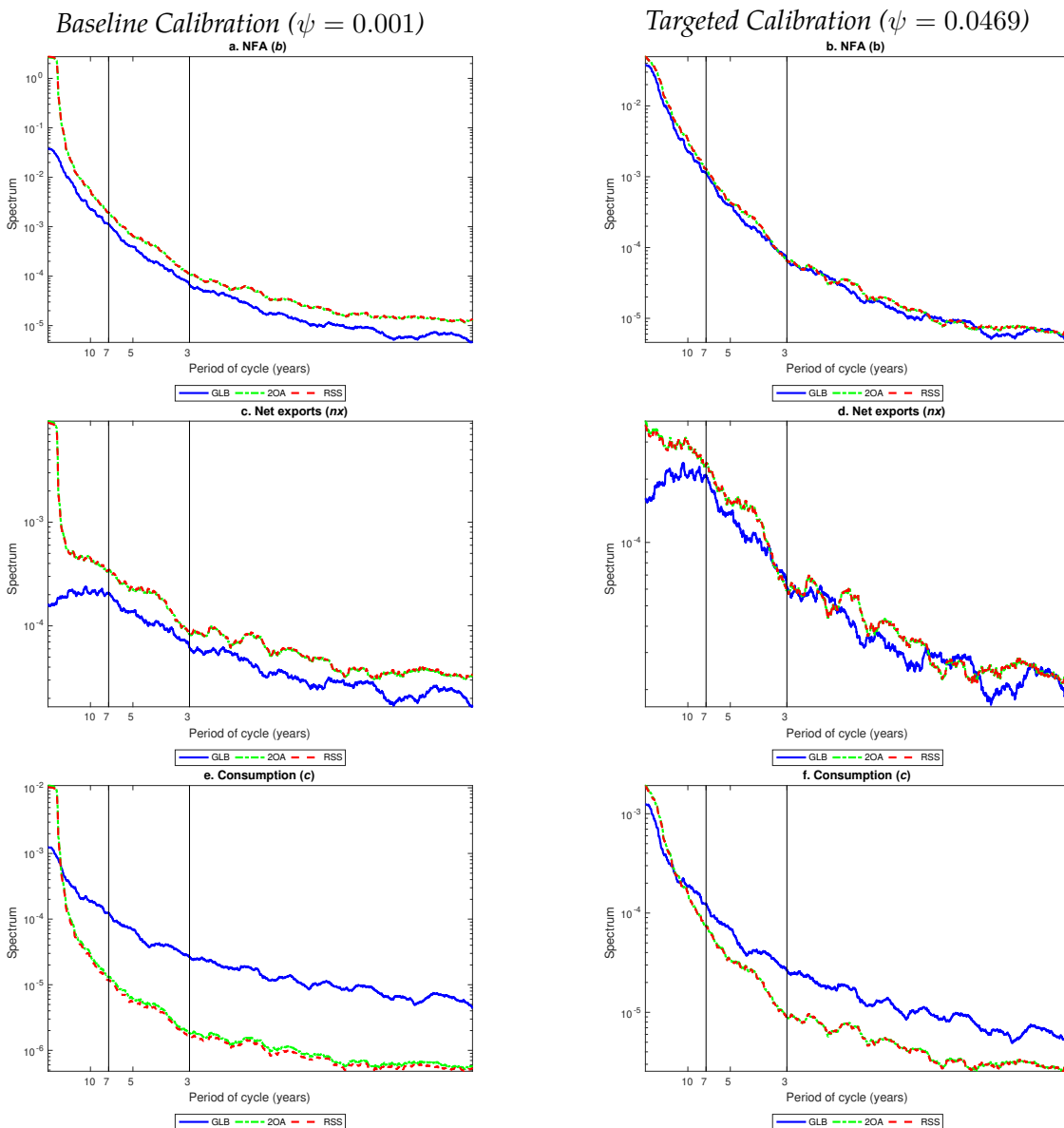
For targeted calibrations, the periodograms of  $b$  are nearly the same in the global and local solutions almost by construction, because the targeted calibrations are built to match the AR(1) coefficient of the GLB solution. However, the periodograms of  $c$  and  $nx$  for the local solutions still differ sharply from the GLB ones. They still underestimate significantly the contribution of consumption fluctuations at business cycle and higher frequencies to overall consumption variance.

The frequency analysis shows that the results of GLB and local methods differ at most frequencies, and not just in business cycle moments and long-run averages. For the endowment economy with the baseline calibrations, local methods overestimate significantly the contribution of low-frequency movements to the variability of NFA and net exports ( $nx$ ), in line with the result indicating that they overestimate the autocorrelation of NFA. The local methods also overestimate

---

<sup>8</sup>We follow Hamilton (1994) in setting the value of the smoothing parameter. The results for parametric estimates of the spectral densities are generally smoother but show similar patterns as those of the nonparametric estimates.

Figure 2: Spectral Density Functions in the Endowment Economy Model



Note: These graphs show parametric estimates of spectral density functions. GLB, 2OA and RSS denote the global, second-order and risky-steady state solution, respectively.

(underestimate) the contribution of low-frequency (high-frequency) movements to consumption fluctuations. The targeted calibrations perform better at approximating the spectral density of NFA and  $nx$ , but for consumption they still underestimate the contribution of high-frequency fluctuations by a large margin. Similar results are obtained for NFA,  $nx$  and consumption in the RBC model.

### B.3.5 Interest rate shocks

The analysis presented in Section 2.4 of the main draft featured additional results with interest rate shocks, which are based on joint endowment and interest rate shocks. This joint process is derived based on a Simple Persistence Markov chain estimation for the endowment and interest rate processes. Specifically, the Simple Persistence Markov chain is defined by a set of pairs of realizations  $(z, z^R)$  and a matrix  $\pi$  of transition probabilities of moving across pairs in one period. Each shock has two realizations equal to +/- one standard deviation of each shock ( $z_1 = -z_2 = 0.0327, z_1^R = -z_2^R = \sigma_{z^R}$ , with  $\sigma_{z^R}$  ranging from 0 to 2.5 percent). The Simple Persistence rule produces a  $\pi$  matrix with elements defined by a formula such that the standard deviations of the shocks match the realization values, and the correlation and autocorrelations of the shocks match their calibrated values. See the main draft for the results with the interest rate shocks.

### B.3.6 Alternative calibration of local solutions: Targeting mean vs. autocorrelation of NFA

In our analysis presented in the main draft, we argued that while calibrating the elasticity of the discount factor for the local solutions, targeting the autocorrelation of NFA gives the local solution the best chance to match the global solution. In this section, we explore an alternative calibration strategy, specifically, targeting the mean of NFA implied by the global solution. Table 3 summarizes how local solutions would behave based on this alternative calibration strategy (see second through fourth columns). For reference, we also report the moments for the global solution (first column) and the moments of the local solutions for the targeted calibration reported in the main draft.

For the local solution with DEIR, recalibration of discount factor ( $\psi$ ) to match the mean NFA of GLB yields  $\psi$  values of 0.002511 and 0.0005727 for 2OA and the partial RSS solutions, respectively. For the full RSS solution, we recalibrated the discount factor ( $\beta$ ), which yields 0.94413158 with  $\beta \cdot R$  nearing one (recall that the baseline value of  $\beta$  used for full RSS solution is 0.94, the same value used for GLB). For the local solutions with DEIR, targeting the mean implies higher order moments much more different than GLB, compared to targeting the autocorrelation of NFA. For instance, variability of NFA and variability of consumption relative to that of income are much higher with targeting the mean, relative to targeting the autocorrelation of NFA. Income correlations with consumption and net exports as well as autocorrelations get closer to the global solution by targeting the autocorrelation, relative to targeting the mean of NFA.

For the full RSS solution, although the mean NFA is now identical to the global solution, by

Table 3: Alternative Calibration for Local Methods: Targeting Mean vs. Autocorrelation of NFA

	GLB	Target mean of NFA			Target autocorr. of NFA	
		2OA	RSS		2OA	RSS
		DEIR	$\beta R < 1$	DEIR	DEIR	DEIR
$\beta$	0.94	0.944	0.94413158	0.944	0.944	0.944
$\psi$	n.a.	0.002511	n.a.	0.0005727	0.047	0.047
<i>Averages</i>						
$E(c)$	0.694	0.694	0.694	0.694	0.689	0.689
$E(nx/y)$	0.022	0.022	0.023	0.023	0.028	0.028
$E(b)$	-0.410	-0.410	-0.410	-0.410	-0.500	-0.506
<i>Variability relative to variability of income</i>						
$\sigma(c)/\sigma(y)$	0.995	1.186	17.987	2.049	1.001	0.997
$\sigma(nx)/\sigma(y)$	0.663	1.087	8.674	1.611	0.730	0.730
$\sigma(b)/\sigma(y)$	7.497	28.051	378.184	58.465	6.647	6.576
<i>Income correlations</i>						
$\rho(y, c)$	0.751	0.297	0.034	0.150	0.684	0.684
$\rho(y, nx/y)$	0.704	0.683	0.044	0.477	0.705	0.708
$\rho(y, b)$	0.266	0.190	0.009	0.094	0.489	0.488
<i>First-order autocorrelations</i>						
$\rho_c$	0.838	0.989	0.999	0.997	0.929	0.929
$\rho_{nx}$	0.536	0.737	0.999	0.876	0.583	0.582
$\rho_b$	0.977	0.997	0.999	0.999	0.977	0.977

Note: GLB refers to the global solution.  $\sigma(\cdot)$  denotes the coefficient of variation for  $c$  and  $b$ , and the standard deviation for  $nx$ .

construction, all of the higher order moments are significantly different with this alternative calibration relative to the baseline full RSS results shown in Table 3 of the main draft. Consumption, NFA and net exports behave get closer to unit-root, implying very low income correlations for these variables.

To sum up, we found that targeting the autocorrelation of NFA gives the local solutions with DEIR their best chance to match the behavior implied by the global solution. For the full RSS, targeting the mean of NFA requires increasing  $\beta$  so high that endogenous variables approach near-unit root.

### B.3.7 Alternative local solutions: 2OA vs. 3OA

In this section, we explore how third-order approximation (3OA) differ from 2OA. Table 4 summarizes the long-run moments for both 2OA and 3OA. As shown in the table, with the targeted calibration, moments from pruned third-order-approximation (3OA) solutions obtained using [Andreasen et al. \(2018\)](#) and 2OA solutions are the same up to the third decimal for most variables. With the baseline calibration, moments are also generally similar, with moments continuing to be identical up to the

third decimal for most variables and differing only slightly for variability ratios. But even for these variables, the differences between 2OA and 3OA are not economically meaningful.

Table 4: Alternative local solutions: 2OA vs. 3OA

	Baseline Calibration		Targeted Calibration	
	2OA	3OA	2OA	3OA
$\psi =$	0.001	0.001	0.0469	0.0469
<i>Averages</i>				
$E(c)$	0.702	0.702	0.689	0.689
$E(nx/y)$	0.015	0.015	0.028	0.028
$E(b/y)$	-0.286	-0.286	-0.502	-0.502
<i>Variability relative to variability of income</i>				
$\sigma(c)/\sigma(y)$	1.577	1.651	1.000	0.997
$\sigma(nx)/\sigma(y)$	1.335	1.379	0.730	0.730
$\sigma(b)/\sigma(y)$	63.033	66.854	6.648	6.641
<i>Income correlations</i>				
$\rho(y, c)$	0.200	0.190	0.684	0.684
$\rho(y, nx/y)$	0.568	0.557	0.705	0.706
$\rho(y, b)$	0.126	0.119	0.489	0.489
<i>First-order autocorrelations</i>				
$\rho_c$	0.995	0.995	0.929	0.929
$\rho_{nx}$	0.821	0.832	0.582	0.581
$\rho_b$	0.999	0.999	0.977	0.977

Note:  $\sigma(\cdot)$  denotes the coefficient of variation for  $c$  and  $b$ , and the standard deviation for  $nx$ .

### B.3.8 Comparison of DEIR vs. Endogenous Discounting

In this section, we examine the implications of endogenizing the discount factor as an alternative approach to induce stationarity in open-economy, incomplete-markets models. Although the most commonly used method in the literature is the use of DEIR function, as surveyed in Tables 1 and 2, the endogenous discount factor (ED) is also widely used. We compare below local (2OA) ED solutions with GLB solutions and 2OA solutions with DEIR for the same endowment economy model of Section 2 in the paper.

#### *Analytical comparison of DEIR and Endogenous Discounting (ED)*

Section 8.2 of [Schmitt-Grohé and Uribe \(2003\)](#) presents a simplified endowment economy closed with an endogenous discount factor without internalization (henceforth, ED) and finds that  $h_b = 1 - \theta c^*$ , where  $\theta$  and  $c^*$  are given by the functional form

$$\beta(c_t) = \frac{(1 + c_t - c^*)^{-\theta}}{1 + r}. \quad (61)$$

As with the DEIR model, we assume  $\rho_z = 0$ ,  $\sigma = 1$ , and  $1 = \beta(1 + r)$ . The IOA decision rule for the ED specification (with  $r \neq 0$  and  $c^* = 1$ ) is given by

$$h_b = h_z = 1 - \theta \quad \text{and} \quad g_b = g_z = \frac{r + \theta}{r + 1}, \quad (62)$$

and with  $r = 0$ ,  $g_b = g_z = \theta$ . Thus, the  $h_b$  coefficient of the DEIR and ED models are identical if  $r = 0$ ,  $c^* = 1$  and if

$$\frac{\theta}{2} = \frac{\psi}{\psi + \sqrt{\psi^2 + 4\psi}}. \quad (63)$$

Thus, while there is a mapping from  $\psi$  to  $\theta$  when matching  $h_b$ , the relationship is nonlinear.

It is not possible to solve a SOA of the UE model when  $r = 0$  because  $h_{\sigma\sigma}$  is undefined. Instead, solving with  $r > 0$ , the 2OA coefficients for the ED specification are given by

$$h_{bb} = h_{bz} = \frac{(\theta - 1)\theta(\theta + r)^2}{(r + 1)(r - (\theta - 2)\theta)}, \quad (64)$$

$$h_{zz} = \frac{(\theta - 1)^2(r^2 + 3\theta r + r + \theta(\theta + 2))}{(r + 1)(r - (\theta - 2)\theta)}, \quad (65)$$

$$h_{\sigma\sigma} = -\frac{(\theta + r)(-r^2 - 3\theta r + r + \theta((\theta - 4)\theta + 2))}{r(r + 1)(r - (\theta - 2)\theta)}. \quad (66)$$

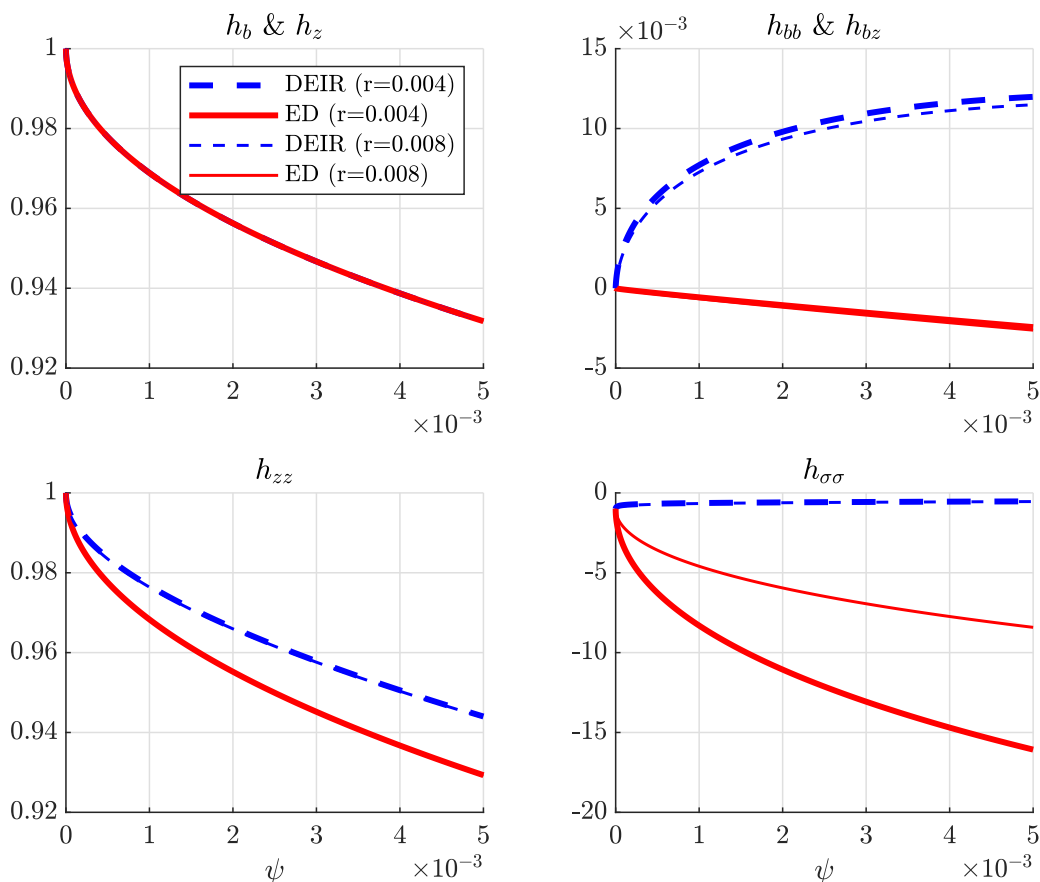
When  $r = 0$ , we have  $h_b = h_y = 1 - \theta$ ,  $g_b = g_y = \theta$ ,  $h_{bb} = h_{by} = -(1 - \theta)\theta^2/(2 - \theta)$ , and  $h_{yy} = (2 - 3\theta + \theta^3)/(2 - \theta)$  with  $h_{\sigma\sigma}$  undefined. When  $\theta = 0$ , then  $h_{bb} = h_{by} = 0$ ,  $h_{yy} = 1$  and  $h_{\sigma\sigma} = (r - 1)/(r + 1)$ .

Figure 3 shows the coefficients of the policy function for DEIR vs. ED under various calibrations. The x-axis varies  $\psi$  (and  $\theta$  for the ED model that it delivers the same  $h_b$ ). It shows that the DEIR decision rule at second-order has more non-linearity arising from  $h_{bb}$ , whereas the ED decision rule has a more significant shift term arising from  $h_{\sigma\sigma}$ . Moreover,  $h_{\sigma\sigma}$  is sensitive to small values of  $r$  for the ED decision rule. Figure 4 highlights the differences for the calibration of  $r = 0.005$  and  $\psi = 0.001$ . Notice is that the shift term ( $h_{\sigma\sigma}$ ) is very important for UE model, whereas the DEIR model has more curvature coming from  $h_{bb}$ .

### ***Comparison of DEIR and Endogenous Discounting (ED) with local and global solutions***

When ED is used, period utility of date  $t + 1$  is discounted by a factor  $\theta_{t+1}$  such that  $\theta_{t+1} =$

Figure 3: Coefficients of the SOA: DEIR vs. ED



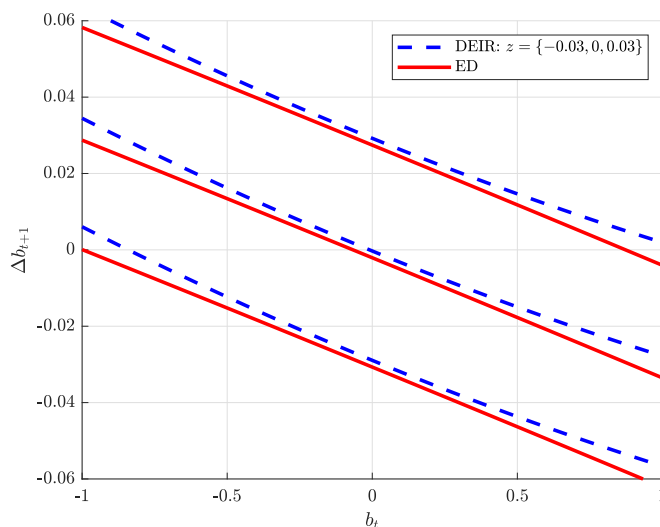
Note: The x-axis is always  $\psi$ . For the ED model,  $\theta$  has been chosen to match  $h_b$ . Under ED,  $h_{\sigma\sigma}$  is sensitive to  $r$  and is undefined ( $h_{\sigma\sigma} \rightarrow -\infty$ ) for  $r = 0$ .

$\beta(c_{t+1})\theta_t$  where:

$$\beta(c) = (1 + c)^{-\psi^{ED}},$$

and  $\psi^{ED}$  denotes the elasticity of the period discount factor with respect to consumption. Preferences with this endogenous discount factor are known as Uzawa-Epstein (UE) preferences. They feature a rate of time preference for date  $t$  that is an increasing function of the history of consumption up to date  $t$ , and an “impatience effect” by which agents take into account that increasing date- $t$  consumption reduces the discount factor that applies to all utility flows from date- $t$  forward. In closing the small open economy with ED for the local solutions, Schmitt-Grohe and Uribe (2003) proposed an alternative formulation in which the impatience effect is removed by assuming that  $\beta(\cdot)$  depends on “aggregate consumption” so that agents do not internalize the dependency of the discount factor on consumption. We denote this formulation as SGU-ED. With this assumption,

Figure 4: SOA decision rules: DEIR vs. ED



Note: For  $\sigma_z = 0.03$ ,  $r = 0.008$  and  $\psi = 0.001$  and a  $\theta$  that delivers the same  $h_b$ . Decision rules are plotted for  $z = \{-0.03, 0, 0.03\}$ . The close-to-linear decision rules are the ED specification whereas the convex decision rules are the DEIR specification.

the Euler Equation for NFA becomes:

$$u_c(c_t) = (1 + r)\beta(\tilde{c}_t)E_t[u_c(c_{t+1})],$$

where  $\tilde{c}_t$  denotes aggregate consumption, which household takes as given but equals  $c_t$  at equilibrium. Schmitt-Grohe and Uribe found that local solutions using UE or SGU-ED are nearly identical, but SGU-ED has a much simpler representation since it removes the impatience effect. Hence our choice to use SGU-ED for the analysis conducted here. The rest of the endowment model structure remains the same as described in the paper.

To explore how using SGU-ED affects long-run moments and precautionary savings we compare local solutions to two alternative variants of the GLB solution, one with  $\beta R < 1$  preferences and the other with Uzawa-Epstein (UE) preferences (the comparison of the GLB solutions under these two preferences was discussed in section B.3.9). The results are shown in Table 5. For the local solutions, we present 2OA results for the baseline DEIR case shown in the paper and for two cases of the SGU-ED setup: Case I, which is calibrated to match the same elasticity of the discount factor as in the GLB-UE calibration. In this case,  $\psi^{ED} = 0.109$  and the GLB-UE and 2OA-SGU-ED solutions have the same  $b^{dss} = -0.44$  by construction. Case II, in which the elasticity of the discount factor was set to match the deterministic steady state of NFA in the GLB- $\beta R < 1$  solution.

Table 5: Long-run Moments: Comparison of GLB vs SGU-ED in the Endowment Economy Model

	GLB		DEIR	2OA	
	$\beta R < 1$	UE		SGU-ED	
				UE calib	$\beta R < 1$ calib
<i>Averages</i>					
$E(c)$	0.694	0.694	0.701	0.694	0.690
$E(nx/y)$	0.023	0.022	0.015	0.023	0.027
$E(b/y)$	-0.413	-0.415	-0.285	-0.424	-0.496
<i>Variability relative to variability of income</i>					
$\sigma(c)/\sigma(y)$	0.991	0.958	1.594	0.972	0.977
$\sigma(nx)/\sigma(y)$	0.663	0.941	1.327	0.953	0.953
$\sigma(b)/\sigma(y)$	7.508	18.653	62.327	8.100	8.094
<i>Income correlations</i>					
$\rho(y, c)$	0.751	0.417	0.202	0.405	0.405
$\rho(y, nx/y)$	0.704	0.759	0.572	0.753	0.751
$\rho(y, b)$	0.267	0.268	0.128	0.259	0.259
<i>First-order autocorrelations</i>					
$\rho_c$	0.845	0.972	0.995	0.978	0.978
$\rho_{nx}$	0.545	0.662	0.819	0.673	0.672
$\rho_{nx/y}$	0.554	0.667	0.826	0.679	0.679
$\rho_b$	0.977	0.994	0.999	0.994	0.994

Note: GLB refers to the global solution, UE refers to the global solution with Uzawa-Epstein preferences, SGU-ED denotes local solution with endogenous discounting.  $\sigma(\cdot)$  denotes the coefficient of variation for variables in levels and the standard deviation for variables in ratios ( $nx/y$  and  $b/y$ ).

In this case,  $\psi^{ED} = 0.11$  and again the 2OA and GLB solutions have the same deterministic steady state by construction but now set at  $b^{dss} = -0.51$ .

It is important to note that the similarity of the two GLB solutions, particularly the first moments, is largely by construction and not a general result. It reflects the calibration strategy for the two solutions that we adopted from [Durdu et al. \(2009\)](#). They calibrated the GLB-UE solution by setting the elasticity of the discount factor so that the deterministic steady state,  $b^{dss}$ , matched the average NFA-GDP ratio ( $b/y$ ) in the Mexican data (-44%), while the calibration of the  $\beta R < 1$  solution was done by setting  $\beta$  so as to approximate the same -44% target but as the *average* of the stochastic model solution (at about -42%). The deterministic steady state was set at the debt limit ( $b^{dss} = \phi = -0.51$ ) so as to match the standard deviation of consumption in the Mexican data, jointly with the mean  $b/y$  at -44%. These two calibrations result in the mean NFA of the two GLB solutions being very similar (-0.413 with UE vs. -0.415 with  $\beta R < 1$ ). Still, they imply very different results for precautionary savings (namely, for the excess of mean NFA relative to  $b^{dss}$ ), which reaches 2.5% of GDP in the UE solution v. 9.7% in the  $\beta R < 1$  solution. Moreover, as Durdu et

al. showed, for given parameter values, the UE setup yields significantly smaller precautionary savings than the  $\beta R < 1$  model as the variability or persistence of the income shocks rises. In turn, as explained in Section 2.4 of the paper, precautionary savings incentives are weaker with ED because the marginal benefit of savings falls as  $\beta_t$  falls when agents borrow more.

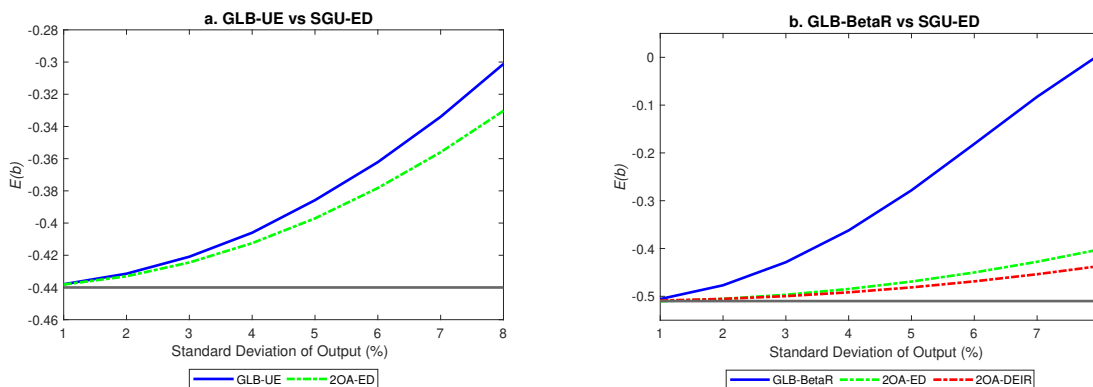
We move now to compare the 2OA ED solutions with their GLB counterparts and the baseline DEIR solution. In Case I, we find that the 2OA ED solution yields  $E(b/y)^{ED} = -42.4\%$ , which is very close to the GLB-UE solution. Hence, in this case, the GLB and 2OA solutions have identical deterministic steady states by construction and yield very similar mean NFA, and since mean NFA is also close to  $b^{dss}$  it follows that the 2OA-ED and GLB-UE solutions are similar because at the calibrated parameters (particularly the 2.6% standard deviation of income) precautionary savings are small in both solutions. Hence, since  $E(b/y)$  is close to  $b^{dss}$ , the local approximations ought to be accurate. This is akin to giving the 2OA ED solution the mean of NFA of the GLB-UE solution as center of approximation in a setting in which precautionary savings are negligible.

Case II, which calibrates the ED elasticity in the 2OA solution to match  $b^{dss}$  in the GLB- $\beta R < 1$  solution, also yields the result that precautionary savings are small in the local solution (the 2OA-ED solution yields  $E(b/y)^{ED} = -0.496$  compared with  $b^{dss} = -0.51$ ). Relative to the GLB- $\beta R < 1$  solution, however, the 2OA solution underestimates precautionary savings, because the GLB solution yields  $E(b/y)^{GLB} = -0.413$  while the local solution yields  $E(b/y)^{ED} = -0.496$  and both solutions have the same  $b^{dss}$ . Hence, the 2OA-ED solution underestimates precautionary savings by 8.3 percentage points. Thus, once precautionary savings become relevant, the local ED solutions display a similar shortcoming as the DEIR solutions in that they approximate poorly the stock of precautionary savings predicted by the GLB solutions.

To provide further evidence of the above finding, we show in Figure 5 how the mean NFA position changes as the variability of income increases in the calibrations of Cases I and II. Plot a. on the left shows results for the comparable GLB-UE and 2OA-ED solutions, and plot b. on the right does the same for the comparable GLB- $\beta R < 1$  and 2OA-ED solutions. In both plots, we include horizontal lines that correspond to the  $b^{dss}$  that is common to GLB and 2OA solutions in each case. These plots make it clear that the 2OA solutions are similar to the GLB solutions only when the variability of income is small enough for precautionary savings to be negligible. As income variability rises by enough to make precautionary savings relevant in the GLB solution (either UE or  $\beta R < 1$ ), the 2OA solutions always underestimate both the mean of NFA and precautionary savings. Moreover, we include in plot b. the solutions produced by the DEIR targeted calibration,

which is the same calibration as in the 2OA-ED solution in Case II (except it uses DEIR instead of ED to induce stationarity). The graph shows that the mean NFA predicted by both local solutions is similar, and both underestimate significantly the comparable GLB solution. This result suggests that  $\psi^{ED}$  (which is slightly higher in plot b. than in plot a.) plays a role analogous to the higher  $\psi$  of the targeted DEIR calibrations in that it acts to make deviations of NFA from steady state costly, and thus results in mean NFA staying close to that steady state as income variability rises.

Figure 5: Average NFA in the endowment economy as the variability and persistence of output rise



Note: GLB-BetaR refers to the global solution with  $\beta R < 1$  preferences, GLB-UE refers to the global solution with Uzawa-Epstein preferences, 2OA-ED denotes local solution with endogenous discounting, 2OA-DEIR denotes the local solution with DEIR preferences and the targeted calibration  $\psi$  value of 0.0469. The horizontal black lines show the respective deterministic steady state value of  $-0.44$  and  $-0.51$ .

Finally, we compare the 2OA ED solutions with the baseline DEIR solution. The first- and higher-order moments are very different. In particular, DEIR yields sharply higher mean NFA and it also overestimates significantly the mean of NFA and the stock of precautionary savings produced by the GLB solutions, as explained in the paper. Hence, from this perspective, and since the first moments of the local ED solutions are closer to the GLB ones, it would appear that adopting ED should be a preferable means to induce stationarity in local solutions, instead of DEIR. However, as explained earlier, this is not a general property but an implication of the negligible precautionary savings in the GLB-UE solution because of its baseline calibration combined with the calibration strategy we took from [Durdu et al. \(2009\)](#) that made the GLB-UE and GLB- $\beta R < 1$  solutions yield similar mean NFA. Moreover, using ED to induce stationarity also has the disadvantage that  $\psi^{ED}$  cannot be set independently of  $b^{dss}$ , whereas using DEIR  $\psi^{ED}$  is independent of  $b^{dss}$ . In terms of capturing precautionary savings effects of higher income volatility, however, both ED and DEIR

fail to yield solutions comparable to those of the GLB solutions.

### B.3.9 Comparison of global solutions

In this section, we compare alternative global solutions of the endowment economy model. We first compare the *FiPIt* solution v. the solution produced by a standard Value Function Iteration (VFI) algorithm using identical calibrations.

The first three data columns of Table 6 show the comparable long-run moments of NFA, consumption and net exports for the two alternative variations of *FiPIt*, and VFI solutions. The bonds grid has 1,000 nodes in the VFI solution v. 200 in the *FiPIt* solution. The latter requires fewer nodes because it uses interpolation of the decision rules to solve the bonds Euler equation. The income process has 5 nodes in *FiPIt*-5 point column and VFI solution (see Section 2.4 of the paper for full details about the endowment model calibration). We also report *FiPIt* solution with income process approximated using 11 nodes. As the Table shows, two alternative versions of *FiPIt* solutions as well as VFI method produce nearly identical moments. These results provide further evidence of the accuracy of the *FiPIt* method, in addition to the evidence we provided in the paper based on Euler equation errors for the endowment, RBC and Sudden Stops models.

We next examine the sensitivity of our baseline results to the use of 5-point Markov Chain in the estimation of the endowment shocks using Tauchen and Hussey algorithm. To this end in figure 6 we report the implied average NFA for changes in variability of income shock when the income shock is approximated by 5-point Markov Chain vs. 11-point Markov Chain. The results show that increasing the number of nodes in the Markov Chain from five to 11 has virtually no effect on the implied average NFA.

### B.3.10 Linear with occasionally binding constraint method: DynareOBC

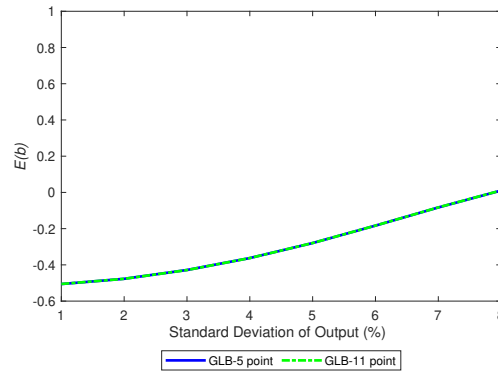
In this section, we provide details on the DynareOBC approach applied to the endowment economy model with an occasionally binding constraint (the ad-hoc debt limit) that we considered in the main draft and also presented in Section B. We consider alternative parameterizations in which the constraint in the reference regime (i.e., at the deterministic steady-state) is binding or not. We use this example to illustrate how DynareOBC constructs solutions using perfect foresight paths along a time-series simulation. This example demonstrates that unconditional mean values for endogenous variables differ from the deterministic steady state even with a first-order approximation and without the presence of precautionary savings.

Table 6: Long-run Moments: Endowment Economy Model

	GLB		
	$\beta R < 1$		
	FiPIt-5 point	FiPIt-11 point	VFI
<i>Averages</i>			
$E(c)$	0.694	0.694	0.694
$E(nx/y)$	0.023	0.023	0.022
$E(b/y)$	-0.413	-0.414	-0.411
<i>Variability relative to variability of income</i>			
$\sigma(c)/\sigma(y)$	0.991	0.991	0.991
$\sigma(nx)/\sigma(y)$	0.663	0.664	0.660
$\sigma(b)/\sigma(y)$	7.508	7.522	7.456
<i>Income correlations</i>			
$\rho(y, c)$	0.751	0.751	0.755
$\rho(y, nx/y)$	0.704	0.704	0.704
$\rho(y, b)$	0.267	0.267	0.268
<i>First-order autocorrelations</i>			
$\rho_c$	0.845	0.844	0.840
$\rho_{nx}$	0.545	0.545	0.543
$\rho_{nx/y}$	0.554	0.554	0.551
$\rho_b$	0.977	0.977	0.977

Note: GLB refers to the global solution.  $\sigma(\cdot)$  denotes the coefficient of variation for variables in levels and the standard deviation for variables in ratios ( $nx/y$  and  $b/y$ ). FiPIt-5 point reports the results of FiPIt solution, which uses a 5-point Markov Chain, and the next column with FiPIt-11 point uses 11-point Markov Chain.

Figure 6: Average NFA in the endowment economy: 5-point vs. 11-point Markov Chains



Note: This figure compares the implied average NFA endowment shock approximated with 5-point vs. 11-point Markov Chains. The figure shows that the results are identical with two specifications.

For tractability, we rewrite the model here. Assume that the problem of the representative agent

is given by

$$\max_{c_t} \sum_{t=0}^{\infty} \frac{c_t^{1-\sigma}}{1-\sigma} \quad \text{s.t.} \quad c_t + q_t b_{t+1} = e^{z_t} + b_t, \quad b_{t+1} \geq \varphi, \quad (67)$$

where  $b_{t+1}$  is bonds,  $\varphi$  is the ad-hoc debt limit, and the endowment process is  $z_{t+1} = \rho z_t + \sigma_z \varepsilon_{t+1}$ . Denote the Lagrange multiplier on the constraint by  $q_t c_t^{-\sigma} \lambda_t$ . The FOC is given by

$$1 - \lambda_t = \beta \mathbb{E}_t \left( \frac{c_{t+1}}{c_t} \right)^{-\gamma} r_t, \quad (68)$$

where

$$r_t = 1/q_t = 1/\beta + \psi \left( e^{b^* - b_{t+1}} - 1 \right). \quad (69)$$

$b^*$  denotes the bond value in the DEIR specification. Typically, this value is set to the deterministic steady state that the model calibration targets. In this example, however, the deterministic steady state  $b^{\text{dss}}$  would be equal to the greater of  $b^*$  and ad-hoc debt limit  $\varphi$ . Put differently, the steady state (or the reference regime) is unconstrained if  $b^* > \varphi$  and constrained if  $b^* \leq \varphi$ .

- Unconstrained SS:  $b = b^*, r = 1/\beta, c = 1 + (1 - 1/r)b^*, \lambda = 0$ .
- Constrained SS:  $b = \varphi, r = 1/\beta + \psi \left( e^{b^* - \varphi} - 1 \right) < 1/\beta, c = 1 + (1 - 1/r)\varphi, \lambda = 1 - \beta r > 0$ .

In DynareOBC the equilibrium conditions are written as follows for Regime 1:

$$1 - \lambda_t = \beta \mathbb{E}_t \left( \frac{c_{t+1}}{c_t} \right)^{-\gamma} r_t, \quad (70)$$

$$c_t + q_t b_{t+1} = e^{z_t} + b_t, \quad (71)$$

$$r_t = 1/q_t = 1/\beta + \psi \left( e^{b^* - b_{t+1}} - 1 \right), \quad (72)$$

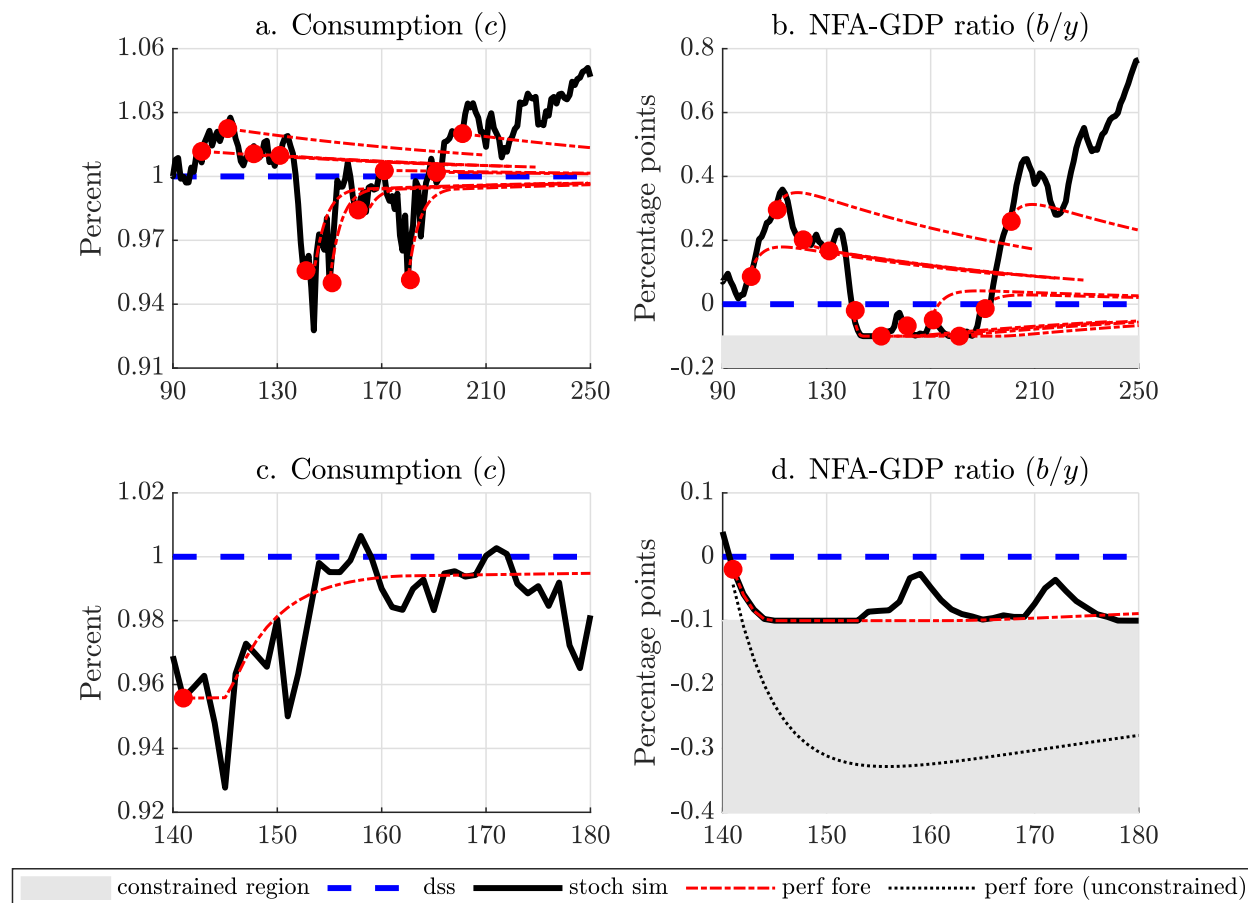
$$0 = \max \left( \varphi, b^* - \log \left( \frac{1}{\psi \beta} \left( \frac{c_{t+1}}{c_t} \right)^{\sigma} + 1 \right) \right). \quad (73)$$

For illustration, Figure 7 displays a stochastic simulation of the model.<sup>9</sup> The black line plots the realized path for consumption and bonds, respectively. At each date, for a given state vector,  $x_t$ , DynareOBC solves for a perfect foresight path, presented by the red-dash lines. These represent the equilibrium paths for the economy at each point in time conditional on no future shocks such that

<sup>9</sup>Note that  $\varphi$  is set to  $-0.1$  in this example, hence the constraint is nonbinding in the deterministic steady state.

the economy converges back to the deterministic steady-state in  $T$  periods. The red-dashed line starting, for example, in period  $t$  is used to generate the realized economic outcome in period  $t + 1$ . For the purposes of the stochastic simulation, the rest of that perfect foresight path is discarded. In  $t + 1$  the economy is hit by a news shock and the state vector is given by  $x_{t+1}$ . DynareOBC then generates a new perfect foresight path, and so on. The bottom row of Figure 7 focuses on a

Figure 7: Perfect foresight paths for DynareOBC

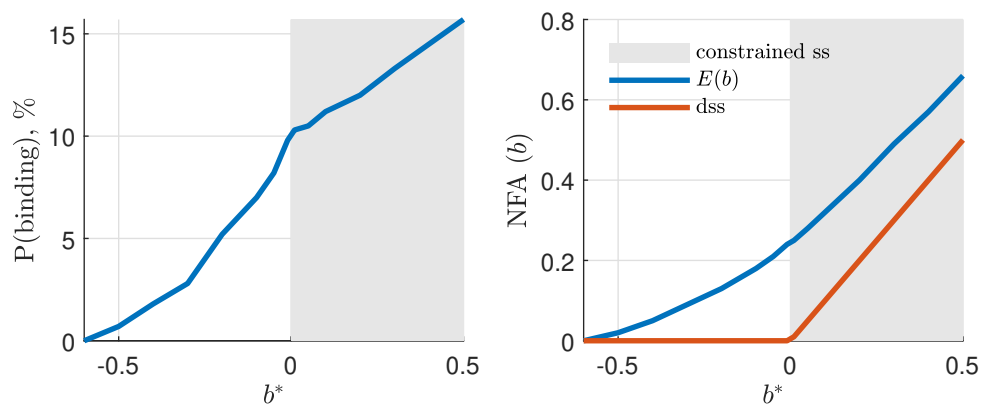


single perfect foresight path from period 141 in the stochastic simulation. In solving for this perfect foresight path, the algorithm needs to determine the periods in which the constraint is binding. This problem is not trivial. The naive (unconstrained) perfect foresight path given by the black-dashed line suggests that the constraint might bind immediately and continue to bind past period 180. In fact, the equilibrium perfect foresight path with the constraint is one in which the constraint is expected to start binding in period 144 (3 periods after the shock) and remain so until only period 163. Of course, subsequent shocks meant that the constraint became unbinding even earlier in

period 153. The implication of this analysis is that when the NFA process is highly persistent, the method requires long extended perfect foresight paths (i.e.,  $T$  needs to be sufficiently high) to find a solution. Additionally, the number of time periods used for the simulations also need to be sufficiently long to achieve convergence of long-run moments.<sup>10</sup>

We next illustrate how alternative values for the ad-hoc debt limit, in relation to the  $b^*$  value in the DEIR specification, affects the deterministic steady state and long-run value of NFA. Figure 8 shows the results. Some useful insights can be derived from this figure that can guide intuition for our results in the main draft. The reference regime is constrained (unconstrained) when  $\varphi$  is higher (lower) than the  $b^*$  value of 0. Regardless of whether the reference regime is constrained or unconstrained the unconditional mean of NFA is always higher than the deterministic steady state value of NFA as long as the constraint binds with a positive probability. This implied higher value of NFA is mainly due to the model's asymmetric (or nonlinear) response to shocks in the presence of an occasionally binding constraint. A shock that causes the constraint to bind causes households to lower bond holdings slower than an increase the same shock with an opposite sign would lead to. As a result, the realized upward movements in bonds is greater than the downward movements, causing the economy to endogenously move away from the constraint. This move away from the constraint would be realized even without a precautionary savings incentive.

Figure 8: Comparative statics



The shaded area illustrates the constrained region. As the constraint becomes tighter the prob-

<sup>10</sup>For the solution of the Sudden Stops model, we set the `TimeToEscapeBounds` option equal to 60. That is, the algorithm searches for a path for the endogenous variables for which the economy returns back to the reference regime within 60 quarters from the current period. This is necessary because, with near-unit root debt dynamics, it can take a long period of time for the economy to revert back to the reference regime.

ability of the constraint being binding increases monotonically as shown in the left panel. When the  $\varphi$  is less than 0, the deterministic steady state value of NFA (shown in orange) equals  $b^*$ . When  $\varphi$  is higher than 0, the deterministic steady state value of NFA equals  $\varphi$ . The unconditional mean of NFA increases with  $\varphi$  and it is always higher than the deterministic steady state of NFA as long as the probability of the constraint being binding is non-zero.

### B.3.11 Analytical solution under savings-under-uncertainty framework

The models we considered for the endowment model both in the main draft and in the appendix do not feature analytical solutions under CRRA preferences. So, it is not possible to assess how GLB solution compares to an analytical or true solution, although our premise is that GLB is nearly identical to the true solution. To understand this issue better, we analyze how global and local solutions compare to the true solution using [Levhari and Srinivasan \(1969\)](#) savings-under-uncertainty framework, which features an analytical solution. We start with describing the model.

At each period  $t$ , a household either consumes his entire wealth  $b_t$  or invests part of it using a risky asset. Denoting consumption as  $c_t$ , investment will then be  $b_t - c_t$ . The random return on investment from the risky asset is given by an exogenous interest rate  $R_t$ . The objective of the household then is to maximize

$$E \left[ \sum_{t=0}^{\infty} \beta^t \frac{c_t^{1-\sigma}}{1-\sigma} \right] \quad \text{s.t.} \quad (74)$$

$$b_{t+1} = (b_t - c_t)R_{t+1}, \quad (75)$$

where  $b_0$  is given and  $b_t \geq c_t \geq 0$ . The optimality conditions for this model is given as

$$c_t^{-\sigma} = \beta \mathbb{E}_t (c_{t+1}^{-\sigma} R_{t+1}), \quad (76)$$

$$b_{t+1} = (b_t - c_t) R_{t+1}, \quad (77)$$

where  $\log(R_{t+1}) = \mu + \sigma_\varepsilon \varepsilon_{t+1}$ ,  $\varepsilon_{t+1} \sim (0, 1)$ . This model is different from the other models we considered in the main draft in that the true solution is a random walk, hence long-run averages for variables in levels (consumption or investment) are not well-defined. However, we can solve this model by detrending. In particular, we can normalize the variables by  $b_t$  to give

$$x_t^{-\sigma} = \beta \mathbb{E}_t (x_{t+1}^{-\sigma} g_{t+1}^{-\sigma} R_{t+1}), \quad (78)$$

$$g_{t+1} = (1 - x_t) R_{t+1}, \quad (79)$$

where  $x_t \equiv c_t/b_t$  and  $g_t = b_t/b_{t-1}$ . Substituting the constraint into the Euler equation gives

$$x_t^{-\sigma} = \beta \mathbb{E}_t (x_{t+1}^{-\sigma} (1 - x_t)^{-\sigma} R_{t+1}^{1-\sigma}). \quad (80)$$

The model contains neither endogenous nor exogenous state variables. Thus, the decision rule is a constant:  $x_t = \lambda$ , and the exact analytical solution is given by

$$\lambda^{EXA} = 1 - \beta^{1/\sigma} \exp\left(\frac{1-\sigma}{\sigma} \mu\right) \exp\left(\frac{(1-\sigma)^2 \sigma_\varepsilon^2}{2}\right). \quad (81)$$

For the solution of the model, note that variance matters but persistence does not, and as we mentioned above, there is no long-run average of the model in levels. The ones in detrended form are well defined. Now we discuss how we can derive the global and local approximations for this model.

**Global solution** The global solution to this problem can easily be derived by implementing FiPIt for the Euler Equation (80). The solution will start with a guess of  $x_j$  in iteration  $j$  to be plugged in to the right hand side of the Euler equation to derive an updated guess of  $x_{j+1}$ . If  $\|x_{j+1} - x_j\| < \epsilon$  then the solution is achieved, otherwise we update our guess with  $x_{j+1}$  and iterate to convergence. We found that for all parameterizations, the GLB solution converges to the exact analytical solution.

**First-order approximation and risk-adjusted steady state solution** To derive the first-order approximation (1OA) and RSS solution we follow the following steps.

Step 1: Substitute the decision rule into the equilibrium condition to give

$$F(\sigma_\varepsilon) \equiv \beta \mathbb{E}_t (\exp((1-\sigma)(\mu + \sigma_\varepsilon \varepsilon_{t+1}))) - (1-\lambda)^\sigma = 0. \quad (82)$$

Step 2: For RSS, take a second-order approximation with respect to  $\sigma_\varepsilon$  to give

$$0 = F(0) + \frac{\sigma_\varepsilon^2}{2} F''(0), \quad (83)$$

$$= \beta \exp((1-\sigma)\mu) \left(1 + (1-\sigma)^2 \frac{\sigma_\varepsilon^2}{2}\right) - (1-\lambda)^\sigma. \quad (84)$$

Rearranging gives the following 1OA and analytical RSS solution:

$$\lambda^{1OA} = 1 - \beta^{1/\sigma} \exp\left(\frac{1-\sigma}{\sigma}\mu\right), \quad (85)$$

$$\lambda^{RSS} = 1 - \beta^{1/\sigma} \exp\left(\frac{1-\sigma}{\sigma}\mu\right) \left(1 + (1-\sigma)^2 \frac{\sigma_\varepsilon^2}{2}\right)^{1/\sigma}. \quad (86)$$

**Higher-order perturbation approximation** Define the decision rule as  $x_t = f(\sigma_\varepsilon)$ . The second-order approximation (2OA) around the deterministic steady state is given by  $\lambda^{2OA} = f(0) + f''(0) \frac{\sigma_\varepsilon^2}{2}$  (since odd-derivatives are generically zero). The methodology proceeds as follows:

Step 1: Substitute the decision rule into the equilibrium condition to give

$$F(\sigma_\varepsilon) \equiv \beta \mathbb{E}_t \exp((1-\sigma)(\mu + \sigma_\varepsilon \varepsilon)) - (1 - f(\sigma_\varepsilon))^\sigma = 0, \quad (87)$$

Step 2:  $F(0) = 0$  gives

$$\beta \exp((1-\sigma)\mu) - (1 - f(0))^\sigma = 0, \quad (88)$$

$$f(0) = 1 - \beta^{1/\sigma} \exp\left(\frac{1-\sigma}{\sigma}\mu\right) \quad (89)$$

Step 3:  $F''(0) = 0$  gives

$$0 = (1-\sigma)^2 + \sigma(1-f(0))^{-1} f''(0), \quad (90)$$

$$f''(0) = -\frac{(1-\sigma)^2}{\sigma} (1-f(0)). \quad (91)$$

Combining these results gives

$$\lambda^{2OA} = 1 - \beta^{1/\sigma} \exp\left(\frac{1-\sigma}{\sigma}\mu\right) \left(1 + \frac{(1-\sigma)^2 \sigma_\varepsilon^2}{2}\right). \quad (92)$$

In fact, perturbation methods produce a Taylor expansion of the exact decision rule. Thus, the 4OA is given by

$$\lambda^{4OA} = 1 - \beta^{1/\sigma} \exp\left(\frac{1-\sigma}{\sigma}\mu\right) \left(1 + \theta \sigma_\varepsilon^2 + \frac{\theta^2}{2} \sigma_\varepsilon^4\right), \quad (93)$$

where  $\theta \equiv (1-\sigma)^2 / (2\sigma)$ .

To illustrate how local solutions differ from the analytical (or GLB) solution, we plot the savings rate implied by each solution as we vary the variance parameter  $\sigma_\varepsilon$  (see panel (a) in Figure 9).<sup>11</sup> We also plot the ratio of the savings rate implied by the GLB solution to each of the local solution (see pane (b)). In the graphs, the vertical black line corresponds to the level of  $\sigma_\varepsilon$  above which the implied GLB savings rate becomes infeasible. This is the point at which the GLB savings rate crosses the horizontal red line in panel (a). At this level of  $\sigma_\varepsilon$  implied savings rate reaches 1, hence consumption equals 0. Further increases in  $\sigma_\varepsilon$  would imply negative consumption. As can be seen from both panels, 1OA, 2OA or RSS solutions all imply significantly different savings rate relative to the GLB solution for a wide range of  $\sigma_\varepsilon$  values. 4OA solution is quite close to the GLB solution for virtually all  $\sigma_\varepsilon$  values.

To further illustrate the discrepancy implied by local solutions relative to the GLB, we next plot the simulated series for the logarithm of bond decisions and logarithm of consumption for  $\sigma_\varepsilon$  value set to 0.4601. With this parameterization, the implied savings rate for each solution is as follows: GLB=0.99577, 1OA=0.70314, RSS=0.86118, 2OA=0.94825, and 4OA=0.99045. Figure 10 show the bond decisions on the left and consumption on the right.<sup>12</sup> Rearranging the budget constraint and using the optimality decision rule for consumption, we can show that the bond decision behaves as a random walk with drift

$$\log(b_{t+1}) = \log(1 - \lambda) + \log(b_t) + \log(R_t). \quad (94)$$

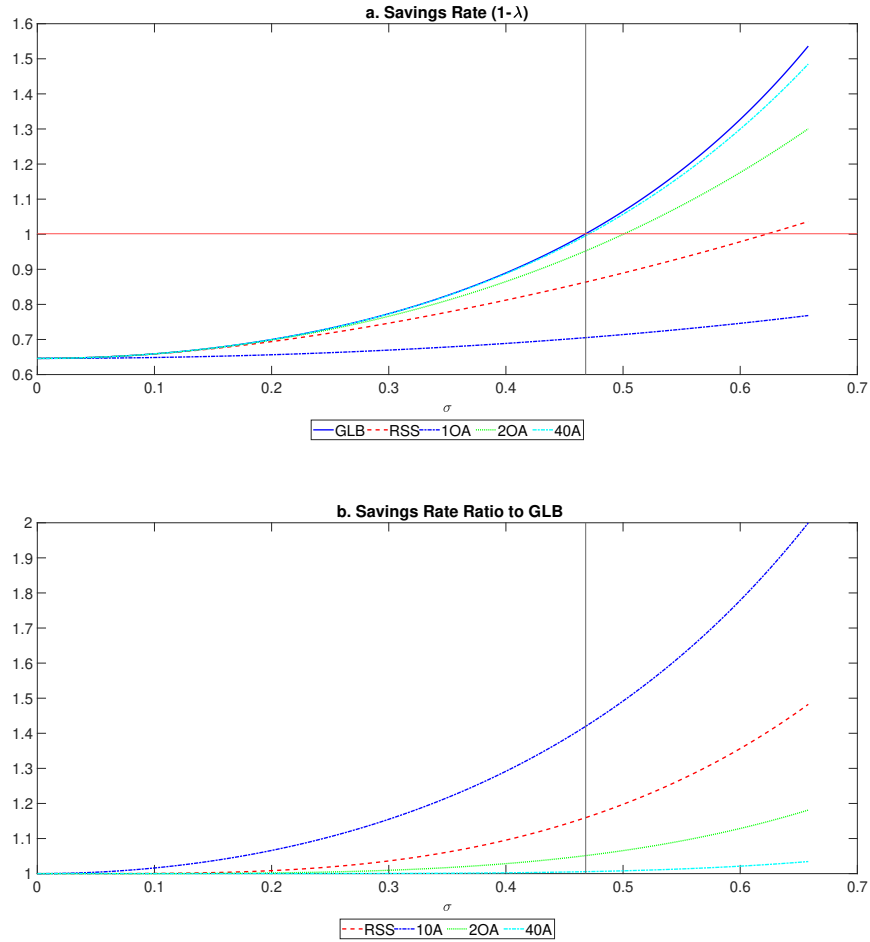
With the exception of 4OA, the drift component ( $\log(1 - \lambda)$ ) yields large differences for local solutions relative to the GLB.

The analysis in this section shows that GLB is identical to the true analytical solution, but all the local solutions with the exception of 4OA imply large differences relative to the analytical solution. However, the accuracy of 4OA we see for this model does not extend to the models in the main draft, because in those models, the center of approximation is not known with local approximations, hence they need to be induced by imposing DEIR.

<sup>11</sup>We set the other parameters as follows.  $\beta$  is 0.94, mean interest rate is 1.7. As we increase  $\sigma_\varepsilon$ , we recompute  $\mu = 1.7 - \sigma_\varepsilon^2/2$ , so that we implement a mean preserving spread increase in interest rate.

<sup>12</sup>For each simulation, the time interval is annual and we start with the same initial conditions and burn the first 200 years.

Figure 9: Implied savings rate



Note: These graphs show the implied savings rate  $1 - \lambda$  in panel a and the ratio of the GLB savings rate to the local solution savings rate in panel b. The vertical line in each chart shows the level of  $\sigma_\varepsilon$  above which the savings rate becomes infeasible for the analytical solution. This point is reached when the GLB line crosses the red horizontal line in panel a.

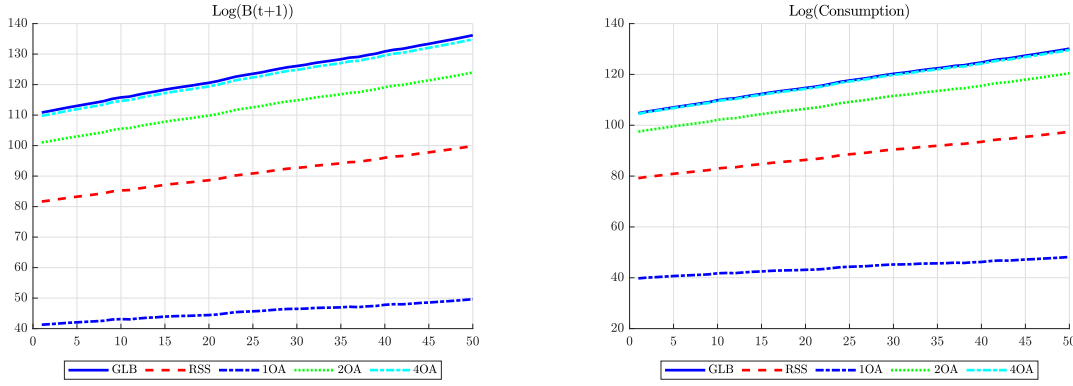
## C The RBC and Sudden Stops models

This section presents a complete description of the Sudden Stops model used for local solutions. The RBC model has the same set of optimality conditions but shuts down the occasionally binding borrowing constraint. The equations are written consistent with using a Dynare compatible toolbox. There are 26 variables

$$b_{t+1}, ca_t, c_t, g_t, i_t, l_t, \lambda_t, r_t^k, R_t, tb_{t+1}, \nu_t, w_t, y_t^{gdp}, y_t, s_t, q_t, k_{t+1}, b_{t+1}$$

$$\varepsilon_t^A, \varepsilon_t^P, \varepsilon_t^r, \mu_t, eb_{t+1}, x_{1,t}, x_{2,t}, lev_t,$$

Figure 10: Time-series simulation of bond decisions and consumption



Note: This figure shows the simulated series of bond decisions and consumption in log terms for all solution methods.

and 26 equations, (95)—(119), given below. Equation (95) is the occasionally binding constraint, written using a max operator. The first term inside the max operator shows the value of capital consistent with the borrowing constraint binding. The second term shows the optimal value of capital derived from the capital Euler equation (equation 98) and the capital demand equation (equation 103) when the Lagrange multiplier on the borrowing constraint,  $\mu_t = 0$ .

Borrowing constraint:

$$k_{t+1} = \max \left( \frac{\phi R_t (w_t l_t + e^{\varepsilon_t^P} p \nu_t) - \frac{b_{t+1}}{R_t}}{\kappa q_t}, \left( \frac{x_{2,t}}{x_{1,t}} \right)^{\frac{1}{\alpha-1}} \right) \quad (95)$$

Aggregate resource constraint:

$$c_t + i_t + g_t = b_t - b_{t+1}/R_t + y_t - e^{\varepsilon_t^P} p \nu_t - (R_t - 1) \phi (w_t l_t + e^{\varepsilon_t^P} p \nu_t) \quad (96)$$

Bond Euler equation:

$$1 = \beta R_t \mathbb{E}_t \lambda_{t+1} / \lambda_t + \mu_t / \lambda_t \quad (97)$$

Capital Euler equation:

$$1 + a \left( \frac{k_t - k_{t-1}}{k_{t-1}} \right) = \beta \mathbb{E}_t \frac{\lambda_{t+1}}{\lambda_t} \left( r_{t+1}^k + 1 - \delta + a \left( \frac{k_{t+1} - k_t}{k_t} \right) + \frac{a}{2} \left( \frac{k_{t+1} - k_t}{k_t} \right)^2 \right) + \frac{\mu_t}{\lambda_t} \kappa q_t \quad (98)$$

Marginal utility of consumption and labour supply:

$$\lambda_t (1 + g) = \left( c_t - \theta \frac{l_t^\omega}{\omega} \right)^{-\gamma}, \quad (99)$$

$$\lambda_t w_t = \theta l_t^{\omega-1} (c_t - \theta l_t^\omega / \omega) \quad (100)$$

Capital accumulation:

$$i_t = \delta k_{t-1} + (k_{t+1} - k_t) \left( 1 + \frac{a}{2} \left( \frac{k_{t+1} - k_t}{k_t} \right) \right) \quad (101)$$

Labour demand:

$$w_t = \eta A e^{\varepsilon_t^A} k_t^\alpha l_t^{\eta-1} \nu_t^{1-\alpha-\eta} - (R_t - 1) \phi w_t - R_t \phi w_t \mu_t / \lambda_t \quad (102)$$

Capital demand:

$$r_t^k = \alpha A e^{\varepsilon_t^A} k_t^{\alpha-1} l_t^\eta \nu_t^{1-\alpha-\eta} \quad (103)$$

Intermediate input demand:

$$e^{\varepsilon_t^P} p = (1 - \alpha - \eta) A e^{\varepsilon_t^A} k_t^\alpha l_t^\eta \nu_t^{-\alpha-\eta} - (R_t - 1) \phi e^{\varepsilon_t^P} p - R_t \phi e^{\varepsilon_t^P} p \mu_t / \lambda_t \quad (104)$$

Debt-elastic interest rate:

$$R_t = e^{\varepsilon_t^R} (1 + r) + \psi \left( e^{\left( \frac{b^*}{y g d p} - \frac{b_{t+1}}{y g d p} \right)} - 1 \right) \quad (105)$$

Auxiliary equations:

$$x_{1,t} = \beta \mathbb{E}_t \frac{\lambda_{t+1}}{\lambda_t} \alpha A e^{\varepsilon_t^A} l_{t+1}^\eta \nu_{t+1}^{1-\alpha-\eta}, \quad (106)$$

$$x_{2,t} = 1 + a \left( \frac{k_t - k_{t-1}}{k_t} \right) - \beta \mathbb{E}_t \frac{\lambda_{t+1}}{\lambda_t} \left( 1 - \delta + a \left( \frac{k_{t+1} - k_t}{k_t} \right) + \frac{a}{2} \left( \frac{k_{t+1} - k_t}{k_t} \right)^2 \right) \quad (107)$$

Excess borrowing:

$$e b_t = b_{t+1} / R_t - R_t \phi \left( w_t l_t + e^{\varepsilon_t^P} p \nu_t \right) + \kappa q_t k_{t+1} \quad (108)$$

Current account, net exports and domestic savings:

$$ca_t = -b_{t+1} + b_t, \quad (109)$$

$$nx_t = y_t - e^{\varepsilon_t^P} p\nu_t - c_t - i_t - g_t, \quad (110)$$

$$s_t = (-b_t + b_{t+1}) + i_t \quad (111)$$

GDP and production function:

$$y_t^{gdp} = y_t - e^{\varepsilon_t^P} p\nu_t \quad (112)$$

$$y_t = Ae^{\varepsilon_t^A} k_t^\alpha l_t^\eta \nu_t^{1-\alpha-\eta} \quad (113)$$

Price of capital and government spending:

$$q_t = 1 + a \left( \frac{k_t - k_{t-1}}{k_{t-1}} \right), \quad (114)$$

$$g_t = g \times c_t \quad (115)$$

Leverage:

$$lev_t = \frac{\frac{b_{t+1}}{R_t} - R_t \phi (w_t l_t + e^{\varepsilon_t^P} p\nu_t)}{q_t k_{t+1}} \quad (116)$$

Shocks:

$$\varepsilon_t^A = \rho_a \varepsilon_{t-1}^A + \sigma_a \varepsilon_t^1 + \sigma_{ar} \varepsilon_t^3 \quad (117)$$

$$\varepsilon_t^P = \rho_p \varepsilon_{t-1}^P + \sigma_p \varepsilon_t^2 \quad (118)$$

$$\varepsilon_t^r = \rho_r \varepsilon_{t-1}^r + \sigma_{ar} \varepsilon_t^1 + \sigma_r \varepsilon_t^3, \quad (119)$$

where  $(\varepsilon_t^1, \varepsilon_t^2, \varepsilon_t^3)$  are mean zero i.i.d. random variables with variance-covariance matrix  $I_3$ .

## C.1 *FiPit* Global Solution Method

This section provides a short description of the fixed-point iteration method we used to solve the RBC and Sudden Stops models. This method is developed by [Mendoza and Villalvazo \(2020\)](#) (see article for full details, a users guide and Matlab codes). *FiPit* has two major advantages over other

global methods that are used for solving models with more than one endogenous state variable: It solves Euler equations without requiring a non-linear solver (unlike standard time iteration methods that need to solve them as a non-linear system) and it uses simple multi-linear interpolation (unlike the endogenous grids method that needs interpolation techniques for irregular grids such as Delaunay interpolation). We summarize the algorithm focusing on the Sudden Stops model. The RBC algorithm is the same but with the  $\kappa$  parameter set high enough so that the collateral constraint never binds (in which case the algorithm never enters step 5 in the description provided below).

The *FiPlt* method is in the class of “Euler equation” methods that solve for recursive equilibria using a model’s optimality conditions in recursive form. For the RBC and SS models we solved, the state space consists of two endogenous states,  $[b, k]$ , and three exogenous states  $\varepsilon = [\varepsilon^A, \varepsilon^R, \varepsilon^P]$ .<sup>13</sup> The optimality conditions in recursive form are the following:

$$\left( c(b, k, \varepsilon) - \frac{L(b, k, \varepsilon)}{\omega} \right)^{-\sigma} = \lambda(b, k, \varepsilon)(1 + \tau) \quad (120)$$

$$\alpha A k^\gamma L(b, k, \varepsilon)^{\alpha-1} v(b, k, \varepsilon)^\eta = w(b, k, \varepsilon) \left( 1 + \phi(R - 1) + \frac{\mu(b, k, \varepsilon)}{\lambda(b, k, \varepsilon)} \phi R \right) \quad (121)$$

$$\alpha A k^\gamma L(b, k, \varepsilon)^\alpha v(b, k, \varepsilon)^{\eta-1} = p \left( 1 + \phi(R - 1) + \frac{\mu(b, k, \varepsilon)}{\lambda(b, k, \varepsilon)} \phi R \right) \quad (122)$$

$$\lambda(b, k, \varepsilon) = R\beta E[\lambda'(b, k, \varepsilon), k'(b, k, \varepsilon), \varepsilon'] + \mu(b, k, \varepsilon) \quad (123)$$

$$\lambda(b, k, \varepsilon) = \frac{1}{q(b, k, \varepsilon)} \beta E[\lambda[b'(b, k, \varepsilon), k'(b, k, \varepsilon), \varepsilon'] (d(b'(b, k, \varepsilon), k'(b, k, \varepsilon), \varepsilon') \quad (124)$$

$$+ q'(b'(b, k, \varepsilon), k'(b, k, \varepsilon), \varepsilon'))] + \mu(b, k, \varepsilon)\kappa$$

$$d(b, k, \varepsilon) = \gamma A k^{\gamma-1} L(b, k, \varepsilon)^\alpha v(b, k, \varepsilon) - \delta \frac{a (k'(b, k, \varepsilon) - k)^2}{k^2} \quad (125)$$

$$q(b, k, \varepsilon) = 1 + a \left( \frac{k'(b, k, \varepsilon) - k}{k} \right) \quad (126)$$

$$w(b, k, \varepsilon) = L(b, k, \varepsilon)^{\omega-1} (1 + \tau) \quad (127)$$

$$(1 + \tau)c(b, k, \varepsilon) + i(b, k, \varepsilon) = e^{\varepsilon^A} F(k, L, v) - e^{\varepsilon^P} p v - \phi(R - 1)(wL(b, k, \varepsilon) \quad (128)$$

$$+ e^{\varepsilon^P} p v(b, k, \varepsilon)) - q^b b'(b, k, \varepsilon) + b$$

where  $i(b, k, \varepsilon) = \delta k + (k'(b, k, \varepsilon) - k) \left[ 1 + \frac{a}{2} \left( \frac{k'(b, k, \varepsilon) - k}{k} \right) \right]$ ,  $F(k, L, v) = A k^\gamma L^\alpha v^\eta$  with  $0 \leq \alpha, \gamma, \eta \leq$

<sup>13</sup>We used the same method to solve the endowment model, in which case bonds are the only endogenous state variable and endowment income is the only exogenous shock. The model reduces to a single recursive equilibrium condition, which is the bonds Euler equation (see [Mendoza and Villalvazo \(2020\)](#) for details).

1,  $\alpha + \gamma + \eta = 1$ , and  $A > 0$ . Finally,  $1/q^b \equiv e^{\varepsilon R} R$ , and  $q$  denotes Tobin's  $q$ . The algorithm proceeds in the following eight steps:

1. **Define the discrete state space:** We use a grid of bonds with  $M$  nodes and a grid of capital with  $N$  nodes. The size of the grids for the shocks depends on the approach used to construct the Markov processes of the shocks. In the paper, we used the same Markov processes as in [Mendoza \(2010\)](#), which feature two realizations for each of the three shocks. Hence, the state space has  $M \times N \times 8$  elements.
2. **Initial conjectures for iteration  $j$ :** For each iteration  $j$ , define conjectured functions for the price of capital  $\hat{q}_j(b, k, \varepsilon)$ , the decision rule for bonds  $\hat{B}_j(b, k, \varepsilon)$ , and the multiplier ratio  $\hat{\mu}_j(b, k, \varepsilon)$  which is the ratio of the multiplier on the borrowing constraint,  $\mu$ , to the multiplier on the budget constraint,  $\lambda$ . For the first iteration, the conjectures are:  $\hat{\mu}_j(b, k, \varepsilon) = 0$ ,  $\hat{q}_j(b, k, \varepsilon) = 1$  and  $B_j(b, k, \varepsilon) = b$  (i.e., the credit constraint does not bind, Tobin's  $q$  is at the value consistent with a capital decision rule equal to the current state, and the bonds decision rule is also set equal to the current state).
3. **Compute iteration- $j$  implied decision rules.** The conjectures set above and the recursive equilibrium conditions imply the following decision rules:

$$K_j(b, k, \varepsilon) = \frac{k}{a} [\hat{q}_j(b, k, \varepsilon) - 1 + a] \quad (129)$$

$$i_j(b, k, \varepsilon) = (K_j(b, k, \varepsilon) - k) \left[ 1 + \frac{a}{2} \left( \frac{K_j(b, k, \varepsilon) - k}{k} \right) \right] - \delta k \quad (130)$$

$$v_j(b, k, \varepsilon) = \left\{ \frac{e^{\varepsilon A} A k^\beta \eta^{\frac{\omega-\alpha}{\omega}} \frac{\alpha}{1+\tau} \frac{\alpha}{\omega}}{p^{\frac{\omega-\alpha}{\omega}} [1 + \phi(R-1) + \hat{\mu}_j(b, k, \varepsilon) \phi R]} \right\}^{\frac{\omega}{\omega(1-\eta)-\alpha}}, \quad (131)$$

$$L_j(b, k, \varepsilon) = \left\{ \frac{\alpha}{\eta(1+\tau)} p v_j(b, k, \varepsilon) \right\}^{\frac{1}{\omega}}, \quad (132)$$

$$y_j(b, k, \varepsilon) = e^{\varepsilon A} A k^\beta L_j(b, k, \varepsilon)^\alpha v_j(b, k, \varepsilon)^\eta, \quad (133)$$

$$(1+\tau)c_j(b, k, \varepsilon) = y_j(b, k, \varepsilon) - p v_j(b, k, \varepsilon) - \phi(R-1) [(1+\tau)L_j(b, k, \varepsilon)^\omega + p v_j(b, k, \varepsilon)] - i_j(b, k, \varepsilon) - \frac{\hat{B}_j(b, k, \varepsilon)}{R} + b. \quad (134)$$

4. **Solve for "new" (i.e.,  $j + 1$ ) decision rules assuming the credit constraint does not bind.**

Assume  $\hat{\mu}_{j+1}(b, k, \varepsilon) = 0$ , and proceed as follows:

- The optimality conditions for factor allocations and the production function can be

solved separately from the rest of the solution to obtain:

$$v_{j+1}(b, k, \varepsilon) = \left\{ \frac{e^{\varepsilon^A} k^\beta \eta \frac{\omega - \alpha}{\omega} \frac{\alpha}{1 + \tau} \frac{\alpha}{\omega}}{p \frac{\omega - \alpha}{\omega} [1 + \phi(R - 1)]} \right\}^{\frac{\omega}{\omega(1 - \eta) - \alpha}} \quad (135)$$

$$L_{j+1}(b, k, \varepsilon) = \left\{ \frac{\alpha}{\eta(1 + \tau)} p v_{j+1}(b, k, \varepsilon) \right\}^{\frac{1}{\omega}} \quad (136)$$

$$y_{j+1}(b, k, \varepsilon) = e^{\varepsilon^A} A k^\beta L_{j+1}(b, k, \varepsilon)^\alpha v_{j+1}(b, k, \varepsilon)^\eta \quad (137)$$

- $c_{j+1}$  is solved directly from the bonds Euler equation (this step uses fixed-point iteration):

$$\begin{aligned} & c_{j+1}(b, k, \varepsilon) \\ &= \left\{ \beta R E \left[ \left( c_j(\hat{B}_j(b, k, \varepsilon), K_j(b, k, \varepsilon), \varepsilon') - \frac{L_j(\hat{B}_j(b, k, \varepsilon), K_j(b, k, \varepsilon), \varepsilon')^\omega}{\omega} \right)^{-\sigma} \right] \right\}^{-\frac{1}{\sigma}} \\ & \quad + \frac{L_{j+1}(b, k, \varepsilon)^\omega}{\omega} \end{aligned} \quad (138)$$

Bi-linear interpolation of the labor and consumption functions is used to determine the values of  $c_j(\hat{B}_j(b, k, \varepsilon), K_j(b, k, \varepsilon), \varepsilon')$  and  $L_j(\hat{B}_j(b, k, \varepsilon), K_j(b, k, \varepsilon), \varepsilon')$ .

- Solve for  $B_{j+1}(b, k, \varepsilon)$  using the resource constraint:

$$\begin{aligned} B_{j+1}(b, k, \varepsilon)/R &= y_{j+1}(b, k, \varepsilon) - p v_{j+1}(b, k, \varepsilon) - \phi(R - 1) [(1 + \tau) L_{j+1}(b, k, \varepsilon)^\omega + p v_{j+1}(b, k, \varepsilon)] \\ & \quad - i_j(b, k, \varepsilon) - (1 + \tau) c_{j+1}(b, k, \varepsilon) + b \end{aligned} \quad (139)$$

- Evaluate if the collateral constraint binds. If

$$\frac{B_{j+1}(b, k, \varepsilon)}{R} - \phi R [(1 + \tau) L_{j+1}(b, k, \varepsilon)^\omega + p v_{j+1}(b, k, \varepsilon)] + \kappa \hat{q}_j(b, k, \varepsilon) K_j(b, k, \varepsilon) \geq \varepsilon^b \quad (140)$$

for small  $\varepsilon^b$ , the constraint does not bind at the point  $(b, k, \varepsilon)$ , the functions with  $j + 1$  subscripts are saved, and the algorithm jumps to step 6. Otherwise, the constraint binds, the  $j + 1$  functions are discarded and we move to Step 5.

5. **Solve for  $j + 1$  decision rules when the credit constraint binds.** Now we impose that the collateral constraint holds with equality for the coordinate  $(b, k, \varepsilon)$  at which the constraint binds in the previous step. Since  $\hat{q}_j(\cdot)$  has not changed, we use the same  $j$ -indexed functions

$K'_j(\cdot)$  and  $\tilde{i}_j(\cdot)$  as before. This step requires a non-linear solver to solve for the values of  $L_{j+1}(\cdot), v_{j+1}(\cdot), c_{j+1}(\cdot), B_{j+1}(\cdot), \tilde{\mu}_{j+1}(\cdot)$  by solving the following equation system formed by the recursive optimality conditions, expressed as a function of  $\tilde{\mu}$  for simplicity.<sup>14</sup>

$$v(\tilde{\mu}) = \left\{ \frac{e^{\varepsilon^A} Ak^\beta \eta^{\frac{\omega-\alpha}{\omega}} \frac{\alpha}{1+\tau} \frac{\alpha}{\omega}}{p^{\frac{\omega-\alpha}{\omega}} [1 + \phi(R-1) + \tilde{\mu}\phi R]} \right\}^{\frac{\omega}{\omega(1-\eta)-\alpha}} \quad (141)$$

$$L(\tilde{\mu}) = \left\{ \frac{\alpha}{\eta(1+\tau)} pv(\tilde{\mu}) \right\}^{\frac{1}{\omega}} \quad (142)$$

$$\frac{B(\tilde{\mu})}{R} = -\kappa \hat{q}_j K_j + \phi R pv(\tilde{\mu}) \left[ 1 + \frac{\alpha}{\eta} \right] \quad (143)$$

$$(1+\tau)c(\tilde{\mu}) = e^{\varepsilon^A} Ak^\beta L(\tilde{\mu})^\alpha v(\tilde{\mu})^\eta - pv(\tilde{\mu}) - \phi(R-1)pv(\tilde{\mu}) \left[ 1 + \frac{\alpha}{\eta} \right] - i_j - \frac{B(\tilde{\mu})}{R} + b \quad (144)$$

In addition to the above four equations, the non-linear system also includes the following condition for  $\tilde{\mu}_{j+1}(b, k, \varepsilon)$  that represents the Euler equation for bonds:

$$\tilde{\mu}_{j+1}(b, k, \varepsilon) = 1 - \frac{\beta RE \left[ \left( c_j(\hat{B}_j(b, k, \varepsilon), K_j(b, k, \varepsilon), \varepsilon') - \frac{L_j(\hat{B}_j(b, k, \varepsilon), K_j(b, k, \varepsilon), \varepsilon')^\omega}{\omega} \right)^{-\sigma} \right]}{\left( c(\tilde{\mu}_{j+1}(b, k, \varepsilon)) - \frac{L(\tilde{\mu}_{j+1}(b, k, \varepsilon))^\omega}{\omega} \right)^{-\sigma}} \quad (145)$$

The numerator in the right-hand-side of this expression is using again fixed-point iteration because it uses  $j$ -indexed functions to compute the entire expected marginal utility term. The values of the functions  $c_j(\hat{B}_j(b, k, \varepsilon), K_j(b, k, \varepsilon), \varepsilon')$  and  $L_j(\hat{B}_j(b, k, \varepsilon), K_j(b, k, \varepsilon), \varepsilon')$  are again determined by bi-linear interpolation.

Algebraic manipulation of the five equations in the nonlinear system reduces the system to

---

<sup>14</sup>The non-linear solver is needed only because when the constraint binds the value of  $\tilde{\mu}$  needs to be solved together with the allocations and prices. If the multiplier could be solved separately, as it is the case for a large class of credit constraints, FiPIt does not need a non-linear solver anywhere (see [Mendoza and Villalvazo \(2020\)](#) for details).

a single nonlinear equation in  $\tilde{\mu}_{j+1}(\cdot)$  for each coordinate  $(b, k, \varepsilon)$  where the constraint binds:

$$\begin{aligned}
(1 - \tilde{\mu}_{j+1}(\cdot)) & \left\{ C_1^{\frac{\omega}{(1-\eta)\omega-\alpha}} \left[ \frac{\alpha}{1 + \phi(R-1) + \tilde{\mu}_{j+1}(\cdot)\phi R} \right]^{\frac{\eta\omega+\alpha}{(1-\eta)\omega-\alpha}} \right. \\
& - \left. \left[ \frac{\alpha C_1}{1 + \phi(R-1) + \tilde{\mu}_{j+1}(\cdot)\phi R} \right]^{\frac{\omega}{(1-\eta)\omega-\alpha}} C_2 \right. \\
& \left. - \left( \frac{i_j(\cdot) - \kappa \hat{q}_j(\cdot) K_j(\cdot) - b}{1 + \tau} \right) \right\}^{-\sigma} \\
& = \beta RE \left[ \left( c_j(\hat{B}_j(\cdot), K_j(\cdot), \varepsilon') - \frac{L_j(\hat{B}_j(\cdot), K_j(\cdot), \varepsilon')^\omega}{\omega} \right)^{-\sigma} \right]
\end{aligned} \tag{146}$$

where:

$$C_1 \equiv \left( \frac{1}{1 + \tau} \right)^{1-\eta} e^{\varepsilon^A} A k^\beta \left( \frac{\eta}{\alpha p} \right)^\eta \quad \text{and} \quad C_2 \equiv \frac{1}{\omega} + \frac{\eta}{\alpha} + \phi \left( 1 + \frac{\eta}{\alpha} \right) (2R - 1). \tag{147}$$

Once  $\tilde{\mu}_{j+1}(b, k, \varepsilon)$  is solved, the rest of the functions can be updated to their  $j+1$  forms using the previous equations as follows:

$$v_{j+1}(b, k, \varepsilon) = \left\{ \frac{e^{\varepsilon^A} A k^\beta \eta^{\frac{\omega-\alpha}{\omega}} \frac{\alpha}{1+\tau} \frac{\alpha}{\omega}}{p^{\frac{\omega-\alpha}{\omega}} [1 + \phi(R-1) + \tilde{\mu}_{j+1}(b, k, \varepsilon)\phi R]} \right\}^{\frac{\omega}{\omega(1-\eta)-\alpha}} \tag{148}$$

$$L_{j+1}(b, k, \varepsilon) = \left\{ \frac{\alpha}{\eta(1 + \tau)} p v_{j+1}(b, k, \varepsilon) \right\}^{\frac{1}{\omega}} \tag{149}$$

$$B_{j+1}(b, k, \varepsilon) = R \left\{ -\kappa \hat{q}_j(b, k, \varepsilon) K_j(b, k, \varepsilon) + \phi R p v_{j+1}(b, k, \varepsilon) \left[ 1 + \frac{\alpha}{\eta} \right] \right\} \tag{150}$$

$$\begin{aligned}
(1 + \tau) c_{j+1}(b, k, \varepsilon) & = e^{\varepsilon^A} A k^\beta L_{j+1}(b, k, \varepsilon)^\alpha v_{j+1}(b, k, \varepsilon)^\eta \\
& - p v_{j+1}(b, k, \varepsilon) - \phi(R-1) p v_{j+1}(b, k, \varepsilon) \left[ 1 + \frac{\alpha}{\eta} \right] \\
& - i_j(b, k, \varepsilon) - \frac{B_{j+1}(b, k, \varepsilon)}{R} + b
\end{aligned} \tag{151}$$

The functions with  $j + 1$  subscripts are saved, and we move to Step 5.

6. **Complete iteration- $j$  solutions for the entire state space:** Return to Step 3 and repeat for all triples  $(b, k, \varepsilon)$  in the state space.

7. **Compute the new capital pricing function:** The new pricing function is solved for by applying the new decision rules for  $c_{j+1}(\cdot)$ ,  $L_{j+1}(\cdot)$ ,  $b'_{j+1}(\cdot)$ ,  $\tilde{\mu}_{j+1}(\cdot)$  to the Euler equation for capital and solving it so as to obtain the following analytical solution for  $q_{j+1}(b, k, \varepsilon)$ :

$$q_{j+1}(b, k, \varepsilon) = \frac{\beta E_t \left[ \left( c_{j+1} \left( b'_{j+1}(\cdot), k'_j(\cdot), \varepsilon' \right) - \frac{L_{j+1} \left( b'_{j+1}(\cdot), k'_j(\cdot), \varepsilon' \right)^\omega}{\omega} \right)^{-\sigma} \left[ d'(\cdot) + \hat{q}_j \left( b'_{j+1}(\cdot), k'_j(\cdot), \varepsilon' \right) \right] \right]}{\left( c_{j+1}(\cdot) - \frac{L_{j+1}(\cdot)^\omega}{\omega} \right)^{-\sigma} (1 - \kappa \tilde{\mu}_{j+1}(\cdot))} \quad (152)$$

where

$$d' \left( b'_{j+1}(\cdot), k'_j(\cdot), \varepsilon' \right) = \gamma A' k'_j(\cdot)^{\gamma-1} L_{j+1} \left( b'_{j+1}(\cdot), k'_j(\cdot), \varepsilon' \right)^\alpha v_{j+1} \left( b'_{j+1}(\cdot), k'_j(\cdot), \varepsilon' \right)^\eta - \delta + \frac{a \left( k'_j \left( b'_{j+1}(\cdot), k'_j(\cdot), \varepsilon' \right) - k'_j(\cdot) \right)^2}{2 k'_j(\cdot)^2}$$

This step also uses fixed-point iteration, because the capital price used in the right-hand-side of (152) is the conjecture set in step 2, and since all the functions in the right-hand-side are known, the equation solves directly for  $q_{j+1}(b, k, \varepsilon)$ . The values of  $c_{j+1} \left( b'_{j+1}(\cdot), k'_j(\cdot), \varepsilon' \right)$ ,  $L_{j+1} \left( b'_{j+1}(\cdot), k'_j(\cdot), \varepsilon' \right)$  and  $\hat{q}_j \left( b'_{j+1}(\cdot), k'_j(\cdot), \varepsilon' \right)$  are determined by bi-linear interpolation. The value of  $d'(\cdot)$  is obtained by applying bi-linear interpolation to evaluate  $L_{j+1} \left( b'_{j+1}(\cdot), k'_j(\cdot), \varepsilon' \right)$ ,  $v_{j+1} \left( b'_{j+1}(\cdot), k'_j(\cdot), \varepsilon' \right)$  and  $k'_j \left( b'_{j+1}(\cdot), k'_j(\cdot), \varepsilon' \right)$ . Notice that the decision rule setting the value of  $b_{t+1}$  at which all these functions are interpolated is a  $j+1$ -indexed function but over the capital dimension we are still using the  $j$ -indexed decision rule.

8. **Check convergence:** Evaluate the convergence of the relevant functions using the following criteria, for small  $\varepsilon^f$ :

$$\|q_{j+1}(b, k, \varepsilon) - \hat{q}_j(b, k, \varepsilon)\| \leq \varepsilon^f \quad (153)$$

$$\|B_{j+1}(b, k, \varepsilon) - \hat{B}_j(b, k, \varepsilon)\| \leq \varepsilon^f \quad (154)$$

$$\|\tilde{\mu}_{j+1}(b, k, \varepsilon) - \hat{\mu}_j(b, k, \varepsilon)\| \leq \varepsilon^f \quad (155)$$

If all of these conditions hold, the recursive equilibrium of the Sudden Stops model has been solved. If convergence fails, update the conjectured functions using a convex combination of the last conjectures and the new functions to dampen possible overshooting using:

$$\hat{x}_j^{new}(b, k, \varepsilon) = \rho \hat{x}_j(b, k, \varepsilon) + (1 - \rho) x_{j+1}(b, k, \varepsilon) \quad (156)$$

for  $x = q, B, \tilde{\mu}$  and some  $-1 \leq \rho \leq 1$ . Set  $\hat{x}_j(b, k, \varepsilon) = \hat{x}_j^{new}(b, k, \varepsilon)$  for all functions, return to step 2 and repeat until convergence is attained.

## C.2 Calibration of the RBC and Sudden Stops models

Calibration of the RBC model follows the approach used for the Sudden Stops model presented in the main paper except for a few variables (see Table 7).  $\kappa$  is set to a very low value so the collateral constraint never binds. We set  $\beta$  and the lower bound of the NFA grid so the model solution is close to the target data moments, and express  $\varphi$  as a ratio of that lower bound to  $y^{dss}$ . Setting  $\beta = 0.92$  and  $\varphi = -0.764$  (implied by a NFA lower bound of -300) we obtain  $E(b/y) = -0.372$  (v. -0.44 in the data) and a variability ratio of consumption to GDP of 1.29 (v. 1.25 in the data).

For the Sudden Stops model, we set  $\kappa = 0.2$  as in [Mendoza \(2010\)](#) and set the lower bound of the bonds grid to solve the SS model at -200 (i.e., a tighter  $\varphi$  than in the RBC solution), which yields  $b^{dss}/y^{dss} = -0.51$ , because strong precautionary savings due to the credit constraint imply that  $b_{t+1}/y_t$  never falls below  $-0.19$  in the SS model's ergodic distribution. Hence, we can increase  $\varphi$  so as to use fewer nodes in the bond grid to make the algorithm more efficient.

The TFP, price and interest-rate shock processes follow the same diagonal VAR structure and calibration structure described in Section 3 of the paper and taken from [Mendoza \(2010\)](#). In the GLB solution of both the RBC and SS model, the shocks are approximated using symmetric two-point Markov processes defined with the Simple Persistence Rule. These processes are defined by a set  $\mathbb{E}$  that includes all triples of realizations of the shocks  $\varepsilon_t = (\varepsilon_t^A, \varepsilon_t^R, \varepsilon_t^P)$ , and a matrix  $\pi$  that includes the transition probabilities of moving from  $\varepsilon_t$  to  $\varepsilon_{t+1}$ . Each shock has two realizations equal to +/- one-standard-deviation of their corresponding data counterparts:  $\varepsilon_1^A = -\varepsilon_2^A = 0.0134$ ,  $\varepsilon_1^R = \varepsilon_2^R = 0.0196$ ,  $\varepsilon_1^P = -\varepsilon_2^P = 0.0335$ , so  $\mathbb{E}$  contains 8 triples. The Simple Persistence Rule produces an 8x8 matrix  $\pi$  which yields variances, correlations and autocorrelations for all the shocks that match those in the data, except that the procedure requires shocks that are correlated (i.e.,  $\varepsilon^A$  and  $\varepsilon^R$ ) to have the same autocorrelation. As noted above, we set  $\rho^A = \rho^R = 0.555$ . This restriction is immaterial, because the two shocks have very similar autocorrelation coefficients in the data ( $\rho^A = 0.537$ ,  $\rho^R = 0.572$ ).

## C.3 Quantitative results of the RBC Model

This section presents quantitative results of the RBC model without the occasionally binding collateral constraint. We first highlight additional details on the solution method, describe the cali-

Table 7: Calibration of the RBC Model

Notation	Parameter/Variable	Value
<b>1. Common parameters</b>		
$\sigma$	Coefficient of relative risk aversion	2.0
$R$	Gross world interest rate	1.0857
$\alpha$	Labor share in gross output	0.592
$\gamma$	Capital share in gross output	0.306
$\eta$	Imported inputs share in gross output	0.102
$\delta$	Depreciation rate of capital	0.088
$\omega$	Labor exponent in the utility function	1.846
$\phi$	Working capital constraint coefficient	0.2579
$a$	Investment adjustment cost parameter	2.75
$\tau$	Consumption tax	0.168
$\kappa$	Collateral constraint coefficient	0.20
$y^{dss}$	GDP at the deterministic steady state	396
<b>2. RBC global solution parameters</b>		
$\beta$	Discount factor	0.920
$\varphi$	Ad-hoc debt limit as a share of $y^{dss}$	-0.758
<b>3. RBC local solution parameters</b>		
<i>Common Parameters</i>		
$\beta$	Discount factor	0.9211
$b^{dss}/y^{dss}$	NFA/GDP at the deterministic steady state	-0.758
<i>Baseline Calibration</i>		
$\psi$	Inessential DEIR coefficient	0.001
<i>Targeted Calibration</i>		
$\psi$	DEIR coefficient for 2OA	0.0109
$\psi$	DEIR coefficient for RSS	0.008

Note: 2OA and RSS denote the second-order and risky-steady state solutions, respectively.

bration parameters and then present the results.

We solve the RBC model using the same methods as the Sudden Stops model described in the main paper. For the GLB solution, we use *FiPit* with a state space consisting of grids of  $k$  and  $b$  with 30 and 80 nodes, respectively. The algorithm iterates to convergence on the decision rule for bonds and the pricing function for capital. [Mendoza and Villalvazo \(2020\)](#) provide full details and Matlab code.

For local solutions, the DEIR function depends on NFA ratios to steady-state GDP ( $y^{dss}$ ):

$$1 + r_t = e^{\varepsilon^R} \bar{R} + \psi \left[ e^{\frac{B^*}{y^{gdp}} - \frac{b_{t+1}}{y^{dss}}} - 1 \right], \quad (157)$$

The local model is calibrated such that  $B^*/y^{gdp} = \varphi = -0.758$ , the deterministic steady state bond-to-GDP ratio in the GLB model. The elasticity of the interest rate with respect to (small) percent

deviations of  $b_{t+1}$  from  $b^{dss}$  is  $\eta^r \approx \psi b^{dss}/y^{dss}$ . This facilitates comparisons across calibrations of global and local solutions, since  $y^{dss}$  is not equal to 1 (as in the endowment model).

### C.3.1 Coefficients of RBC decision rules

This section gives the numerical values for the RBC decision rules based on local solutions. To facilitate the comparison of coefficients, we report the decision rule coefficients for  $(k_{t+1} - k)/k$  and  $(b_{t+1} - b)/|b|$  with the state vector as follows:  $\mathbb{x}_t \equiv [(k_t - k)/k, (b_t - b)/|b|, \varepsilon_t^A, \varepsilon_t^P, \varepsilon_t^R]'$ . The coefficients of the RSS decision rules are given by

$$g_{\mathbb{x}}^k = \begin{bmatrix} 0.8760 & 0.0039 & 0.0890 & -0.0170 & -0.5860 \end{bmatrix},$$

$$g_{\mathbb{x}}^b = \begin{bmatrix} 0.1013 & 0.9980 & 0.3164 & -0.0222 & 0.7237 \end{bmatrix}.$$

For 2OA:

$$g_{\mathbb{x}}^k = \begin{bmatrix} 0.8757 & 0.0006 & 0.0894 & -0.0164 & -0.5840 \end{bmatrix}, \quad (158)$$

$$g_{\mathbb{x}}^b = \begin{bmatrix} 0.3387 & 0.9961 & 1.0643 & -0.0748 & 1.0676 \end{bmatrix}, \quad (159)$$

$$g_{\mathbb{xx}}^k = \begin{bmatrix} -0.0733 & -0.0008 & 0.0522 & -0.0096 & -0.3959 \\ -0.0008 & -0.0009 & -0.0021 & 0.0002 & -0.0014 \\ 0.0522 & -0.0021 & 0.0532 & -0.0080 & -0.0943 \\ -0.0096 & 0.0002 & -0.0080 & 0.0013 & 0.0198 \\ -0.3959 & -0.0014 & -0.0943 & 0.0198 & 0.9408 \end{bmatrix}, \quad (160)$$

$$g_{\mathbb{xx}}^b = \begin{bmatrix} -0.0373 & 0.0067 & 0.6618 & -0.0588 & 0.8642 \\ 0.0067 & 0.0034 & 0.0103 & -0.0013 & 0.9158 \\ 0.6618 & 0.0103 & 2.2172 & -0.2094 & 1.2487 \\ -0.0588 & -0.0013 & -0.2094 & 0.0181 & -0.1721 \\ 0.8642 & 0.9158 & 1.2487 & -0.1721 & -3.1692 \end{bmatrix}, \quad (161)$$

$$g_{\sigma\sigma} = \begin{bmatrix} 0.0064 & -0.0029 \end{bmatrix}. \quad (162)$$

Both the RSS and 2OA decision rules for capital have negligible coefficients on lagged NFA. A relevant statistic on how the GLB decision rule for capital behaves in the bonds dimension is the

following elasticity:

$$\frac{\partial k'(b, k, \varepsilon)}{b} \times \frac{b}{k}$$

Excluding the state space in which the ad-hoc debt limit binds, the maximum value of this elasticity is 0.088 and the mean value (computed using the ergodic distribution of the GLB solution) is 0.001. These imply a negligible 1% change in bonds imply 0.001 % (mean) and 0.088% (max) change in  $k'$ .

### C.3.2 Long-run moments and performance metrics

Table 8 presents unconditional moments of GLB, 2OA and RSS solutions. 1OA results are omitted because, as with the endowment model, second- and higher-order moments are nearly identical to those obtained with 2OA.<sup>15</sup> First, we highlight the differences between the RBC and endowment results in the GLB solutions: The RBC model predicts higher variability of consumption relative to GDP and countercyclical net exports, both of which bring the model closer the data. These changes are due to the presence of the working capital constraint and capital accumulation. The former amplifies the effects of TFP and input price shocks, and induces higher imports of inputs during expansions in response to the countercyclical interest-rate shocks. Capital accumulation also incentivizes higher imports and external deficits during expansions, because of the positive autocorrelation of the model's three shocks: "Good times," (high TFP, low input prices and interest rates), have positive persistence, which makes it optimal to borrow from abroad to finance investment due to the expectation that favorable realizations of the shocks will continue in the near future. The countercyclical net exports due to these effects contributes to the excess variability in consumption relative to GDP.

Compare next the RSS and 2OA solutions under the baseline calibration. The moments for consumption, net exports and NFA differ slightly between these two solutions in the endowment model, but in the RBC model the differences are larger. This is, however, consistent with the arguments presented earlier, because  $b^{rss}$  and  $b^{dss}$  differ sharply in the RBC model (36 v. -76 in percent of GDP), while in the endowment model the difference was too small to matter. The first-order coefficients of the decision rules are again similar for 2OA and RSS(see Appendix C.4.1), and the second-order coefficients of the 2OA solution yield again negligible effects, but the large difference between  $b^{rss}$  and  $b^{dss}$  yields larger differences in long-run moments. This is particularly the case for the means of the ratios of net exports and NFA to GDP, which are -4.2 and 73.2 percent respectively

---

<sup>15</sup>As reported in Appendix C.4.1, the first-order coefficients of the 1OA and 2OA decision rules are identical, and those for higher-order terms in the 2OA solution, except the variance, are negligible again.

in the 2OA solution v. -18.5 and 255.9 percent in the RSS solution.

Comparing GLB v. local solutions under the baseline calibration, the performance of the latter at approximating the GLB solution for  $E(b/y)$  worsens markedly in the RBC model v. the endowment model. In particular, while for the endowment model the 2OA and RSS methods produced  $E(b/y)$  values of -0.28 and -0.45, relative to -0.41 in the GLB solution, in the RBC model they produce *positive* ratios of 0.73 and 2.56 respectively (i.e., the economy is a net lender) relative to -0.37 in the GLB solution. Hence, the precautionary savings motive is sharply overstated by the local solutions. This is partly because the RBC model includes interest-rate shocks, and we documented earlier that when these shocks are included 2OA and RSS solutions overestimate significantly  $E(b/y)$ , even in the endowment model.<sup>16</sup> These findings are also in line with results reported by [de Groot \(2014\)](#), showing large, positive mean NFA-GDP ratios of 3.6 and 41 in the two stable equilibria produced by the full RSS method for an endowment economy.<sup>17</sup>

For second- and higher-order moments, the results are largely in line with those obtained for the endowment model. In particular, the local solutions overestimate the persistence of net exports. The GLB solution generates an autocorrelation of net exports around 0.71 whereas both local methods generate values around 0.85. This occurs again because NFA is a near-unit root process and small differences in its autocorrelation (0.997 in GLB v. 0.999 in 2OA and 0.998 in RSS) imply large differences in the autocorrelation of net exports. Moreover, the local solutions overestimate markedly again the variability of consumption, net exports and NFA relative to GDP.

Despite the differences in the moments for consumption, net exports and NFA, the cyclical moments for investment, capital, imported inputs, labor and output are similar across solutions. For investment and the capital stock, this occurs because, as shown in [Mendoza \(1991\)](#) the Fisherian separation of investment from savings and consumption decisions that holds strictly under perfect foresight, holds approximately in the RBC model. Intuitively, the RBC model is in the wide class of models consistent with negligible equity premia, and in the limit with zero premium Fisherian separation holds exactly. In addition, the GHH structure of preferences prevents consumption and savings from affecting labor supply, and hence output and all factors of production. The near-Fisherian separation property is verified in the negligible coefficients of the capital decision rules on lagged NFA in the 2OA and RSS solutions and the near-zero numerical derivatives of the decision rule for  $k'(b, k, \varepsilon)$  with respect to  $b$  in the GLB solutions (the largest of which was 0.0064).

---

<sup>16</sup>In the endowment model with  $\sigma_{zR} = 0.025$ , 2OA (RSS) yields  $E(b/y)$  of 0.806 (0.942), v. -0.38 in the GLB solution.

<sup>17</sup>Interestingly, [de Groot \(2014\)](#)'s analysis showing spurious multiplicity of the full RSS solution shows an additional weakness of this method, namely that it can produce two stable solutions whereas the global solution is unique.

Consider next the local solutions with targeted calibrations. Matching the GLB value of  $\rho_b$  required  $\psi = 0.0109$  and  $\psi = 0.008$  in the 2OA and RSS solutions, respectively (see Table ??). These are smaller than the value needed for the targeted calibrations of the endowment economy (0.0469 for both 2OA and RSS). These differences, together with the different NFA-GDP ratios in the deterministic steady states of the endowment and RBC models, imply values of  $\eta^r$  of 0.0083 and 0.0061 for the 2OA and RSS solutions of the RBC model respectively, lower by a factor of 3 than the 0.0239 for the endowment model solutions. This is the case mainly because the GLB solution of  $\rho_b$  is higher in the RBC than in the endowment model (0.996 v. 0.977).

The lower  $\psi$  values for the targeted calibrations of the RBC model v. the endowment model also imply that the mean of NFA can now rise above the deterministic steady state by non-trivial margins, because the implicit cost of deviating from  $b^{dss}$  is smaller. This is even more the case for the targeted RSS solution, which has a lower  $\psi$  than the 2OA solution and thus allows  $E(b/y)$  to rise by more ( $-0.397$  v.  $-0.62$  in the 2OA solution and  $-0.758$  in the deterministic steady state).

The gap between  $b^{rss}$  and  $b^{dss}$  in the RSS and 2OA solutions narrows in the targeted calibrations relative to the baseline calibrations:  $b^{rss}$  is now  $-0.591$ , compared with  $-0.758$  for  $b^{dss}$ . With this smaller difference, we recover the result that the decision rules for RSS and 2OA yield similar second- and higher-order moments and similar impulse response functions, as shown below.

As with the endowment model, targeted calibrations generally yield moments closer to the GLB solution than baseline calibrations. It is still the case, however, that targeted calibrations require knowing the GLB solution for  $\rho_b$ . Targeted RSS performs markedly better than 2OA in that it yields  $E(b/y)$  much closer to the GLB solution. 2OA yields  $-0.62$ , nearly 24 percentage points lower than the global value ( $-0.38$ ), whereas RSS yields about  $-0.4$ , just 1.3 percentage points below the global value. The targeted RBC calibrations, however, do not get as close to the other GLB solution moments as in the case of the endowment model, even with the RSS solution: The variability of the NFA-GDP ratio is roughly half of what the GLB solution yields and its correlation with GDP is 3.5 times bigger. The leverage ratio is also much less variable and has a much lower correlation with GDP. Fisherian separation continues to approximately hold, so moments for output, investment, and factors of production are similar in the targeted calibrations and the GLB solution.

In terms of execution times, the local solutions take about 2/3rds of the time taken up by the GLB solution (which takes 61 seconds). 1OA and 2OA have similar execution times and, as explained earlier, yield similar second- and higher-order moments.<sup>18</sup> Local methods show similar

---

<sup>18</sup>Execution time reported for RSS solution reflects pre-processing and solution steps taken by Schmitt-Grohe-Urbe

limitations in terms of accuracy as with the endowment model: they yield much larger Euler equation errors (for capital and NFA with RSS and for capital with 2OA), the average (maximum) differences in the decision rules for  $k$  and  $c$  are in the 1.7–1.9 (5.1–6.6) percent range, and those for NFA are much larger at above 8 (50) percent for the average (maximum) respectively. These large differences occur at the debt limit  $\varphi$ , because local methods do not handle it as occasionally binding.

We conducted a robustness analysis of the results reported here by altering the values of some of the model’s key parameters (see Appendix C.3.5). We examined scenarios increasing the variability of TFP, input price and interest-rate shocks one at a time, as well as increasing the coefficient of relative risk aversion, the correlation between interest rate and TFP shocks, and the subjective discount factor. As in the case of the endowment model, local solutions with a fixed value of  $\psi$  calibrated to match  $\rho_b$  in the baseline GLB solution are not useful for analyzing the effects of any of these parameter changes, because they yield solutions that differ sharply from the GLB solutions for the same parameter variations. In particular, the local solutions continue to perform poorly at capturing precautionary savings effects (i.e., the GLB solution for  $E(b/y)$  differs sharply from what the local solutions yield).<sup>19</sup> In addition, the local solutions underestimate the variability of NFA and net exports, overestimate (underestimate) the correlations of NFA and consumption (net exports) with GDP, and underestimate the autocorrelation of net exports. The local solutions are closer to the GLB solutions if we re-calibrate  $\psi$  to target the new value of  $\rho_b$  from the GLB solution for each new parameterization, but this implies obtaining the GLB solution first and in addition the long-run moments are not as close to those of the GLB solution as with the endowment model.

### C.3.3 Impulse response functions

Figures 11 and 12 show impulse response functions to a negative one-standard-deviation TFP shock.<sup>20</sup> All impulse responses return to zero in about 500 periods, but only the first 100 are shown to highlight the differences across the solutions. As in the endowment model, 1OA and 2OA impulse responses are nearly identical under baseline and targeted calibrations. This occurs because again the first-order coefficients of decision rules are identical, and the second-order terms (other than the variance terms) are quantitatively irrelevant.

toolbox. These times are indicative and alternative toolboxes, such as Dynare, might have faster solution times.

<sup>19</sup>The only exception was the experiment doubling the variability of input price shocks. This has minor effects because imported inputs are only 10 percent of gross output, so that their share in GDP net of working capital is 11 percent ( $0.1/(1 - 0.1) = 0.11$ ). Thus, rising  $\sigma_{\epsilon P}$  from 3.4 to 6.8 percent increases net income variability just a notch.

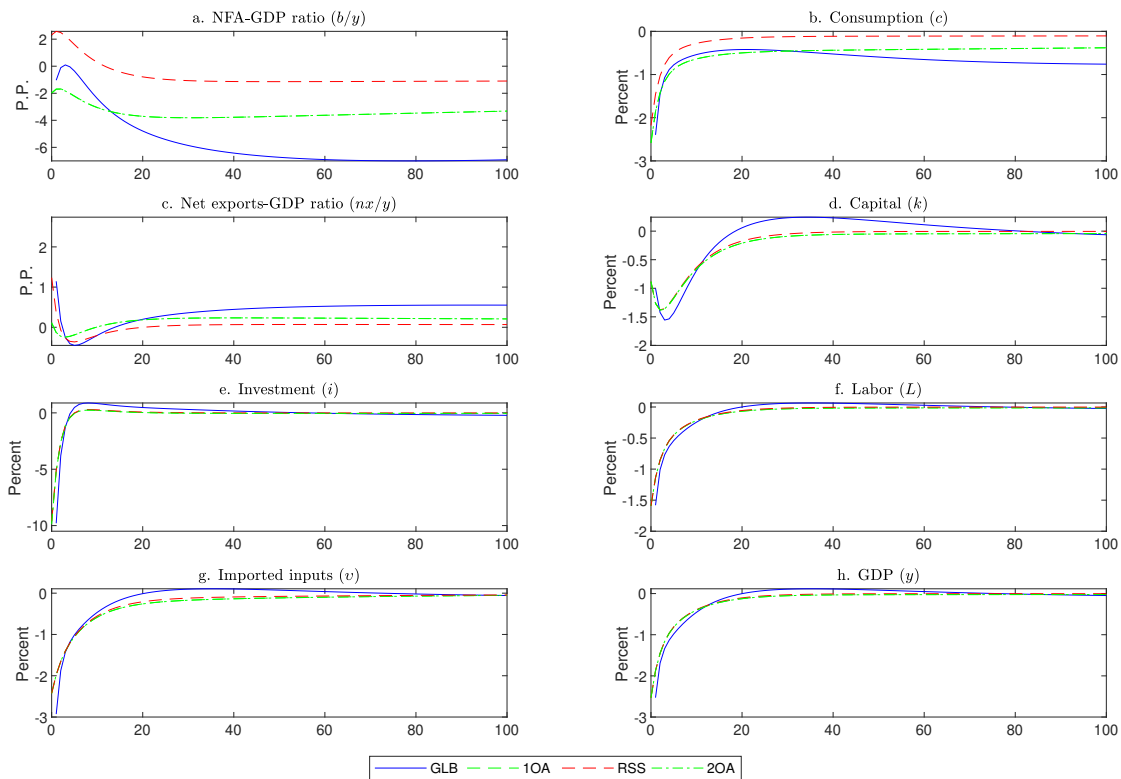
<sup>20</sup>We examine impulse response functions for interest-rate and input price shocks in Appendix D.

Table 8: Long-run Moments: RBC model

	GLB	Baseline Calibration		Targeted Calibration	
		2OA	RSS	2OA	RSS
$\psi =$	na	0.001	0.001	0.0109	0.008
<i>Averages</i>					
$E(y)$	393.847	397.269	396.190	397.370	397.210
$E(c)$	264.021	295.599	342.850	259.519	265.420
$E(i)$	67.53	68.631	67.747	68.666	68.063
$E(nx/y)$	0.045	-0.042	-0.185	0.065	0.046
$E(b/y)$	-0.372	0.732	2.559	-0.620	-0.397
$E(lev.rat.)$	-0.286	-0.237	-1.100	0.400	0.295
$E(v)$	42.649	43.009	42.852	43.021	42.975
$E(L)$	18.433	18.523	18.499	18.525	18.528
<i>Variability relative to variability of GDP</i>					
$\sigma(y)$	0.040	0.039	0.039	0.041	0.040
$\sigma(c)/\sigma(y)$	1.291	1.752	1.412	1.252	1.212
$\sigma(i)/\sigma(y)$	3.386	3.448	3.493	3.305	3.388
$\sigma(nx/y)/\sigma(y)$	0.885	1.389	1.212	0.718	0.731
$\sigma(b/y)/\sigma(y)$	7.589	15.064	12.909	3.822	4.269
$\sigma(lev.rat.)/\sigma(y)$	3.614	7.149	6.084	1.884	2.053
$\sigma(v)/\sigma(y)$	1.481	1.493	1.504	1.461	1.482
$\sigma(L)/\sigma(y)$	0.596	0.600	0.600	0.597	0.598
<i>Correlations with GDP</i>					
$\rho(y, c)$	0.773	0.613	0.509	0.928	0.904
$\rho(y, i)$	0.640	0.632	0.628	0.660	0.648
$\rho(y, nx/y)$	-0.227	-0.280	0.026	-0.476	-0.381
$\rho(y, b/y)$	0.090	0.207	-0.160	0.508	0.343
$\rho(y, lev.rat.)$	0.112	0.212	0.150	0.528	-0.366
$\rho(y, v)$	0.834	0.831	0.830	0.839	0.835
$\rho(y, L)$	0.995	0.995	0.995	0.995	0.995
<i>First-order autocorrelations</i>					
$\rho(y)$	0.830	0.825	0.820	0.841	0.853
$\rho(b)$	0.996	0.999	0.998	0.996	0.996
$\rho(c)$	0.885	0.947	0.918	0.874	0.862
$\rho(i)$	0.516	0.511	0.509	0.519	0.513
$\rho(nx/y)$	0.711	0.869	0.843	0.560	0.563
$\rho(lev.rat.)$	0.997	0.999	0.998	0.991	0.995
$\rho(v)$	0.780	0.777	0.774	0.788	0.782
$\rho(L)$	0.808	0.803	0.799	0.819	0.810
<i>Performance metrics</i>					
Time in sec.	61.0	2.5	40.6	2.5	39.6
ratio rel. to GLB	1.0	0.620	0.666	0.621	0.649
Max. Abs. $b$ Euler eq. error	1.17E-07	1.33E-07	6.21E-04	1.43E-07	1.13E-03
Max. Abs. $k$ Euler eq. error	3.84E-16	4.52E-07	8.92E-05	3.95E-07	6.59E-05
Decision rule diff $b$		0.089 (0.546)	0.089 (0.546)	0.081 (0.505)	0.081 (0.505)
Decision rule diff $k$		0.017 (0.051)	0.017 (0.051)	0.017 (0.049)	0.017 (0.049)
Decision rule diff $c$		0.019 (0.066)	0.019 (0.066)	0.019 (0.077)	0.019 (0.077)

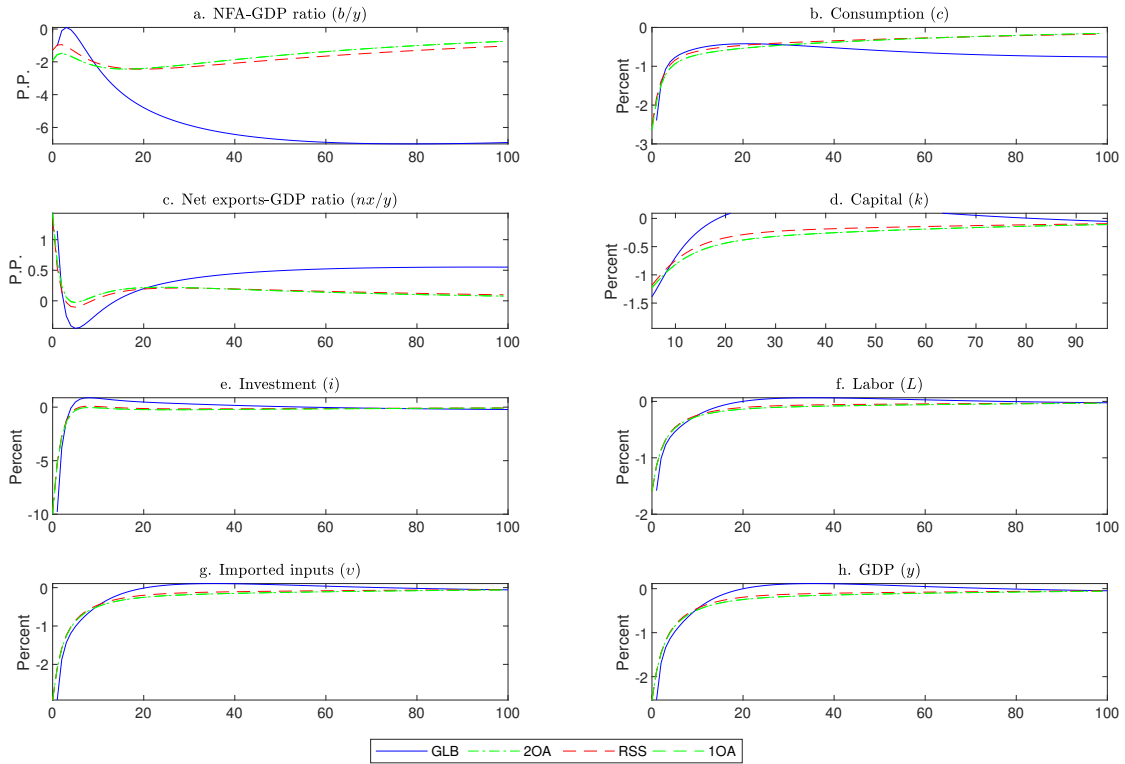
GLB, 2OA and RSS refer to the global, second-order and risky steady state solutions, respectively.  $\sigma(\cdot)$  denotes the coefficient of variation for variables in levels and the standard deviation for variables in ratios ( $nx/y$ ,  $b/y$  and the leverage ratio  $lev/rat.$ ). Euler equation errors and decision rule differences are computed for all  $(b, z)$  pairs in the state space of the GLB solution. Decision rule differences in the last two rows are differences between the local and GLB solutions in percent of the latter. We report mean and maximum (maximum in brackets) differences conditional on bond values that have positive probability in the ergodic distribution of the GLB solution.

Figure 11: RBC Impulse Response Functions to a Negative TFP shock: Baseline Calibration



Note: GLB, 1OA, 2OA, RSS refer to the global, first-order, second-order and risky-steady state solution, respectively. GLB impulse responses are forecast functions of the equilibrium Markov processes of the endogenous variables with initial conditions set to  $E[b]$ ,  $E[k]$  and a value of TFP equal to a one-standard-deviation shock. Variables are plotted as percent deviations from long-run means, with the exception of NFA and net exports, which are plotted as differences relative to their long-run means (since these variables are measured as GDP ratios, and hence are already in percent).

Figure 12: RBC Impulse Response Functions to a Negative TFP Shock: Targeted Calibration



Note: GLB, 1OA, 2OA, RSS refer to the global, first-order, second-order and risky-steady state solution, respectively.

For the baseline calibration, RSS yields markedly different responses for  $b/y$  (panel a.), consumption (panel b.) and the net exports-GDP ratio ( $nx/y$ ) (panel c.) than 2OA. This is because, as noted earlier, the gap between  $b^{rss}$  and  $b^{dss}$  is large enough to affect the results. However, since near-Fisherian separation still holds, the other variables (capital, investment, labor, imported inputs and GDP) display similar responses in the two local solutions.

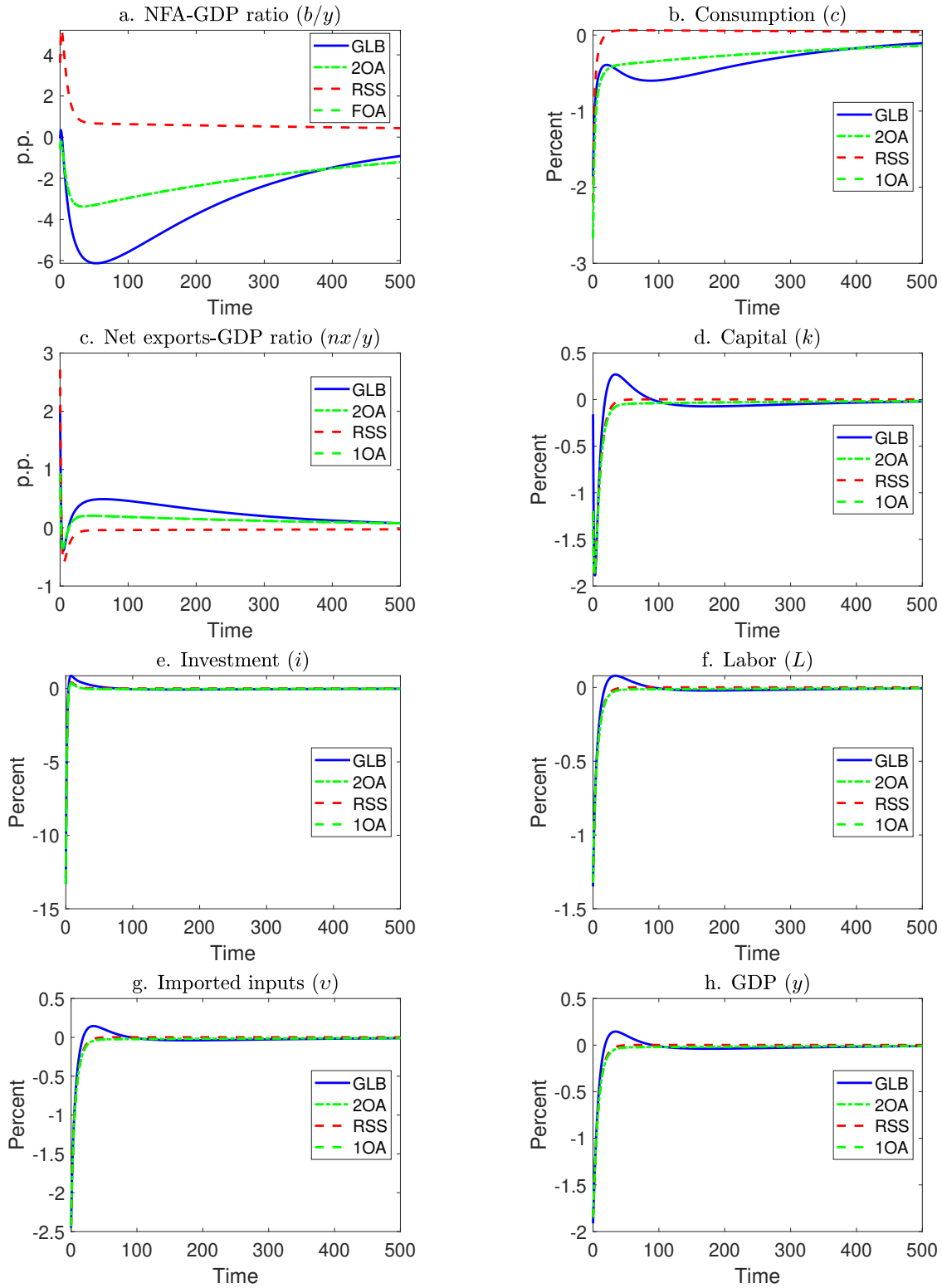
2OA and RSS baseline impulse responses differ sharply from those of the GLB solution. In particular, RSS overestimates the initial rise in  $b/y$  while 2OA underestimates it (see panel a.). In fact, RSS yields above-average  $b/y$  for the first 17 periods, while in both GLB and 2OA the NFA position is always below average. After the 15th period, the local solutions predict mean deviations of  $b/y$  that remain uniformly above the GLB solution until mean reversion is attained. These differences in NFA are reflected in differences in consumption and net exports (see panels b. and c.). Initially, the mean deviation of consumption under the GLB solution is lower (higher) than in the RSS (2OA) solution. After the 30th period, the GLB solution yields smaller mean deviations of

consumption than the two local solutions and the opposite is observed for the net exports-GDP ratio. Differences in investment, output and factors of production are smaller because near-Fisherian separation holds, but still capital falls slightly more initially in the GLB than in the local solutions, and then between periods 15 and 80 the GLB solution rises above the local ones. Since there is no wealth effect on labor supply, these differences in capital dynamics yield qualitatively similar but quantitatively smaller differences in labor, imported inputs and GDP.

Under the targeted calibrations (Figure 12), the gap between  $b^{rss}$  and  $b^{dss}$  becomes again too small to make a difference for 2OA and RSS impulse responses. Hence, our findings for the endowment and RBC models indicate that, if the choice is limited to local methods, 1OA is simpler and nearly identical to 2OA and RSS. Relative to the GLB solution, targeted local solutions still fail to match important features of GLB impulse responses. Initial differences are smaller than with the baseline solutions, and now  $b/y$  always shows negative deviations from its mean in all three solutions. Beyond the 15th to 20th period, however,  $b/y$ , consumption and the net exports-GDP ratio in the targeted solutions differ sharply from the GLB solution, with similar qualitative features as with respect to the baseline solutions, and in some cases with even larger quantitative differences. The reason for this is that, even though the targeted calibrations force the same  $\rho_b$  across global and local solutions, the required higher values of  $\psi$  imply that NFA has much less variability than in the GLB solution (see Table 8). The higher volatility with similar persistence in the GLB solution yield an impulse response for  $b/y$  that rises more initially and then drops more before returning to zero in the long run. In contrast, in the local solutions the high  $\psi$  values make large mean deviations in  $b/y$  too costly, and hence  $b/y$  never falls more than about 2 percentage points below its mean (v. about 7 percentage points in the GLB solution).

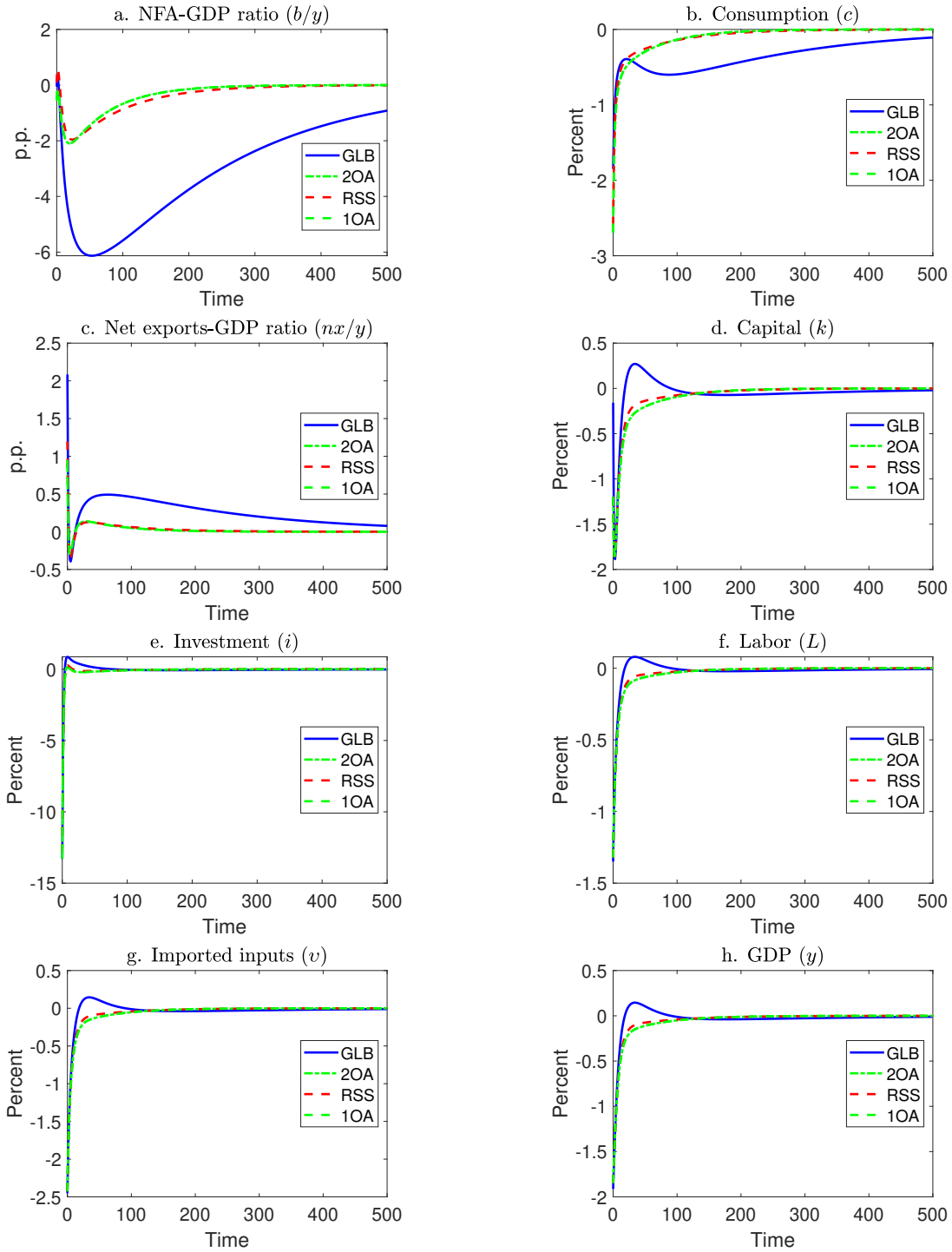
Next we complete the analysis of impulse response functions by adding to the analysis of TFP shocks described above a discussion of the impulse response functions for the other shocks. Figures 13 to 16 show the impulse responses to one-standard-deviation positive interest rate and one-standard-deviation negative imported input price shocks for both baseline and targeted calibrations. The results generally echo the findings obtained with TFP shocks. Focusing on the baseline calibration results, RSS yields markedly different responses for the NFA-GDP ratio (Panel a.), consumption (Panel b.) and the net exports-GDP ratio (Panel c.) than 2OA. This is because, as noted earlier, the gap between  $b^{rss}$  and  $b^{dss}$  is sufficiently large to affect the results. However, since near-Fisherian separation still holds, the other variables (capital, investment, labor, imported inputs and GDP) display similar responses in the two local solutions.

Figure 13: Impulse Response Functions to Interest Rate shocks: Baseline Calibration



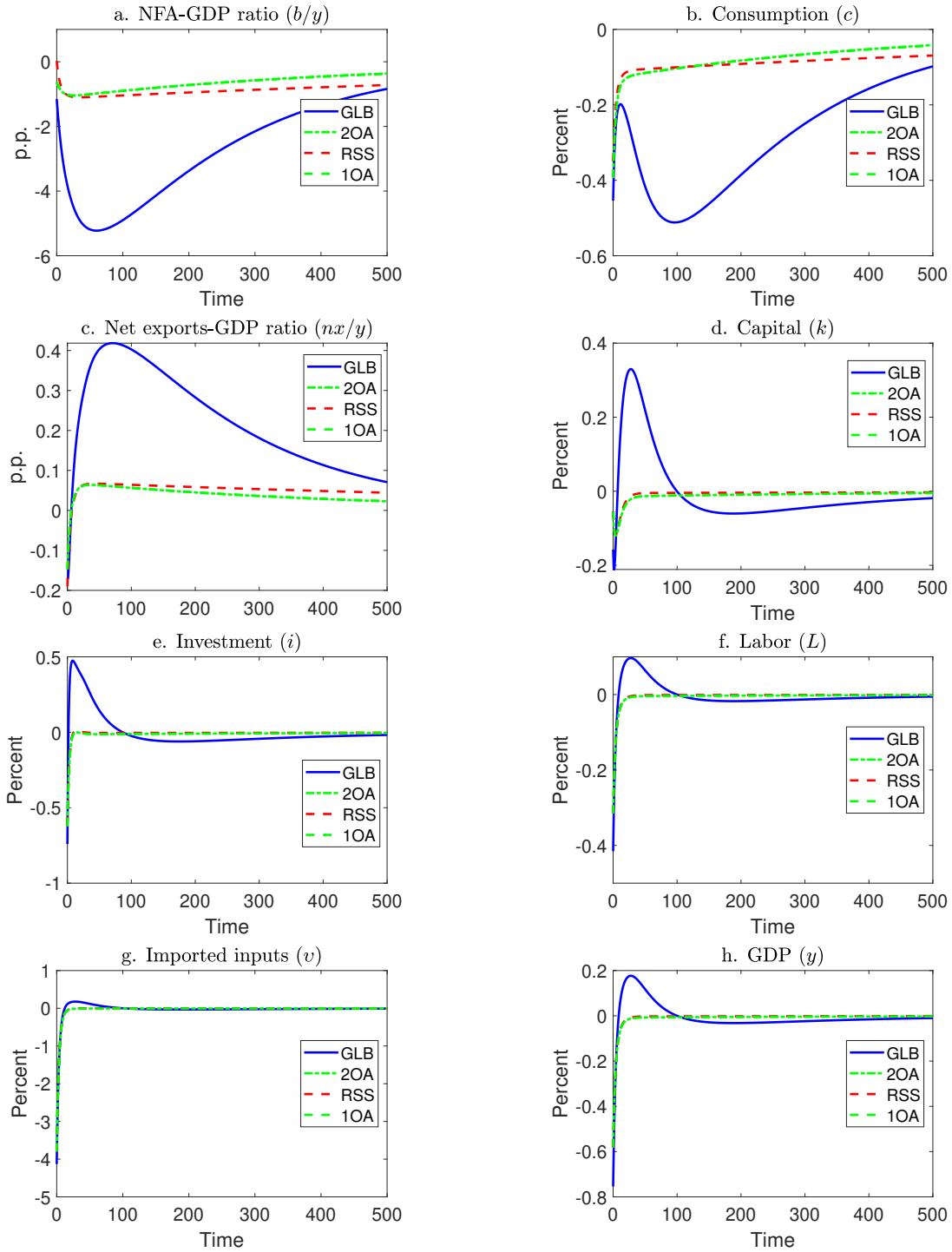
Note: These graphs show the impulse responses. GLB refers to global solution, 2OA refers to second-order solution, RSS refers to risky-steady state solution.

Figure 14: Impulse Response Functions to Interest Rate shocks: Targeted Calibration



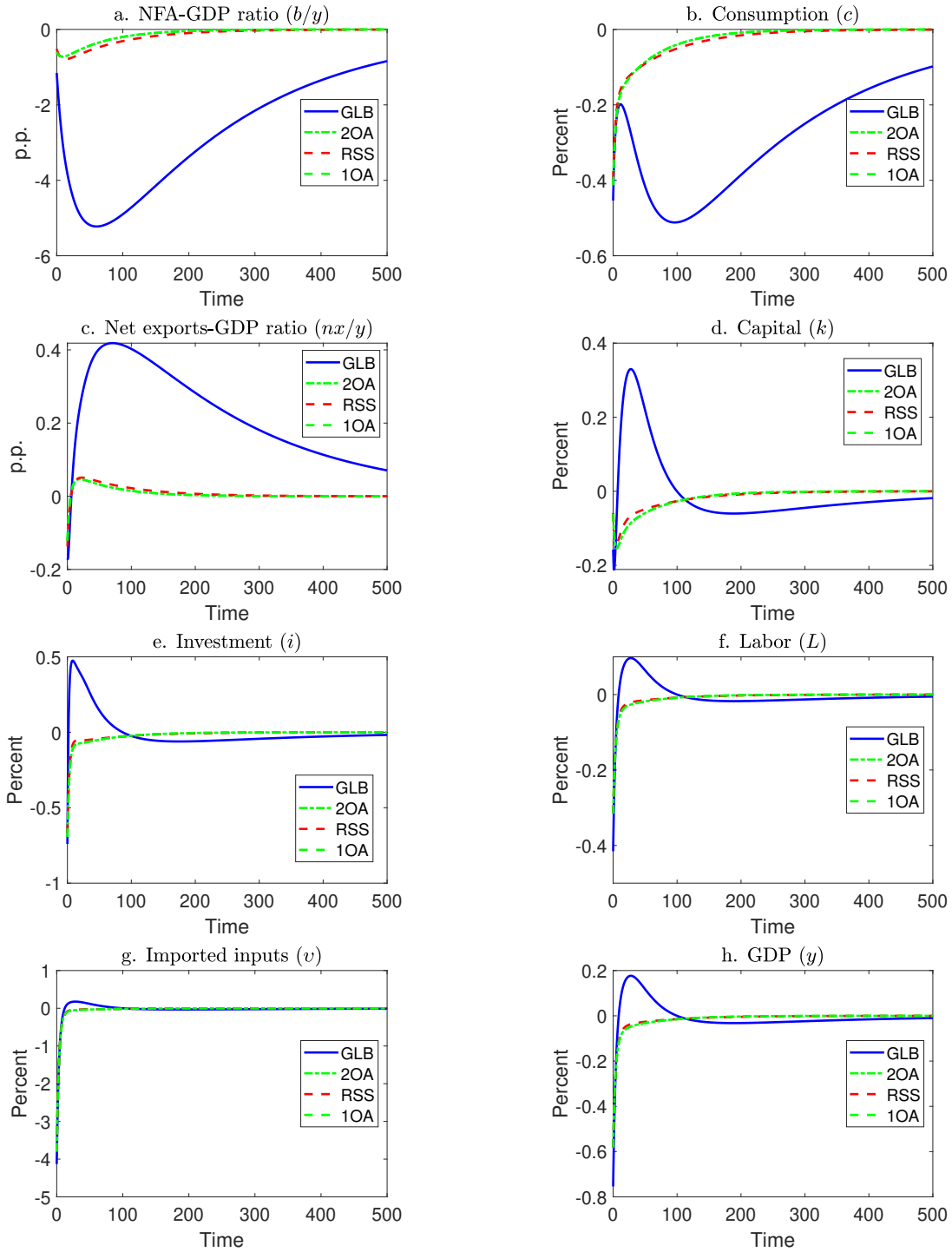
Note: These graphs show the impulse responses. GLB refers to global solution, 2OA refers to second-order solution, RSS refers to risky-steady state solution.

Figure 15: Impulse Response Functions to Imported Input Price shocks: Baseline Calibration



Note: These graphs show the impulse responses. GLB refers to global solution, 2OA refers to second-order solution, RSS refers to risky-steady state solution.

Figure 16: Impulse Response Functions to Imported Input Price shocks: Targeted Calibration



Note: These graphs show the impulse responses. GLB refers to global solution, 2OA refers to second-order solution, RSS refers to risky-steady state solution.

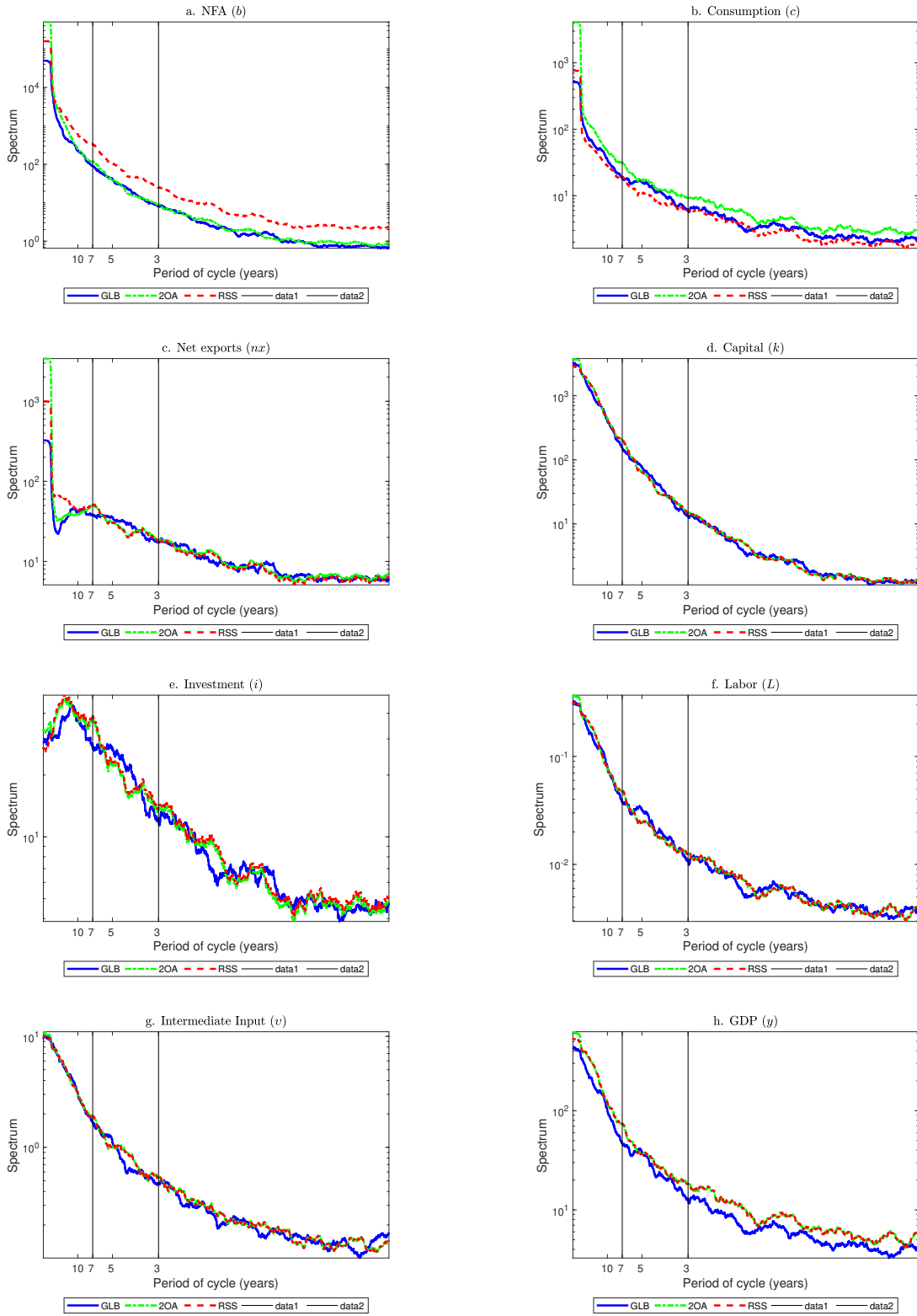
Impulse responses produced by baseline 2OA and RSS solutions differ sharply from those of the GLB solution. In particular, RSS overestimates the initial deviation of the NFA-GDP ratio relative to

its long-run mean while 2OA underestimates it (see panel a.). The local solutions remain uniformly above the GLB solution until mean reversion is attained. These differences in NFA are reflected in differences in consumption and net exports (see panels b. and c.). Differences in investment, output and factors of production are less noticeable because near-Fisherian separation holds, but still the capital stock declines slightly more initially in the GLB solution than in the local solutions. Since there is no wealth effect on labor supply, these differences in capital stock dynamics translate into qualitatively similar but quantitatively smaller differences in labor, intermediate goods and GDP. Under the targeted calibrations, the gap between  $b^{rss}$  and  $b^{dss}$  becomes again too small to make a difference for the 2OA and RSS results, so impulse responses for both look about the same. Relative to the GLB solution, the targeted local solutions still fail to match important features of the GLB impulse response functions. Initial differences are smaller than with the baseline solutions, and now the NFA-GDP ratio always shows negative deviations from its mean in all three solutions.

### C.3.4 Spectral analysis

Figures 17 and 18 show nonparametric periodograms for key variables of the RBC model. As with the endowment model, all the periodograms are downward sloping, indicating that lower frequencies contribute more to the variability of the simulated data than business cycle and higher frequencies. In contrast with the endowment model, however, 2OA and RSS yield different periodograms for NFA, consumption and net exports under the baseline calibration, because in the RBC baseline calibration the gap between  $b^{rss}$  and  $b^{dss}$  is large enough for 2OA and RSS results to differ. The other periodograms for 2OA and RSS are similar because of the near-Fisherian-separation property noted earlier. Relative to the GLB solution, 2OA and RSS periodograms show differences that are less stark than for the endowment model, but RSS still overstates the contribution of business cycle and higher frequencies to the variability of NFA, and 2OA and RSS still overstate the contribution of very low frequencies to the variability of NFA, consumption and net exports, as well as the contribution of business cycle and higher frequencies to GDP variability.

Figure 17: Spectral Density Functions for the RBC model: Baseline Calibration



Note: These graphs show parametric estimates of spectral density functions. GLB, 2OA, and RSS refer to the global, second-order and risky-steady state solution, respectively.

For the targeted calibrations, the 2OA and RSS periodograms are nearly identical, reflecting the result that in this case the gap between  $b^{rss}$  and  $b^{dss}$  is too small to affect the results. Relative to the GLB solution, both RSS and 2OA yield periodograms that approximate their GLB counterparts better than under the baseline calibration, in line with what we found for the endowment model. The local methods underestimate slightly overall NFA and GDP variability. The periodograms for investment and factors of production are very similar to those under both the GLB solution and the local baseline calibrations, again because of the near-Fisherian-separation property.

In summary, the RBC model yields several key results in line with those obtained with the endowment model: Local methods do poorly at quantifying the effects of precautionary savings. Local methods with baseline calibrations yield very different results than the global solution for consumption, net exports and NFA. Targeted calibrations perform better but targeting  $\psi$  requires solving the model globally to determine the value of  $\rho_b$ , and this needs to be re-done for any parameter variation. 1OA and 2OA yield nearly identical results (other than first moments), because they have identical first-order terms and the second-order terms of the 2OA solution (other than the variance term) are quantitatively irrelevant.

The RBC results differ from the endowment model results in that 2OA and RSS solutions with baseline calibrations differ significantly, because  $b^{rss}$  and  $b^{dss}$  differ enough to yield non-negligible differences in first-order coefficients of the decision rules. In the targeted calibrations, however,  $b^{rss}$  and  $b^{dss}$  are close again, and hence 2OA and RSS solutions are very similar. Thus, with targeted calibrations, 1OA, 2OA and RSS solutions differ only in their first moments, while higher-order moments, impulse responses and spectral density functions are nearly identical. This makes 1OA the preferable local method if first moments are not being studied. A second important difference relative to the endowment model results is that the targeted local solutions are less accurate at approximating the GLB solution results for NFA, consumption and net exports. This is because the required  $\psi$  values make fluctuations in NFA costly, which reduces NFA variability to about half of that in the GLB solution. Investment, output and factor allocations are similar across global and local solutions because Fisherian separation of savings and investment nearly holds.

### C.3.5 Sensitivity Analysis

Table 9 compares the targeted calibration results shown in the paper (Panel (a)) with results for experiments doubling the standard deviation of TFP, interest rate and input price shocks, one at a time keeping the other two at their calibrated values (Panels (b), (c) and (d)). Doubling the vari-

ability of imported input prices has minor effects on all the cyclical moments (compare Panels (a) and (d)). This is because imported inputs are only 10 percent of gross output, so that their share in GDP net of working capital costs is 11 percent ( $0.1/(1 - 0.1) = 0.11$ ). Thus, increasing  $\sigma_{\epsilon^p}$  from 3.4 to 6.8 percent increases net income variability just a notch.<sup>21</sup>

Comparing Panels (b) and (c) with Panel (a) yields findings similar to those obtained for the endowment model: Higher TFP and interest rate variability increases income variability, and therefore induces a large increase in the average NFA-GDP ratio because of a stronger precautionary savings motive, which the local solutions fail to capture (except the RSS solution for the higher variability of interest rate shocks). In the global solutions, doubling the standard deviation of TFP (interest rate) shocks increases the variability of GDP from 4 to 6.1 (5.7) percent, and the mean NFA-GDP ratio rises by 45.6 (81.4) percentage points. The RSS and 2OA solutions yield similar increases in GDP variability (again because Fisherian separation nearly holds), but underestimate significantly the increase in the mean NFA-GDP ratio (except for the RSS case in Panel (c)). In addition, the local solutions underestimate the variability of NFA and net exports, overestimate (underestimate) the correlations of NFA and consumption (net exports) with GDP, and underestimate the autocorrelation of net exports. In short, changing the variability of the shocks worsens markedly the ability of the local solutions with targeted calibrations to approximate the global solutions.

We also conducted robustness analysis for variations in the coefficient of relative risk aversion, the correlation between interest rate and TFP shocks, and the subjective discount factor (see Table 10). The implications are similar as those described above. A higher CRRA coefficient or higher  $\beta$  strengthen precautionary savings, resulting in much larger increases in the mean NFA-GDP ratio with the global solutions than the local solutions with targeted calibrations. For changes in  $\beta$  particularly, the local solutions remain unchanged because they cannot accommodate variations in the discount factor that deviate from the inverse of the steady-state interest rate.

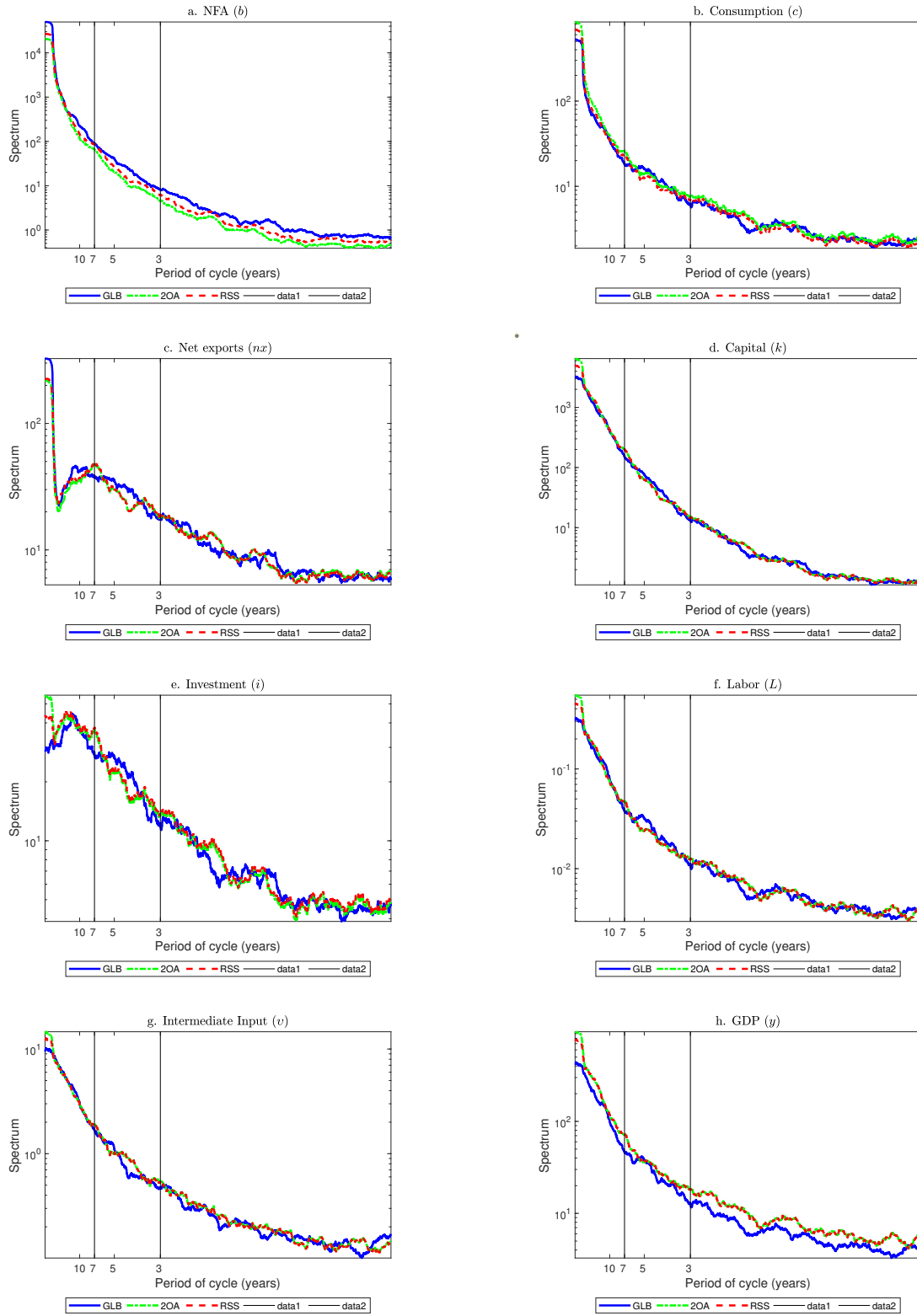
In summary, this sensitivity analysis of the RBC model shows that, as was the case with the sensitivity analysis of the endowment model, local solutions with a fixed value of  $\psi$  (set to match the value of  $\rho_b$  in the baseline GLB solution) are not useful for analyzing the effects of parameter changes, because they yield solutions that differ sharply from GLB solutions for the same parameter variations. Keeping the local solutions close to the GLB solutions would require solving the

---

<sup>21</sup>With inelastic labor, one can show that 1.2% ( $0.11^2$ ) of  $\sigma_{\epsilon^p}^2$  is added to the variance of GDP net working capital costs.

model globally each time a parameter is altered to pin down the corresponding new value of  $\rho_b$ , and then re-targeting the value of  $\psi$  in the local solutions to match it.

Figure 18: Spectral Density Functions for the RBC model: Targeted Calibrations



Note: These graphs show parametric estimates of spectral density functions. GLB, 2OA, and RSS refer to the global, second-order and risky-steady state solution, respectively.

Table 9: RBC Model Sensitivity Analysis: Higher Variability of Shocks

	(a) Targeted Calibration			(b) High TFP Vol.			(c) High Int. Rate Vol.			(d) High Inp. Price Vol.		
	GLB	2OA	RSS	GLB	2OA	RSS	GLB	2OA	RSS	GLB	2OA	RSS
<i>Average</i>												
$E(b/y)$	-0.372	-0.62	-0.397	0.149	-0.552	-0.231	0.422	-0.312	0.45	-0.339	-0.617	-0.39
<i>Variability</i>												
$\sigma(y)$	0.04	0.041	0.04	0.061	0.064	0.062	0.055	0.061	0.058	0.041	0.043	0.042
$\sigma(c)/\sigma(y)$	1.291	1.268	1.212	1.206	1.214	1.163	1.109	1.302	1.008	1.3	1.263	1.213
$\sigma(i)/\sigma(y)$	3.386	3.32	3.388	2.406	2.359	2.378	4.652	4.272	4.479	3.275	3.191	3.254
$\sigma(nx/y)/\sigma(y)$	0.885	0.712	0.731	0.827	0.514	0.544	1.246	0.962	0.979	0.894	0.693	0.716
$\sigma(b/y)/\sigma(y)$	7.589	3.758	4.269	9.012	4.099	4.817	9.48	3.333	3.231	8.01	3.847	4.433
$\sigma(lev.rat.)/\sigma(y)$	3.614	1.849	2.053	4.269	1.995	2.306	4.518	1.647	1.465	3.809	1.887	2.129
$\sigma(v)/\sigma(y)$	1.481	1.463	1.482	1.254	1.233	1.244	1.353	1.304	1.329	2.157	2.142	2.185
$\sigma(L)/\sigma(y)$	0.596	0.596	0.598	0.581	0.579	0.579	0.623	0.611	0.616	0.594	0.592	0.593
<i>Correlations with GDP</i>												
$\rho(y, c)$	0.773	0.929	0.904	0.671	0.911	0.877	0.579	0.926	0.887	0.752	0.925	0.898
$\rho(y, i)$	0.64	0.661	0.648	0.726	0.773	0.753	0.558	0.55	0.533	0.634	0.658	0.644
$\rho(y, nx/y)$	-0.227	-0.476	-0.381	0.034	-0.43	-0.278	0.023	-0.402	-0.157	-0.189	-0.456	-0.359
$\rho(y, b/y)$	0.09	0.511	0.343	0.025	0.595	0.429	-0.408	0.358	-0.427	0.087	0.527	0.365
$\rho(y, lev.rat.)$	0.112	-0.532	-0.366	0.041	-0.552	-0.401	-0.432	-0.459	0.362	0.106	-0.537	-0.378
$\rho(y, v)$	0.834	0.839	0.835	0.9	0.908	0.904	0.893	0.904	0.898	0.732	0.734	0.732
$\rho(y, L)$	0.995	0.995	0.995	0.998	0.998	0.998	0.989	0.99	0.99	0.995	0.995	0.995
<i>Autocorrelations</i>												
$\rho(y)$	0.83	0.841	0.832	0.732	0.763	0.747	0.905	0.913	0.903	0.827	0.84	0.831
$\rho(b)$	0.996	0.996	0.996	0.999	0.997	0.998	0.993	0.99	0.976	0.997	0.996	0.996
$\rho(c)$	0.885	0.873	0.862	0.896	0.879	0.872	0.847	0.865	0.791	0.893	0.879	0.87
$\rho(i)$	0.516	0.519	0.513	0.515	0.54	0.525	0.507	0.508	0.503	0.517	0.522	0.515
$\rho(nx/y)$	0.711	0.555	0.563	0.885	0.722	0.742	0.657	0.482	0.465	0.737	0.569	0.581
$\rho(lev.rat.)$	0.997	0.991	0.995	0.998	0.995	0.997	0.992	0.984	0.985	0.998	0.992	0.996
$\rho(v)$	0.78	0.788	0.782	0.729	0.752	0.74	0.834	0.846	0.836	0.762	0.767	0.763
$\rho(L)$	0.808	0.819	0.81	0.723	0.753	0.738	0.869	0.88	0.868	0.807	0.82	0.811

Note: GLB, 2OA and RSS refer to the global, second-order and risky-steady state solutions, respectively. Panel (a) shows the targeted calibration results. Panels (b), (c) and (d) show results doubling the standard deviations of shocks to TFP, interest rate and input prices relative to their calibrated values.

Table 10: RBC Model Sensitivity Analysis: Changes in Preference Parameters and TFP-Interest Rate Correlation.

	(a) Targeted Calibration			(b) Higher CRRA			(c) Higher TFP Int. Rate Corr.			(c) Higher $\beta$		
	GLB	2OA	RSS	GLB	2OA	RSS	GLB	2OA	RSS	GLB	2OA	RSS
<i>Average</i>												
$\mu(b/y)$	-0.372	-0.62	-0.397	-0.255	-0.587	-0.324	-0.365	-0.613	-0.379	0.111	-0.62	-0.397
<i>Variability</i>												
$\sigma(y)$	0.04	0.041	0.04	0.04	0.042	0.04	0.041	0.042	0.041	0.039	0.041	0.04
$\sigma(c)/\sigma(y)$	1.291	1.268	1.212	1.356	1.303	1.237	1.299	1.28	1.218	1.547	1.268	1.212
$\sigma(i)/\sigma(y)$	3.386	3.32	3.388	3.383	3.282	3.371	3.337	3.281	3.349	3.438	3.32	3.388
$\sigma(nx/y)/\sigma(y)$	0.885	0.712	0.731	0.904	0.705	0.729	0.789	0.673	0.687	1.208	0.712	0.731
$\sigma(b/y)/\sigma(y)$	7.589	3.758	4.269	9.133	4.392	5.01	7.47	3.739	4.206	13.178	3.758	4.269
$\sigma(lev.rat.)/\sigma(y)$	3.614	1.849	2.053	4.348	2.169	2.413	3.563	1.85	2.031	6.232	1.849	2.053
$\sigma(v)/\sigma(y)$	1.481	1.463	1.482	1.481	1.448	1.475	1.469	1.449	1.469	1.495	1.463	1.482
$\sigma(L)/\sigma(y)$	0.596	0.596	0.598	0.597	0.595	0.597	0.6	0.599	0.601	0.599	0.596	0.598
<i>Correlations with GDP</i>												
$\rho(y, c)$	0.773	0.929	0.904	0.713	0.921	0.888	0.791	0.939	0.916	0.541	0.929	0.904
$\rho(y, i)$	0.64	0.661	0.648	0.637	0.666	0.65	0.688	0.707	0.696	0.625	0.661	0.648
$\rho(y, nx/y)$	-0.227	-0.476	-0.381	-0.121	-0.503	-0.385	-0.223	-0.562	-0.462	0.002	-0.476	-0.381
$\rho(y, b/y)$	0.09	0.511	0.343	0.083	0.548	0.369	0.106	0.524	0.351	-0.053	0.511	0.343
$\rho(y, lev.rat.)$	0.112	-0.532	-0.366	0.094	-0.565	-0.388	0.117	-0.55	-0.379	-0.056	-0.532	-0.366
$\rho(y, v)$	0.834	0.839	0.835	0.834	0.843	0.836	0.841	0.846	0.842	0.831	0.839	0.835
$\rho(y, L)$	0.995	0.995	0.995	0.995	0.995	0.995	0.996	0.996	0.996	0.995	0.995	0.995
<i>Autocorrelations</i>												
$\rho(y)$	0.83	0.841	0.832	0.832	0.847	0.835	0.838	0.848	0.838	0.825	0.841	0.832
$\rho(b)$	0.996	0.996	0.996	0.996	0.997	0.997	0.996	0.997	0.997	0.997	0.996	0.996
$\rho(c)$	0.885	0.873	0.862	0.915	0.899	0.889	0.886	0.873	0.861	0.929	0.873	0.862
$\rho(i)$	0.516	0.519	0.513	0.517	0.525	0.515	0.517	0.52	0.513	0.511	0.519	0.513
$\rho(nx/y)$	0.711	0.555	0.563	0.821	0.605	0.612	0.774	0.568	0.573	0.883	0.555	0.563
$\rho(lev.rat.)$	0.997	0.991	0.995	0.998	0.994	0.997	0.998	0.992	0.996	0.999	0.991	0.995
$\rho(v)$	0.78	0.788	0.782	0.781	0.793	0.784	0.783	0.791	0.784	0.777	0.788	0.782
$\rho(L)$	0.808	0.819	0.81	0.812	0.826	0.813	0.813	0.822	0.812	0.805	0.819	0.81

Note: GLB, 2OA and RSS denote the global, second-order and risky-steady state solutions, respectively. Panel (a) shows the targeted calibrations results, (b) increases the CRRA coefficient to 2.5 from 2.0, (c) increases the correlation of TFP and interest rate shocks to  $-0.8$  from  $-0.669$ , and (c) increases the discount factor to 0.921 from 0.920.

## C.4 Quantitative results of the Sudden Stops model

The main results for the Sudden Stops model is presented in the main draft. Here we discuss additional quantitative results.

### C.4.1 Spectral analysis

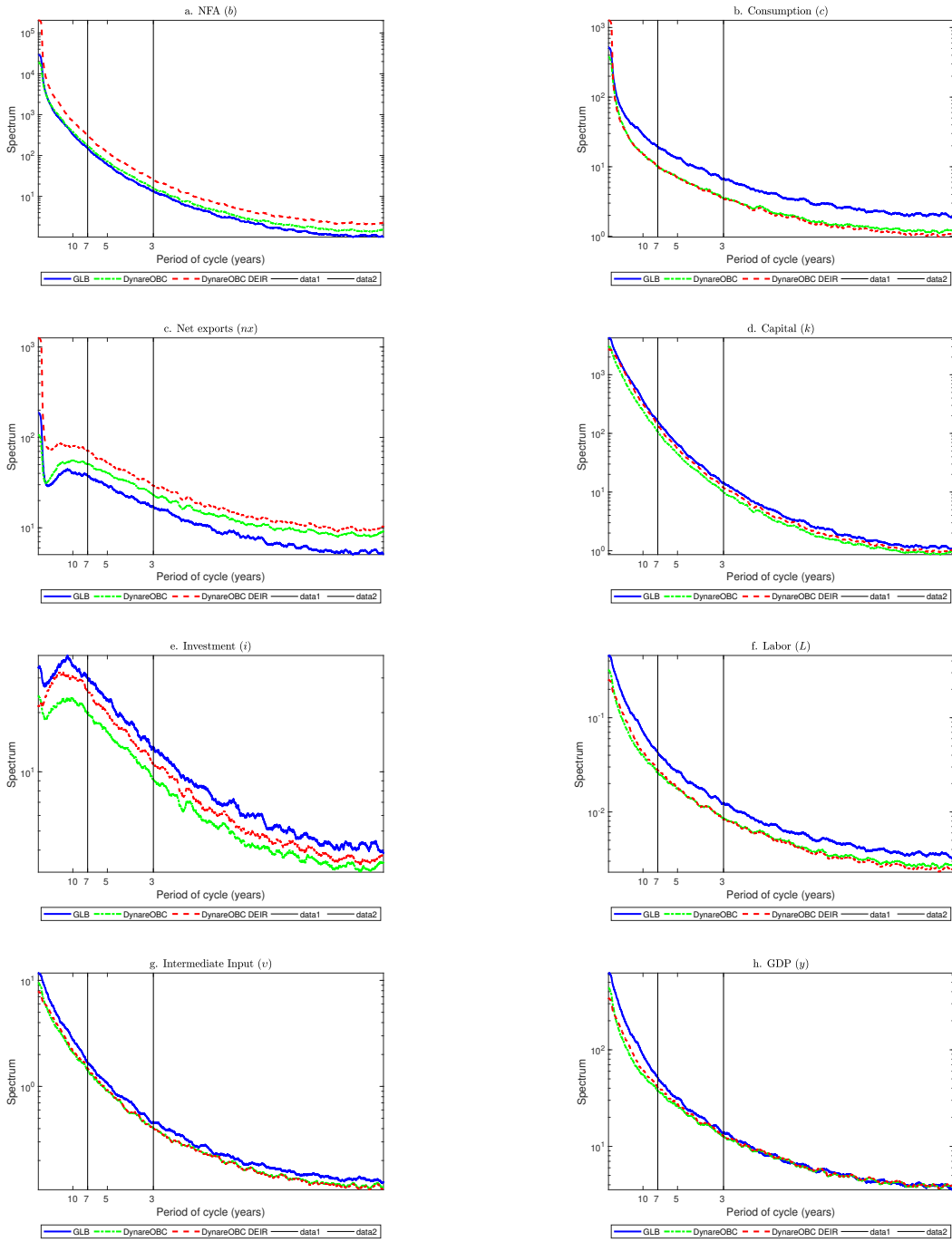
Figure 19 shows the nonparametric periodograms for the DynareOBC and GLB solutions. As in the endowment and RBC models, since all of the variables follow AR(1)-like processes, the periodograms are generally downward sloping, indicating that low frequencies account for a larger fraction of the variance of the variables than business cycle and higher frequencies. Moreover, the periodograms for the GLB solution are very similar to those for the RBC GLB solution, in line with the finding that the GLB impulse responses of the RBC and SS models are similar because the credit constraint binds infrequently. The periodograms of the DynareOBC solution differ from those of the 2OA and RSS solutions of the RBC model, so the local methods fail to match the property of the GLB solutions that spectral densities of the RBC and SS models are similar.

The DynareOBC periodograms for NFA, consumption, net exports, investment and labor differ sharply from the GLB results. Consumption has the highest variance in the GLB solution (121.4), followed by DynareOBC-DEIR (119.2) and DynareOBC- $\beta R < 1$  with a much lower variance (65.8). In contrast, the autocorrelation of consumption is highest in DynareOBC-DEIR (0.91) and about the same in GLB and DynareOBC- $\beta R < 1$  (0.83). As a result, the consumption periodograms for the latter two have the same intercept but the one for GLB is uniformly higher otherwise, while the periodogram for DynareOBC-DEIR has the highest intercept but is generally below the periodogram for GLB. The DynareOBC solutions assign significantly less consumption variability to business cycle and lower frequencies than the GLB solution. Net exports also show higher persistence in the DynareOBC-DEIR solution while DynareOBC- $\beta R < 1$  and GLB have similar persistence, and opposite from what we observe for consumption, the GLB solution has less overall variance and less variability at all frequencies. Investment has higher variance and persistence in the GLB than in the local solutions, and it has uniformly higher variability at all frequencies.

### C.4.2 *FiPit* v. DynareOBC speed comparisons

Table 11 provides additional comparisons of execution times for alternative specifications of the DynareOBC and *FiPit* solutions. As explained in the paper, on one hand, *FiPit* suffers from the

Figure 19: Spectral Density Functions for the Sudden Stops Model



curse of dimensionality typical of GLB methods related to the number of state variables, and more so if the model specification requires using a root-finder when the constraint binds. But once the decision rules are solved for, generating stochastic time-series simulations is very fast. On the other hand, the number of state variables is much less of an issue for DynareOBC, but execution

time rises with the required length of extended perfect-foresight paths for each date- $t$  solution, the length of the full time-series simulation needed for convergence of long-run moments, and the iterations required to compute the news-shocks sequences that implement the constraint.

Table 11: Execution Times: Sudden Stops model

Execution time	
<i>Baseline</i>	
GLB	268.0
DynareOBC	243.5
<i>150,000 period simulations</i>	
GLB	268.0
DynareOBC	350.9
<i><math>\kappa</math> 0.3</i>	
GLB	137.3
DynareOBC	228.4
<i>TFP shock only</i>	
GLB	41.7
DynareOBC	229.9

Note: This table shows the execution times with alternative assumptions for the GLB and DynareOBC with  $\beta R < 1$  solutions. See Table 5 in the main text for the information on the hardware used to record these metrics.

The above tradeoffs between the two algorithms is illustrated by the results shown in Table 11. First-order DynareOBC is much slower than *FiPIt* if the simulation length rises to 150,000 periods (350 seconds v. 268 seconds) or with fewer exogenous shocks so that the curse of dimensionality is less severe for the global solution (with TFP shocks only, *FiPIt* solves in 42 seconds v. 230 seconds with DynareOBC). Increasing borrowing capacity by setting  $\kappa$  to 0.3 also results in *FiPIt* solving much faster than DynareOBC (137 v. 228 seconds).

### C.4.3 Financial premia & quintile analysis for Sudden Stops model

The financial premia for the *FiPIt* solution are computed using their recursive representations. For each coordinate in the state space  $(b, k, \varepsilon)$ , we used the recursive representation of equations (20) and (21) of the paper and the recursive optimal decision rules to obtain the following expressions for the shadow interest premium (*SIP*), the equity premium (*EP*), the risk component of the equity premium (*RP*) and the covariance between marginal utility and equity returns (*COV*):

$$SIP(b, k, \varepsilon) = \frac{R\mu(b, k, \varepsilon)(1 + \tau)}{u'(c(b, k, \varepsilon)) - \mu(b, k, \varepsilon)(1 + \tau)}, \quad (163)$$

$$EP_{\varepsilon'}(b, k, \varepsilon)(b, k, \varepsilon) = E_{\varepsilon'}[R^q(b'(b, k, \varepsilon), k'(b, k, \varepsilon), \varepsilon')] - R, \quad (164)$$

$$\begin{aligned} COV_{\varepsilon'}(b, k, \varepsilon) &= E_{\varepsilon'} \left\{ \left[ u'(c(b'(b, k, \varepsilon), k'(b, k, \varepsilon), \varepsilon')) - E_{\varepsilon'}(u'(c(b'(b, k, \varepsilon), k'(b, k, \varepsilon), \varepsilon')))) \right] \right. \\ &\quad \left. \times \left[ R^q(b'(b, k, \varepsilon), k'(b, k, \varepsilon), \varepsilon') - E_{\varepsilon'}(R^q(b'(b, k, \varepsilon), k'(b, k, \varepsilon), \varepsilon')) \right] \right\} \end{aligned} \quad (165)$$

$$RP_{\varepsilon'}(b, k, \varepsilon) \equiv -\frac{COV_{\varepsilon'}(b, k, \varepsilon)}{E_{\varepsilon'}[u'(c(b'(b, k, \varepsilon), k'(b, k, \varepsilon), \varepsilon'))]}. \quad (166)$$

The conditional expectations and covariance terms in the above expressions are calculated taking expectations over  $\varepsilon'$  using the Markov transition probabilities  $\pi(\varepsilon, \varepsilon')$ :

The means of the financial premia conditional on the quintile distribution of  $\mu > 0$  reported in the paper are constructed as follows: First, we construct the quintile distribution of  $\mu(b, k, \varepsilon) > 0$  using the ergodic distribution  $P(b, k, \varepsilon)$  produced by the *FiPit* algorithm. To compute this quintile distribution, we start by sorting the values of  $\mu(b, k, \varepsilon)$  by size removing all those that are zero. The ergodic distribution of  $\mu(b, k, \varepsilon) > 0$  is given by  $P(b, k, \varepsilon) / \sum_{\{(b, k, \varepsilon); \mu(b, k, \varepsilon) > 0\}} P(b, k, \varepsilon)$ . The associated cumulative ergodic distribution of  $\mu(b, k, \varepsilon) > 0$  is denoted  $CumP_{\mu > 0}(b, k, \varepsilon)$ . Then we assign the values of  $\mu(b, k, \varepsilon) > 0$  into quintiles by identifying the values of  $\mu$  associated with the quintile boundaries at which  $CumP_{\mu > 0}(b, k, \varepsilon) = 0.2, 0.4, 0.6, 0.8, 1$  and then allocating each value of  $\mu(b, k, \varepsilon) > 0$  into its corresponding quintile using these boundaries. Each value of  $\mu(b, k, \varepsilon) > 0$  has associated with it a value for each of the financial premia indicators shown above, since both  $\mu$  and the financial premia are recursive functions of the state variables. Hence, once the quintile distribution of  $\mu(b, k, \varepsilon) > 0$  is formed, the means of the financial premia for each quintile are computed by taking averages using the probability distribution of  $(b, k, \varepsilon)$  within each quintile (i.e., ergodic distributions scaled by the cumulative probability of being in each quintile) and we can also compute means across the entire quintile distribution, which are the same as means conditional on  $\mu(b, k, \varepsilon) > 0$ .

For DynareOBC, we use time-series simulations to construct the financial premia indicators. It is not feasible to construct conditional expectations, so we use realized values over the time-series simulations. To construct the quintile distribution of  $\mu > 0$ , we find the quintile boundaries for the subset of the full time-series simulation solution for which  $\mu_t > 0$ , and associate with each value  $\mu_t$  allocated to each quintile the corresponding values of  $SIP_t, EP_t, COV_t, RP_t$ . Then we compute within-quintile means of these financial premia as the averages of the values allocated to each quintile, and we can also compute averages across all five quintiles which are equivalent to averages conditional on  $\mu_t > 0$ .

## References

- ADJEMIAN, S. AND M. JUILLARD (2013): "Stochastic extended path approach," *Unpublished manuscript*.
- AGUIAR, M. AND G. GOPINATH (2007): "Emerging market business cycles: The cycle is the trend," *Journal of Political Economy*, 115, 69–102.
- ANDREASEN, M. M., J. FERNÁNDEZ-VILLAVERDE, AND J. F. RUBIO-RAMÍREZ (2018): "The pruned state-space system for non-linear DSGE models: Theory and empirical applications," *Review of Economic Studies*, 85, 1–49.
- ARELLANO, C. (2008): "Default risk and income fluctuations in emerging economies," *American Economic Review*, 98, 690–712.
- BENIGNO, G., H. CHEN, C. OTROK, A. REBUCCI, AND E. R. YOUNG (2016): "Optimal capital controls and real exchange rate policies: A pecuniary externality perspective," *Journal of Monetary Economics*, 84, 147–165.
- BIANCHI, J. (2011): "Overborrowing and systemic externalities in the business cycle," *American Economic Review*, 101, 3400–3426.
- BIANCHI, J. AND E. G. MENDOZA (2018): "Optimal, Time-Consistent Macroprudential Policy," *Journal of Political Economy*, 126, 588–634.
- COEURDACIER, N., H. REY, AND P. WINANT (2011): "The risky steady state," *American Economic Review*, 101, 398–401.
- COLLARD, F. AND M. JUILLARD (2001): "Accuracy of stochastic perturbation methods: The case of asset pricing models," *Journal of Economic Dynamics and Control*, 25, 979–999.
- DE GROOT, O. (2013): "Computing the risky steady state of DSGE models," *Economics Letters*, 120, 566–569.
- (2014): "The risky steady state and multiple (spurious) equilibria: The case of the small open economy model," *Unpublished manuscript*.
- DURDU, C. B., E. G. MENDOZA, AND M. E. TERRONES (2009): "Precautionary demand for foreign assets in Sudden Stop economies: An assessment of the New Mercantilism," *Journal of Development Economics*, 89, 194–209.
- GUERRIERI, L. AND M. IACOVIELLO (2015): "OccBin: A toolkit for solving dynamic models with occasionally binding constraints easily," *Journal of Monetary Economics*, 70, 22–38.
- HAMILTON, J. (1994): *Time series econometrics*, Princeton University Press.
- HOLDEN, T. AND M. PAETZ (2012): "Efficient simulation of DSGE models with inequality constraints,"

- Unpublished manuscript.*
- HOLDEN, T. D. (2016): "Computation of solutions to dynamic models with occasionally binding constraints," *Unpublished manuscript.*
- JUDD, K. L. AND K. L. JUDD (1998): *Numerical methods in economics*, MIT press.
- JUILLARD, M. (2011): "Local approximation of DSGE models around the risky steady state," *Unpublished manuscript.*
- LANE, P. R. AND G. M. MILESI-FERRETTI (2007): "The external wealth of nations mark II: Revised and extended estimates of foreign assets and liabilities, 1970–2004," *Journal of International Economics*, 73, 223–250.
- LASÉEN, S. AND L. SVENSSON (2011): "Anticipated alternative policy-rate paths in policy simulations," *Unpublished manuscript.*
- LEVHARI, D. AND T. N. SRINIVASAN (1969): "Optimal savings under uncertainty," *The Review of Economic Studies*, 36, 153–163.
- MCGRATTAN, E. R. (1996): "Solving the stochastic growth model with a finite element method," *Journal of Economic Dynamics and Control*, 20, 19–42.
- MENDOZA, E. G. (1991): "Real business cycles in a small open economy," *American Economic Review*, 797–818.
- (1995): "The terms of trade, the real exchange rate, and economic fluctuations," *International Economic Review*, 101–137.
- (2010): "Sudden stops, financial crises, and leverage," *American Economic Review*, 100, 1941–66.
- MENDOZA, E. G., V. QUADRINI, AND J.-V. RIOS-RULL (2009): "Financial integration, financial development, and global imbalances," *Journal of Political Economy*, 117, 371–416.
- MENDOZA, E. G. AND K. A. SMITH (2006): "Quantitative implications of a debt-deflation theory of sudden stops and asset prices," *Journal of International Economics*, 70, 82–114.
- MENDOZA, E. G. AND S. VILLALVAZO (2020): "FiPIt: A simple, fast global method for solving models with two endogenous states & occasionally binding constraints," *Review of Economic Dynamics*, 37, 81–102.
- MEYER-GOHDE, A. (2015): "Risk-sensitive linear approximations," *Unpublished manuscript.*
- NEUMEYER, P. A. AND F. PERRI (2005): "Business cycles in emerging economies: The role of interest rates," *Journal of Monetary Economics*, 52, 345–380.
- SCHMITT-GROHÉ, S. AND M. URIBE (2003): "Closing small open economy models," *Journal of Interna-*

*tional Economics*, 61, 163–185.

——— (2004): “Solving dynamic general equilibrium models using a second-order approximation to the policy function,” *Journal of Economic Dynamics and Control*, 28, 755–775.

——— (2017): “Is optimal capital control policy countercyclical in open economy models with collateral constraints?” *IMF Economic Review*, 65, 498–527.

URIBE, M. AND V. Z. YUE (2006): “Country spreads and emerging countries: Who drives whom?” *Journal of International Economics*, 69, 6–36.